UNDERSTUDIED EMERGING PARAMYXOVIRUSES: FROM PATHOGENICITY TO CELL-CELL FUSION AND VIRAL ENTRY MECHANISMS

A Dissertation

Presented to the Faculty of the Graduate School

of Cornell University

In Partial Fulfillment of the Requirements for the Degree of

Doctor of Philosophy

by

Eun Jin Choi

December 2021

UNDERSTUDIED EMERGING PARAMYXOVIRUSES:
FROM PATHOGENICITY TO CELL-CELL FUSION AND VIRAL ENTRY MECHANISMS

Eun Jin Choi, Ph. D.
Cornell University 2021

The family *Paramyxoviridae* has a wide host range and includes viruses with high potential to induce future epidemics and pandemics. Two genera of the family, *Morbillivirus* and *Henipavirus*, include many pathogenic viruses. Feline morbillivirus (FeMV) and Mojiang virus (MojV) are two recently identified viruses in these genera, respectively. FeMV was firstly isolated from an infected stray cat in Hong Kong in 2012. Since its first detection, many strains with genetic diversity have been found worldwide. Although previous studies determined some of its characteristics, such as in vitro host range and clinical signs of FeMV-infected cats, further studies are still needed. For instance, FeMV's tropism and viral entry mechanisms are still unknown, and its association with several feline kidney diseases is controversial. MojV is the first rat-originated henipavirus identified in China in 2012. The host cell receptor(s) of the MojV G is still undetermined, and its amino acid identity with other bat-originated henipaviruses is only 20%. Despite its uniqueness, our experimental data suggest that the G proteins of MojV and another deadly pathogenic henipavirus, Nipah (NiV), can complement each other, which confirms that MojV belongs to the genus Henipavirus.

Our study results also showed that the three cysteines on the MojV G stalk domain are involved in many roles in cell-cell fusion and viral entry into host cells. Furthermore, the two surface glycoproteins of MojV, G and the fusion protein (F), are far less N-glycosylated than those of other henipaviruses. Different from MojV F whose two N-glycans were involved in F protein expression, proteolytic F2 cleavage, fusogenic capability, and viral entry levels, the sole N-glycan on the G protein did not show any roles, suggesting that N-glycosylation on MojV G only plays minor roles in modulating cell-cell fusion and viral entry mechanisms. My study highlights the two understudied emerging viruses and expands knowledge on membrane fusion and viral entry mechanisms amongst paramyxoviruses.

BIOGRAPHICAL SKETCH

Eun Jin Choi was born in Jinju, South Korea in 1988. She moved to Seoul to attend Chung-Ang University in 2008 and obtained Bachelor's Degree in the field of Life Science in 2012. In the same year, she started in the Master of Science program at the same university. During her two years at graduate school, she specialized in environmental microbiology in Dr. Che Ok Jeon's lab. She participated in several research projects, such as isolating and characterizing novel bacteria, and defining the biodegradation pathways of toxic compounds of bacteria which was isolated from a gasoline-contaminated tidal flat, and obtained her MS degree in 2014. In 2015 she began her doctoral studies at Cornell University in Ithaca, New York. After rotating several labs, she has been conducting research in the laboratory of Dr. Hector Aguilar-Carreno's lab since 2019. In Dr. Aguilar's lab, she identified the mechanisms of (1) the three cysteines in the stalk domain of receptor binding protein (RBP), and (2) the N-glycans on the Fusion (F) and RBP glycoproteins of the Mojiang virus, which is a recently identified rodent-originated henipavirus, during the host cell membrane fusion and viral entry.

This work is dedicated to my family and my pets.

Thinking of Robin, who passed in 2021.

ACKNOWLEDGMENTS

I would like to thank Dr. Hector Aguilar-Carreno for being a great mentor. I could have not made it without his guidance and warm support. I would also like to thank my minor committee members, Dr. Brian VanderVen and Dr. Colin Parrish for their huge help and advice during every meeting. Also, I thank all the Aguilar lab members, who are very supportive and optimistic. I cannot say thank you enough to my family who has always been on my side. Last but not least, I also want to say that I would have not made it this far without my three supporters, Sabo, Zoro, and Robin.

TABLE OF CONTENTS

LIST OF FIGURES

LIST OF TABLES

LIST OF ABBREVIATIONS

APMV-1	Avian paramyxovirus serotype-1
CDV	Canine distemper virus
CedV	Cedar virus
CeMV	cetacean morbillivirus
CKD	chronic kidney diseases
CL	cell lysate
co-IP	co-immunoprecipitation
CRFK	Crandall–Reese Feline Kidney
CSE	cell surface expression
CT	cytoplasmic tail
CTE	C-terminal extension
DMEM	Dulbecco's modified Eagle's medium
ELISA	enzyme-linked immunosorbent assay
Eph	ephrin
F	fusion
FBS	fetal bovine serum
FeMV	Feline morbillivirus
FP	fusion peptide
G	attachment
GhV	Ghana virus

GlcNAc	N-acetylglucosamine
H	hemagglutinin
HA	hemagglutinin
6HB	6-helix bundle
HEK	human embryonic kidney
HeV	Hendra virus
HN	hemagglutinin-neuraminidase
hpi	hours of post-infection
hPIV3	Human parainfluenza virus type 3
hpt	hours of post-transfection
HR	heptad repeat
ICTV	International Committee on Taxonomy of Viruses
IHC	immunohistochemistry
IP	immunoprecipitation
L	large
M	matrix
MeV	Measles virus
MojV	Mojiang virus
MuV	Mumps virus
N	nucleocapsid
NDV	Newcastle disease virus
NGS	next-generation sequencing
NiV	Nipah virus

NRK	Normal Rat Kidney
P	phosphoprotein
PHI	pre-hairpin intermediate
PIV5	Parainfluenza virus 5
PNGaseF	Peptide-*N*-Glycosidase F
PPRV	peste des petits ruminants virus
RBP	receptor binding protein
RLU	relative light units
RPV	Rinderpest virus
RT-LAMP	reverse transcription loop-mediated isothermal amplification
RT-PCR	reverse transcription polymerase chain reaction
SEM	standard error of measurement
SeV	Sendai virus
SISPA	sequence-independent single primer amplification
SV5	Simian virus
TIN	tubulointerstitial nephritis
TM	transmembrane
VSV	vesicular stomatitis virus

CHAPTER 1

Introduction

1.1 The *Paramyxoviridae* Family

It was reported that future pandemics could be more frequent and impact global economy more devastatingly than the current global pandemic (63, 64). To prevent potential pandemics, it is important to pay close attention to zoonotic pathogenic viruses. The family *Paramyxoviridae* includes enveloped, non-segmented, negative-sense, and single-stranded RNA viruses (1, 2). They infect a large variety of mammalian hosts, such as humans, mice, pandas, hyenas, whales, bats, rats, dogs, and cats, as well as non-mammalian hosts, such as birds and reptiles (3-7). The *Paramyxoviridae* family includes many pathogenic viruses which significantly affect animal and human health such as measles virus (MeV), mumps virus (MuV), Rinderpest virus (RPV), and the two deadly pathogenic Hendra virus (HeV) and Nipah virus (NiV) (4, 8, 9). Based on the most recent classification by the International Committee on Taxonomy of Viruses (ICTV), the family *Paramyxoviridae* is divided into the four subfamilies, 14 genera, and 72 recognized species based on complete L protein amino acid sequences (Table 1.1) (26, 31). The four subfamily groups (*Orthoparamyxovirinae, Metaparamyxovirinae, Rubulavirinae,* and *Avulavirinae*) are divided based on the phylogenic distance from *Sunviridae*, which is the closest outlier from the *Paramyxoviridae* (31).

There are minimally six genes in the genome of paramyxovirus, in the order of 3'-N-P-M-F-RBP-L-5' (Fig. 1.1.A). Most paramyxoviruses encode nine proteins from the coding sequences (Fig. 1.1.B). The negative-strand RNA is tightly bound to the viral nucleocapsid (N) protein and forms a ribonucleoprotein (RNP) complex along with the large (L) RNA-dependent RNA polymerase and the phosphoprotein (P)

Subfamily	Genus	Species
Orthoparamyxovirinae	*Aquaparamyxovirus*	Atlantic salmon paramyxovirus (AsaPV)
	Ferlavirus	fer-de-lance virus (FDLV)
	Jeilongvirus	Beilong virus (BeV)
	Henipavirus	Hendra virus (HeV), Nipah virus (NiV), **Mojiang virus (MojV)**
	Morbillivirus	Measles virus (MeV), Canine distemper virus (CDV), Rinderpest virus (RV), **Feline morbillivirus (FeMV)**
	Narmovirus	Nariva virus (NarPV)
	Respirovirus	Human parainfluenza virus (HPIV) 1,3, Sendai virus (SeV)
	Salemvirus	Salem virus (SalV)
Metaparaymyxovirinae	*Synodonvirus*	Wenling triplecross lizardfish paramyxovirus (WpssPV)
Rubulavirinae	*Orthorubulavirus*	Mumps virus (MuV), Human parainfluenza virus (HPIV) 2,4,5
	Pararubulavirus	Hervey virus (HerPV)
Avulavirinae	*Metaavulavirus*	Avian paramyxovirus (APMV) 2
	Orthoavulavirus	Avian paramyxovirus (APMV) 1 (NDV)
	Paraavulavirus	Avian paramyxovirus (APMV) 3

Table 1.1: Subfamilies, genus, and most representative species of the family. *Paramyxoviridae* based on Rima *et al* (31). Abbreviations are listed in parentheses. The two viruses which will be covered in further chapters were marked in bold.

(10). The RNP complex has a very efficient replication system called the "rule of six," meaning that paramyxoviral genomes are polyhexameric length (6n + 0) so each N protein binds every six RNA nucleotides (11, 12, 90). Also, the two additional proteins, V and W, are encoded by mRNA editing of the P gene. The C protein is also generated from P mRNA using an alternate reading frame (13, 14). The P-derived three proteins are known to inhibit interferon signaling to antagonize host antiviral response (13). The matrix protein (M) is a non-glycosylated peripheral membrane protein involved in virus particle assembly and budding process (15, 16). The two surface glycoproteins, the fusion (F) and the receptor-binding protein (RBP, designated variably as HN/H/G), induce membrane fusion and viral entry into target

cells.

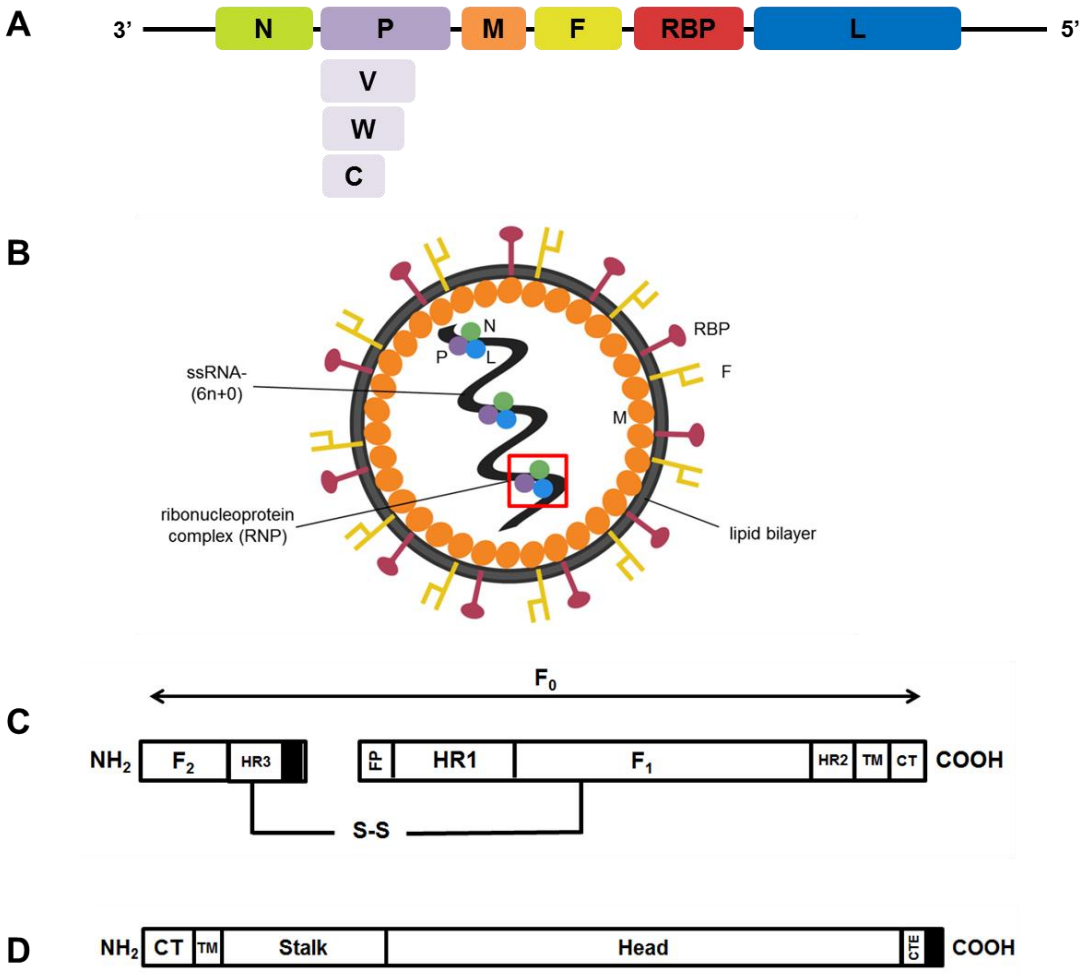

Figure 1.1: Paramyxovirus genome and structure.
(A) Genome organization (3' to 5') of paramyxovirus. Each box indicates the coding sequence of each protein. **(B)** Schematic diagram of paramyxovirus structure. The color of each protein is identical to the coding sequence of Fig. 1.1 A. **(C, D)** Diagram of F (C) and RBP (D) glycoproteins. For F, the 1X FLAG tag (indicated as a black box in F) was inserted at the C-terminus of the F_2 region, and F_1 and F_2 are linked with a disulfide bond (indicated as S-S). As for G, the HA tag (indicated as a black box in G) was attached to the C-terminal end. HR; heptad repeat, FP; fusion peptide, TM; transmembrane, CT; cytoplasmic tail, CTE; C-terminal extension.

1.2 Structure and functions of the surface glycoproteins of paramyxovirus

The F glycoproteins of paramyxovirus are a homotrimeric class I viral fusion

proteins and are characterized by having numerous central N-terminal trimeric α-helical coiled-coils (17). The paramyxoviral F protein is encoded as an inactive precursor (F_0) and transported to the cell surface. The F_0 is then endocytosed and cleaved into F_1 and F_2 in an endosomal compartment by a furin-like protease (18, 19). The fusogenically active F_1 and F_2 are linked by a disulfide bond and transported back to the plasma membrane (3). Each monomer of the F homotrimer has heptad repeat one and two (HR1 and HR2) domains. HR1 is located next to a C-terminus of the fusion peptide, and HR2 is in the proximity of the C-terminus of F_1, adjacent to the transmembrane region (Fig. 1.1.C) (10). It is well known that binding of HR1 and HR2 is a critical for membrane fusion by forming pre-hairpin intermediate (PHI) (3, 89). An additional HR domain (HR3) is located in a C-terminus of the F_2 region. A previous study in my lab reported that the HR3 of the NiV F plays important roles in the membrane fusion cascade (89).

The RBP is various as hemagglutinin-neuraminidase (HN), hemagglutinin (H), and glycoprotein (G) depending on its receptor. For example, the HN protein has receptor-cleaving neuraminidase activity and binds to sialic acid-containing receptors (e.g. mumps virus, APMV-1, and parainfluenza viruses 1 to 5 (PIV 1-5)) (21). The H protein solely has hemagglutinin activity and binds to proteinaceous and immune-related cell surface receptors such as CD46, SLAM (CD150), and an epithelial receptor Nectin-4 (e.g. wild-type measles (MeV) and morbilliviruses) The G protein also recognizes protein receptors including ephrin (Eph)-A2/A5/B2/B3 (e.g. henipavirus) (23-27). For example, NiV and HeV G proteins bind to Eph B2 and B3, which are the EphB class of receptor tyrosine kinases (91). The RBP is a

homotetramer, made up of dimer-of-dimers (28). It is a transmembrane type II protein composing a cytoplasmic tail, transmembrane, 4-helix bundle (4HB) stalk, and a receptor binding globular head domain (Fig. 1.1.D). It is known that the atomic structures of the RBP head domains are highly conserved regardless of their receptors (26).

1.3 Host cell fusion and viral entry mechanism of paramyxovirus

Paramyxovirus membrane fusion is mediated through a pH-independent process and requires the collaborative effort of the RBP and F glycoproteins, which are expressed on the surface of an infected cell (26). Once the head domain of RBP binds to its host receptor protein or sialic acid, it undergoes a conformational change that leads to either exposure of the stalk domain and/or structural change in the stalk itself (65-69). During the pre-fusion stage, the two glycoproteins bind and interact to each other to trigger the conformational change of F. There are two models proposed for this interaction based on the timing of the RBP binds to its receptor (22, 69). Firstly, the dissociation or clamp model suggests that the F and RBP bind to each other before RBP binding to its receptor. This prevents the premature conformational change of F into its post-fusion form (22). It is proposed that many H and G glycoproteins such as MeV or Canine distemper virus (CDV) H, and Nipah virus (NiV) or Hendra virus (HeV) G follow this model (3, 70-73). Previous studies revealed that NiV and HeV F and G show negative correlation between the fusogenicity and F/G interaction, meaning that hyperfusogenic mutants show less F/G avidity in the dissociation model (54, 91). On the other hand, the association or provocateur model explains that RBP which is binding to its receptor triggers F through destabilization

(22). The paramyxoviruses which possess HN glycoprotein such as parainfluenza virus 5 (PIV5), human parainfluenza virus type 3 (hPIV3), avian paramyxovirus serotype-1 (APMV-1) are known to follow this model (3, 74). The subsequent interaction of the RBP stalk domain with F then elicits a conformational change within F. The three hydrophobic N-terminal fusion peptides insert into a membrane of nearby naïve cell, as a form of the PHI (pre-hairpin intermediate), and the two helical regions of F, HR1 and HR2, are exposed and extended. As HR1 and HR2 continuously get closer, the membranes of the infected cell and the naïve cell starts to be pulled in. The HR1 and HR2 eventually bind to each other and form a shape called 6-helix bundle (6HB), which is a highly stable structure. This eventually creates a fusion pore between the two cell membranes (cell-cell fusion). Viruses enter into host cells via the same membrane fusion process between viral and cell membrane (virus-cell fusion). This allows viral genetic materials to enter into the target cell. The fusion cascade continues with neighboring naïve receptor-expressing cells and forms multinuclei cells called as syncytia (3, 26, 91).

Additionally, the studies of headless mutants of paramyxoviruses such as NiV G, MeV H, PIV5 HN, NDV HN, and MuV HN showed that they still sufficiently trigger F protein without requiring receptor binding (21, 29, 30, 66). Specifically, the previous study on headless NiV G revealed the three-step mechanism of the F triggering process (30). The receptor binding of NiV G induces two steps of conformational changes of its head domain, and this triggers the exposure of the stalk domain to interact with F protein for further membrane fusion process (30).

1.4 The two pathogenic genera of *Paramyxoviridae*: *Morbillivirus* and *Henipavirus*

The genera of *Morbillivirus* and *Henipavirus* both belong to the *Orthoparamyxovirinae* subfamily. The *Morbillivirus* contains viruses which can be highly infectious and fatal to both of human and their livestock including MeV, CDV, Rinderpest virus (RPV), and peste des petits ruminants virus (PPRV) (32, 33). The members of *Morbillivirus* use hemagglutinin (H) as their RBP, which interacts with F protein and induces cell-cell fusion. Their principal cellular receptors are SLAM (CD150) and CD46, which are extensively expressed on immune-related cells. A previous study using 28 strains of MeV revealed that SLAM (CD150) serves as a common receptor for all the tested strains (92). This study also suggested that the single amino acid substitution at the position 481 in the H protein determines its binding of CD46, and the binding sites of the two receptors are distinct (92). Another preliminary receptor of the morbillivirus is an epithelial receptor Nectin-4. It is thought that MeV infects and grows in SLAM-expressing lympathic cells. After systemic infection via lymph nodes, the virus is transmitted to the basolateral side of epithelial cells using Nectin-4 and subsequently shed from the apical surface of the cells (34, 35). Furthermore, the viruses in the *Morbillivirus* genus have a possibility of a large outbreak. For example, the feline morbillivirus (FeMV) was newly identified from stray cats in Hong Kong in 2012. So far, many FeMV strains which have genetic diversity have been reported from worldwide including Hong Kong, Japan, Italy, United States, Brazil, Turkey, United Kingdom, Germany, and Malaysia (1, 5, 36-46).

The *Henipavirus* includes highly infectious zoonotic viruses such as NiV and HeV that can have a major global impact in veterinary and medical health, as well as

Cedar (CedV), Ghana (GhV, formally known as Kumasi virus), and Mojiang (MojV) viruses. The natural host reservoirs of henipaviruses except for MojV are mostly bats, but the viruses can be transmitted to numerous other hosts such as humans or other domestic animals by direct contact with infectious body fluids (26, 47).

NiV was first identified in Malaysia in 1998, from an outbreak of the respiratory and neurological disease in pigs and encephalitis in people (4). It was found to be transmitted by a flying fox (pteropid fruit bats) as a natural reservoir host, and transmissions via animal-to-human and human-to-human are both possible (48, 49). The geological range of NiV is broad, including Malaysia, Singapore, India, Bangladesh, Philippines, Cambodia, East Timor, Indonesia, Vietnam, Papua New Guinea, and Thailand (4, 75-81). NiV infection causes symptoms including encephalitis and neurological malfunction which can eventually lead patients to death (48, 50). Despite its high mortality rate (40 to 92%) in humans, there are no efficient treatments nor vaccines approved for humans yet (48, 49, 51).

HeV was firstly reported from infected horses in Australia in 1994 and became the first zoonotic henipavirus (4, 52). It is harbored by Australian flying foxes, and horse-to-human transmission can occur by direct contact with infected horses (4). HeV causes fatal and acute respiratory disease to horses, and can be accompanied with symptoms such as facial swelling, ataxia, and terminally, copious frothy nasal discharge (47, 82). Although the geographical range of the HeV outbreak is limited to eastern Australia, this virus still raises concerns due to its high mortality rate and absence of licensed vaccines for human use (53, 54). However, promisingly, it was reported that a monoclonal antibody which was derived from human, m102.4,

exhibited a high level of cross-neutralization of both NiV and HeV *in vitro* (83). This antibody also proved its ability to prevent lethal NiV and HeV infection from *in vivo* studies using animal models such as ferret and African green monkey (84-86). The m102.4 is known to be capable of neutralizing all known isolates of both NiV and HeV and went through its phase 1 clinical trial recently (87, 88).

CedV is a henipavirus that was isolated from Pteropus bat colonies in Queensland, Australia in 2012 (55). CedV has many similarities with the deadly pathogenic NiV and HeV, such as similar genome size, highly conserved domains in N, M, and L. It also shares the same receptor (Ephrin B2) and shows antibody cross-reactivity with NiV and HeV (55). However, it was reported that CedV did not show pathogenicity to small animals such as ferrets and guinea pigs (55). Also, CedV lacks the RNA editing function of the P gene for coding V and W proteins, which are important for antagonizing the interferon response. This may induce the pathogenic inability of CedV (56, 57).

The viral RNA of the GhV was detected from feces of the African straw-colored fruit bat, *Eidolon helvum* (58). The finding of a novel henipavirus in continental Africa, where Pteropus bats do not exist, suggests a potential endemicity of henipaviruses (58). However, it is still unclear if the live GhV really causes diseases in animals and humans (59). Furthermore, the fusogenicity of GhV is limited to bat-originated cell lines in spite of its binding ability to EphB2, which is a highly conserved receptor among henipaviruses (60). Interestingly, the previous study reported that the truncation of the cytoplasmic tail of GhV G significantly enhanced fusogenicity in cell lines which are not originated from bats (60). This result suggests

that a genetically mutated GhV G may be able to infect a wide range of hosts.

Unlike other bat-borne henipaviruses, the viral RNA of the Mojiang virus (MojV) was detected in a rat (*Rattus flavipectus*) from an abandoned mine. It is circumstantially associated with three human deaths from severe pneumonia in Mojiang Hani Autonomous County in China in 2012 (61). Although the overall genome structure is similar to other henipaviruses, MojV G has several unique characteristics compared to other henipaviral G proteins. First, the amino acid homology between MojV G and other henipaviral G proteins is approximately 20%, which is less than the alignment between other henipaviral G proteins (Table 1.2.). Second, MojV G has a C-terminal extension (CTE) within its head domain, which has not been identified in other henipaviruses, yet, the role(s) of the region is unclear. Lastly, the cellular receptor(s) of MojV G glycoprotein is still undetermined despite previous extensive studies. It was reported that MojV G does not bind to any of the proteinaceous or sialic acid receptors of paramyxoviral RBPs (23). A recent study on the MojV G receptor reported that cell-cell fusion was observed from cells expressing rat Eph A4, human Eph A5, and mouse Eph A1 (62). However, this result does not confirm that Eph A1, A4 and A5 are the main receptors of MojV G due to the low fusion levels and slow kinetics of MojV F and G glycoproteins (62).

	NiV G	HeV G	CedV G	GhV G	MojV G	MeV H
NiV F		78.24	31.69	26.66	20.86	15.96
HeV F	88.1		30.17	27.92	20.45	15.9
CedV F	44.04	42.94		25.3	19.44	16.67
GhV F	53.3	53.11	39.49		19.97	14.59
MojV F	41.56	40.82	34.76	43.23		12.77
MeV F	33.15	33.9	28.79	36.09	34.08	

Table 1.2: Paramyxovirus F and G Percent Identity Analysis.
The table was build using RBP and fusion glycoprotein sequences on the NCBI Protein Database. The protein sequences were aligned using the Clustal Omega Multiple Sequence Alignment Tool (48). The top row indicates the attachment glycoproteins while the left column corresponds to fusion glycoproteins after alignment. The black boxes indicate no comparison was performed, since the boxes corresponded to self (100%). The virus names and accession numbers are as follows: Nipah virus (NiV; G- AEZ01389.1, F- AEZ01388.1), Hendra virus (HeV; G- AEB21198.1, F- AEB21197.1), Cedar virus (CedV; G-AFP87279.1, F- AFP87278.1), Mojiang virus (MojV; G- YP_009094095.1, F- YP_009094094.1), Ghana virus (GhV; G- AFH96011.1, F- AFH96010.1), and Measles virus (MeV; H- AAA75500.1, F- AAA75498.1).

1.5 References

1. Woo, P.C.; Lau, S.K.; Wong, B.H.; Fan, R.Y.; Wong, A.Y.; Zhang, A.J.; Wu, Y.; Choi, G.K.; Li, K.S.; Hui, J., et al. Feline morbillivirus, a previously undescribed paramyxovirus associated with tubulointerstitial nephritis in domestic cats. *Proc Natl Acad Sci U S A* **2012**, *109*, 5435-5440.
2. Park, E.S.; Suzuki, M.; Kimura, M.; Maruyama, K.; Mizutani, H.; Saito, R.; Kubota, N.; Furuya, T.; Mizutani, T.; Imaoka, K., et al. Identification of a natural recombination in the F and H genes of feline morbillivirus. *Virology* **2014**, *468-470*, 524-531.
3. Aguilar, H.C.; Henderson, B.A.; Zamora, J.L.; Johnston, G.P. Paramyxovirus Glycoproteins and the Membrane Fusion Process. *Curr Clin Microbiol Rep* **2016**, *3*, 142-154.
4. Clayton, B.A. Nipah virus: transmission of a zoonotic paramyxovirus. *Curr Opin Virol* **2017**, *22*, 97-104.
5. Marcacci, M.; De Luca, E.; Zaccaria, G.; Di Tommaso, M.; Mangone, I.; Aste, G.; Savini, G.; Boari, A.; Lorusso, A. Genome characterization of feline morbillivirus from Italy. *J Virol Methods* **2016**, *234*, 160-163.
6. Thibault, P.A.; Watkinson, R.E.; Moreira-Soto, A.; Drexler, J.F.; Lee, B. Zoonotic Potential of Emerging Paramyxoviruses: Knowns and Unknowns. *Adv Virus Res* **2017**, *98*, 1-55.
7. Hyndman, T.H.; Shilton, C.M.; Marschang, R.E. Paramyxoviruses in reptiles: a review. *Vet Microbiol* **2013**, *165*, 200-213.
8. Cox, R.M.; Plemper, R.K. Structure and organization of paramyxovirus particles. *Curr Opin Virol* **2017**, *24*, 105-114.
9. Bradel-Tretheway, B.G.; Zamora, J.L.R.; Stone, J.A.; Liu, Q.; Li, J.; Aguilar, H.C. Nipah and Hendra Virus Glycoproteins Induce Comparable Homologous but Distinct Heterologous Fusion Phenotypes. *J Virol* **2019**, *93*.
10. Morrison, T.G. Structure and function of a paramyxovirus fusion protein. *Biochim Biophys Acta* **2003**, *1614*, 73-84.
11. Kolakofsky, D.; Roux, L.; Garcin, D.; Ruigrok, R.W.H. Paramyxovirus mRNA editing, the "rule of six" and error catastrophe: a hypothesis. *J Gen Virol* **2005**, *86*, 1869-1877.
12. Vulliemoz, D.; Roux, L. "Rule of six": how does the Sendai virus RNA polymerase keep count? *J Virol* **2001**, *75*, 4506-4518.
13. Lo, M.K.; Harcourt, B.H.; Mungall, B.A.; Tamin, A.; Peeples, M.E.; Bellini, W.J.; Rota, P.A. Determination of the henipavirus phosphoprotein gene mRNA editing frequencies and detection of the C, V and W proteins of Nipah virus in virus-infected cells. *J Gen Virol* **2009**, *90*, 398-404.
14. Lo, M.K.; Peeples, M.E.; Bellini, W.J.; Nichol, S.T.; Rota, P.A.; Spiropoulou, C.F. Distinct and overlapping roles of Nipah virus P gene products in modulating the human endothelial cell antiviral response. *PLoS One* **2012**, *7*, e47790.

15. El Najjar, F.; Schmitt, A.P.; Dutch, R.E. Paramyxovirus glycoprotein incorporation, assembly and budding: a three way dance for infectious particle production. *Viruses* **2014**, *6*, 3019-3054.
16. Schmitt, A.P.; Leser, G.P.; Waning, D.L.; Lamb, R.A. Requirements for budding of paramyxovirus simian virus 5 virus-like particles. *J Virol* **2002**, *76*, 3952-3964.
17. White, J.M.; Delos, S.E.; Brecher, M.; Schornberg, K. Structures and mechanisms of viral membrane fusion proteins: multiple variations on a common theme. *Crit Rev Biochem Mol Biol* **2008**, *43*, 189-219.
18. Diederich, S.; Moll, M.; Klenk, H.D.; Maisner, A. The nipah virus fusion protein is cleaved within the endosomal compartment. *J Biol Chem* **2005**, *280*, 29899-29903.
19. Iorio, R.M.; Mahon, P.J. Paramyxoviruses: different receptors - different mechanisms of fusion. *Trends Microbiol* **2008**, *16*, 135-137.
20. Gardner, A.E.; Dutch, R.E. A conserved region in the F(2) subunit of paramyxovirus fusion proteins is involved in fusion regulation. *J Virol* **2007**, *81*, 8303-8314.
21. Bose, S.; Song, A.S.; Jardetzky, T.S.; Lamb, R.A. Fusion activation through attachment protein stalk domains indicates a conserved core mechanism of paramyxovirus entry into cells. *J Virol* **2014**, *88*, 3925-3941.
22. Bose, S.; Jardetzky, T.S.; Lamb, R.A. Timing is everything: Fine-tuned molecular machines orchestrate paramyxovirus entry. *Virology* **2015**, *479-480*, 518-531.
23. Rissanen, I.; Ahmed, A.A.; Azarm, K.; Beaty, S.; Hong, P.; Nambulli, S.; Duprex, W.P.; Lee, B.; Bowden, T.A. Idiosyncratic Mojiang virus attachment glycoprotein directs a host-cell entry pathway distinct from genetically related henipaviruses. *Nat Commun* **2017**, *8*, 16060.
24. Aguilar, H.C.; Ataman, Z.A.; Aspericueta, V.; Fang, A.Q.; Stroud, M.; Negrete, O.A.; Kammerer, R.A.; Lee, B. A novel receptor-induced activation site in the Nipah virus attachment glycoprotein (G) involved in triggering the fusion glycoprotein (F). *J Biol Chem* **2009**, *284*, 1628-1635.
25. Takimoto, T.; Taylor, G.L.; Connaris, H.C.; Crennell, S.J.; Portner, A. Role of the hemagglutinin-neuraminidase protein in the mechanism of paramyxovirus-cell membrane fusion. *J Virol* **2002**, *76*, 13028-13033.
26. Azarm, K.D.; Lee, B. Differential Features of Fusion Activation within the Paramyxoviridae. *Viruses* **2020**, *12*.
27. Navaratnarajah, C.K.; Generous, A.R.; Yousaf, I.; Cattaneo, R. Receptor-mediated cell entry of paramyxoviruses: Mechanisms, and consequences for tropism and pathogenesis. *J Biol Chem* **2020**, *295*, 2771-2786.
28. Maar, D.; Harmon, B.; Chu, D.; Schulz, B.; Aguilar, H.C.; Lee, B.; Negrete, O.A. Cysteines in the stalk of the nipah virus G glycoprotein are located in a distinct subdomain critical for fusion activation. *J Virol* **2012**, *86*, 6632-6642.
29. Brindley, M.A.; Suter, R.; Schestak, I.; Kiss, G.; Wright, E.R.; Plemper,

R.K. A stabilized headless measles virus attachment protein stalk efficiently triggers membrane fusion. *J Virol* **2013**, *87*, 11693-11703.
30. Liu, Q.; Stone, J.A.; Bradel-Tretheway, B.; Dabundo, J.; Benavides Montano, J.A.; Santos-Montanez, J.; Biering, S.B.; Nicola, A.V.; Iorio, R.M.; Lu, X., et al. Unraveling a three-step spatiotemporal mechanism of triggering of receptor-induced Nipah virus fusion and cell entry. *PLoS Pathog* **2013**, *9*, e1003770.
31. Rima, B.; Balkema-Buschmann, A.; Dundon, W.G.; Duprex, P.; Easton, A.; Fouchier, R.; Kurath, G.; Lamb, R.; Lee, B.; Rota, P., et al. ICTV Virus Taxonomy Profile: Paramyxoviridae. *J Gen Virol* **2019**, *100*, 1593-1594.
32. Buczkowski, H.; Muniraju, M.; Parida, S.; Banyard, A.C. Morbillivirus vaccines: recent successes and future hopes. *Vaccine* **2014**, *32*, 3155-3161.
33. de Vries, R.D.; Duprex, W.P.; de Swart, R.L. Morbillivirus infections: an introduction. *Viruses* **2015**, *7*, 699-706.
34. Kumar, N.; Barua, S.; Thachamvally, R.; Tripathi, B.N. Systems Perspective of Morbillivirus Replication. *J Mol Microbiol Biotechnol* **2016**, *26*, 389-400.
35. Sato, H.; Yoneda, M.; Honda, T.; Kai, C. Morbillivirus receptors and tropism: multiple pathways for infection. *Front Microbiol* **2012**, *3*, 75.
36. Yilmaz, H.; Tekelioglu, B.K.; Gurel, A.; Bamac, O.E.; Ozturk, G.Y.; Cizmecigil, U.Y.; Altan, E.; Aydin, O.; Yilmaz, A.; Berriatua, E., et al. Frequency, clinicopathological features and phylogenetic analysis of feline morbillivirus in cats in Istanbul, Turkey. *J Feline Med Surg* **2017**, *19*, 1206-1214.
37. Darold, G.M.; Alfieri, A.A.; Muraro, L.S.; Amude, A.M.; Zanatta, R.; Yamauchi, K.C.; Alfieri, A.F.; Lunardi, M. First report of feline morbillivirus in South America. *Arch Virol* **2017**, *162*, 469-475.
38. Furuya, T.; Sassa, Y.; Omatsu, T.; Nagai, M.; Fukushima, R.; Shibutani, M.; Yamaguchi, T.; Uematsu, Y.; Shirota, K.; Mizutani, T. Existence of feline morbillivirus infection in Japanese cat populations. *Arch Virol* **2014**, *159*, 371-373.
39. Sakaguchi, S.; Nakagawa, S.; Yoshikawa, R.; Kuwahara, C.; Hagiwara, H.; Asai, K.I.; Kawakami, K.; Yamamoto, Y.; Ogawa, M.; Miyazawa, T. Genetic diversity of feline morbilliviruses isolated in Japan. *J Gen Virol* **2014**, *95*, 1464-1468.
40. Park, S.W.; Ryou, J.; Choi, W.Y.; Han, M.G.; Lee, W.J. Epidemiological and Clinical Features of Severe Fever with Thrombocytopenia Syndrome During an Outbreak in South Korea, 2013-2015. *Am J Trop Med Hyg* **2016**, *95*, 1358-1361.
41. Stranieri, A.; Lauzi, S.; Dallari, A.; Gelain, M.E.; Bonsembiante, F.; Ferro, S.; Paltrinieri, S. Feline morbillivirus in Northern Italy: prevalence in urine and kidneys with and without renal disease. *Vet Microbiol* **2019**, *233*, 133-139.
42. Mohd Isa, N.H.; Selvarajah, G.T.; Khor, K.H.; Tan, S.W.; Manoraj, H.;

Omar, N.H.; Omar, A.R.; Mustaffa-Kamal, F. Molecular detection and characterisation of feline morbillivirus in domestic cats in Malaysia. *Vet Microbiol* **2019**, *236*, 108382.
43. Donato, G.; De Luca, E.; Crisi, P.E.; Pizzurro, F.; Masucci, M.; Marcacci, M.; Cito, F.; Di Sabatino, D.; Boari, A.; D'Alterio, N., et al. Isolation and genome sequences of two Feline Morbillivirus genotype 1 strains from Italy. *Vet Ital* **2019**, *55*, 179-182.
44. Sieg, M.; Vahlenkamp, A.; Baums, C.G.; Vahlenkamp, T.W. First Complete Genome Sequence of a Feline Morbillivirus Isolate from Germany. *Genome Announc* **2018**, *6*.
45. Sutummaporn, K.; Suzuki, K.; Machida, N.; Mizutani, T.; Park, E.S.; Morikawa, S.; Furuya, T. Association of feline morbillivirus infection with defined pathological changes in cat kidney tissues. *Vet Microbiol* **2019**, *228*, 12-19.
46. Choi, E.J.; Ortega, V.; Aguilar, H.C. Feline Morbillivirus, a New Paramyxovirus Possibly Associated with Feline Kidney Disease. *Viruses* **2020**, *12*.
47. Middleton, D.J.; Weingartl, H.M. Henipaviruses in their natural animal hosts. *Curr Top Microbiol Immunol* **2012**, *359*, 105-121.
48. Biering, S.B.; Huang, A.; Vu, A.T.; Robinson, L.R.; Bradel-Tretheway, B.; Choi, E.; Lee, B.; Aguilar, H.C. N-Glycans on the Nipah virus attachment glycoprotein modulate fusion and viral entry as they protect against antibody neutralization. *J Virol* **2012**, *86*, 11991-12002.
49. Singh, R.K.; Dhama, K.; Chakraborty, S.; Tiwari, R.; Natesan, S.; Khandia, R.; Munjal, A.; Vora, K.S.; Latheef, S.K.; Karthik, K., et al. Nipah virus: epidemiology, pathology, immunobiology and advances in diagnosis, vaccine designing and control strategies - a comprehensive review. *Vet Q* **2019**, *39*, 26-55.
50. Sejvar, J.J.; Hossain, J.; Saha, S.K.; Gurley, E.S.; Banu, S.; Hamadani, J.D.; Faiz, M.A.; Siddiqui, F.M.; Mohammad, Q.D.; Mollah, A.H., et al. Long-term neurological and functional outcome in Nipah virus infection. *Ann Neurol* **2007**, *62*, 235-242.
51. Lam, S.K. Nipah virus--a potential agent of bioterrorism? *Antiviral Res* **2003**, *57*, 113-119.
52. Murray, K.; Selleck, P.; Hooper, P.; Hyatt, A.; Gould, A.; Gleeson, L.; Westbury, H.; Hiley, L.; Selvey, L.; Rodwell, B., et al. A morbillivirus that caused fatal disease in horses and humans. *Science* **1995**, *268*, 94-97.
53. Mire, C.E.; Geisbert, J.B.; Agans, K.N.; Feng, Y.R.; Fenton, K.A.; Bossart, K.N.; Yan, L.; Chan, Y.P.; Broder, C.C.; Geisbert, T.W. A recombinant Hendra virus G glycoprotein subunit vaccine protects nonhuman primates against Hendra virus challenge. *J Virol* **2014**, *88*, 4624-4631.
54. Bradel-Tretheway, B.G.; Liu, Q.; Stone, J.A.; McInally, S.; Aguilar, H.C. Novel Functions of Hendra Virus G N-Glycans and Comparisons to Nipah Virus. *J Virol* **2015**, *89*, 7235-7247.

55. Marsh, G.A.; de Jong, C.; Barr, J.A.; Tachedjian, M.; Smith, C.; Middleton, D.; Yu, M.; Todd, S.; Foord, A.J.; Haring, V., et al. Cedar virus: a novel Henipavirus isolated from Australian bats. *PLoS Pathog* **2012**, *8*, e1002836.
56. Pryce, R.; Azarm, K.; Rissanen, I.; Harlos, K.; Bowden, T.A.; Lee, B. A key region of molecular specificity orchestrates unique ephrin-B1 utilization by Cedar virus. *Life Sci Alliance* **2020**, *3*.
57. Schountz, T.; Campbell, C.; Wagner, K.; Rovnak, J.; Martellaro, C.; DeBuysscher, B.L.; Feldmann, H.; Prescott, J. Differential Innate Immune Responses Elicited by Nipah Virus and Cedar Virus Correlate with Disparate In Vivo Pathogenesis in Hamsters. *Viruses* **2019**, *11*.
58. Drexler, J.F.; Corman, V.M.; Gloza-Rausch, F.; Seebens, A.; Annan, A.; Ipsen, A.; Kruppa, T.; Muller, M.A.; Kalko, E.K.; Adu-Sarkodie, Y., et al. Henipavirus RNA in African bats. *PLoS One* **2009**, *4*, e6367.
59. Behner, L.; Zimmermann, L.; Ringel, M.; Weis, M.; Maisner, A. Formation of high-order oligomers is required for functional bioactivity of an African bat henipavirus surface glycoprotein. *Vet Microbiol* **2018**, *218*, 90-97.
60. Voigt, K.; Hoffmann, M.; Drexler, J.F.; Muller, M.A.; Drosten, C.; Herrler, G.; Kruger, N. Fusogenicity of the Ghana Virus (Henipavirus: Ghanaian bat henipavirus) Fusion Protein is Controlled by the Cytoplasmic Domain of the Attachment Glycoprotein. *Viruses* **2019**, *11*.
61. Wu, Z.; Yang, L.; Yang, F.; Ren, X.; Jiang, J.; Dong, J.; Sun, L.; Zhu, Y.; Zhou, H.; Jin, Q. Novel Henipa-like virus, Mojiang Paramyxovirus, in rats, China, 2012. *Emerg Infect Dis* **2014**, *20*, 1064-1066.
62. Cheliout Da Silva, S.; Yan, L.; Dang, H.V.; Xu, K.; Epstein, J.H.; Veesler, D.; Broder, C.C. Functional Analysis of the Fusion and Attachment Glycoproteins of Mojiang Henipavirus. *Viruses* **2021**, *13*.
63. Dodds W. (2019). Disease Now and Potential Future Pandemics. The World's Worst Problems , 31–44.
64. Michie, S.; West, R. Sustained behavior change is key to preventing and tackling future pandemics. *Nat Med* **2021**, *27*, 749-752.
65. Deng, R.; Wang, Z.; Mahon, P.J.; Marinello, M.; Mirza, A.; Iorio, R.M. Mutations in the Newcastle disease virus hemagglutinin-neuraminidase protein that interfere with its ability to interact with the homologous F protein in the promotion of fusion. *Virology* **1999**, *253*, 43-54.
66. Bose, S.; Zokarkar, A.; Welch, B.D.; Leser, G.P.; Jardetzky, T.S.; Lamb, R.A. Fusion activation by a headless parainfluenza virus 5 hemagglutinin-neuraminidase stalk suggests a modular mechanism for triggering. *Proc Natl Acad Sci U S A* **2012**, *109*, E2625-2634.
67. Ader, N.; Brindley, M.A.; Avila, M.; Origgi, F.C.; Langedijk, J.P.; Orvell, C.; Vandevelde, M.; Zurbriggen, A.; Plemper, R.K.; Plattet, P. Structural rearrangements of the central region of the morbillivirus attachment protein stalk domain trigger F protein refolding for membrane fusion. *J Biol Chem* **2012**, *287*, 16324-16334.

68. Navaratnarajah, C.K.; Oezguen, N.; Rupp, L.; Kay, L.; Leonard, V.H.; Braun, W.; Cattaneo, R. The heads of the measles virus attachment protein move to transmit the fusion-triggering signal. *Nat Struct Mol Biol* **2011**, *18*, 128-134.
69. Navaratnarajah, C.K.; Negi, S.; Braun, W.; Cattaneo, R. Membrane fusion triggering: three modules with different structure and function in the upper half of the measles virus attachment protein stalk. *J Biol Chem* **2012**, *287*, 38543-38551.
70. Plattet, P.; Alves, L.; Herren, M.; Aguilar, H.C. Measles Virus Fusion Protein: Structure, Function and Inhibition. *Viruses* **2016**, *8*, 112.
71. Aguilar, H.C.; Ataman, Z.A.; Aspericueta, V.; Fang, A.Q.; Stroud, M.; Negrete, O.A.; Kammerer, R.A.; Lee, B. A novel receptor-induced activation site in the Nipah virus attachment glycoprotein (G) involved in triggering the fusion glycoprotein (F). *J Biol Chem* **2009**, *284*, 1628-1635.
72. Bishop, K.A.; Stantchev, T.S.; Hickey, A.C.; Khetawat, D.; Bossart, K.N.; Krasnoperov, V.; Gill, P.; Feng, Y.R.; Wang, L.; Eaton, B.T., et al. Identification of Hendra virus G glycoprotein residues that are critical for receptor binding. *J Virol* **2007**, *81*, 5893-5901.
73. Plemper, R.K.; Hammond, A.L.; Gerlier, D.; Fielding, A.K.; Cattaneo, R. Strength of envelope protein interaction modulates cytopathicity of measles virus. *J Virol* **2002**, *76*, 5051-5061.
74. Melanson, V.R.; Iorio, R.M. Amino acid substitutions in the F-specific domain in the stalk of the newcastle disease virus HN protein modulate fusion and interfere with its interaction with the F protein. *J Virol* **2004**, *78*, 13053-13061, doi:10.1128/JVI.78.23.13053-13061.2004.
75. Hayman, D.T.; Suu-Ire, R.; Breed, A.C.; McEachern, J.A.; Wang, L.; Wood, J.L.; Cunningham, A.A. Evidence of henipavirus infection in West African fruit bats. *PLoS One* **2008**, *3*, e2739.
76. Sendow, I.; Field, H.E.; Adjid, A.; Ratnawati, A.; Breed, A.C.; Darminto; Morrissy, C.; Daniels, P. Screening for Nipah virus infection in West Kalimantan province, Indonesia. *Zoonoses Public Health* **2010**, *57*, 499-503.
77. Wacharapluesadee, S.; Boongird, K.; Wanghongsa, S.; Ratanasetyuth, N.; Supavonwong, P.; Saengsen, D.; Gongal, G.N.; Hemachudha, T. A longitudinal study of the prevalence of Nipah virus in Pteropus lylei bats in Thailand: evidence for seasonal preference in disease transmission. *Vector Borne Zoonotic Dis* **2010**, *10*, 183-190.
78. Hasebe, F.; Thuy, N.T.; Inoue, S.; Yu, F.; Kaku, Y.; Watanabe, S.; Akashi, H.; Dat, D.T.; Mai le, T.Q.; Morita, K. Serologic evidence of nipah virus infection in bats, Vietnam. *Emerg Infect Dis* **2012**, *18*, 536-537.
79. Yadav, P.D.; Raut, C.G.; Shete, A.M.; Mishra, A.C.; Towner, J.S.; Nichol, S.T.; Mourya, D.T. Detection of Nipah virus RNA in fruit bat (Pteropus giganteus) from India. *Am J Trop Med Hyg* **2012**, *87*, 576-578.
80. Field, H.; de Jong, C.E.; Halpin, K.; Smith, C.S. Henipaviruses and fruit bats, Papua New Guinea. *Emerg Infect Dis* **2013**, *19*, 670-671.

81. Majid, Z.; Majid Warsi, S. NIPAH virus: a new threat to South Asia. *Trop Doct* **2018**, *48*, 376.
82. Eaton, B.T.; Broder, C.C.; Wang, L.F. Hendra and Nipah viruses: pathogenesis and therapeutics. *Curr Mol Med* **2005**, *5*, 805-816.
83. Zhu, Z.; Bossart, K.N.; Bishop, K.A.; Crameri, G.; Dimitrov, A.S.; McEachern, J.A.; Feng, Y.; Middleton, D.; Wang, L.F.; Broder, C.C., et al. Exceptionally potent cross-reactive neutralization of Nipah and Hendra viruses by a human monoclonal antibody. *J Infect Dis* **2008**, *197*, 846-853.
84. Bossart, K.N.; Zhu, Z.; Middleton, D.; Klippel, J.; Crameri, G.; Bingham, J.; McEachern, J.A.; Green, D.; Hancock, T.J.; Chan, Y.P., et al. A neutralizing human monoclonal antibody protects against lethal disease in a new ferret model of acute nipah virus infection. *PLoS Pathog* **2009**, *5*, e1000642.
85. Geisbert, T.W.; Daddario-DiCaprio, K.M.; Hickey, A.C.; Smith, M.A.; Chan, Y.P.; Wang, L.F.; Mattapallil, J.J.; Geisbert, J.B.; Bossart, K.N.; Broder, C.C. Development of an acute and highly pathogenic nonhuman primate model of Nipah virus infection. *PLoS One* **2010**, *5*, e10690.
86. Rockx, B.; Bossart, K.N.; Feldmann, F.; Geisbert, J.B.; Hickey, A.C.; Brining, D.; Callison, J.; Safronetz, D.; Marzi, A.; Kercher, L., et al. A novel model of lethal Hendra virus infection in African green monkeys and the effectiveness of ribavirin treatment. *J Virol* **2010**, *84*, 9831-9839.
87. Broder, C.C.; Geisbert, T.W.; Xu, K.; Nikolov, D.B.; Wang, L.F.; Middleton, D.; Pallister, J.; Bossart, K.N. Immunization strategies against henipaviruses. *Curr Top Microbiol Immunol* **2012**, *359*, 197-223.
88. Playford, E.G.; Munro, T.; Mahler, S.M.; Elliott, S.; Gerometta, M.; Hoger, K.L.; Jones, M.L.; Griffin, P.; Lynch, K.D.; Carroll, H., et al. Safety, tolerability, pharmacokinetics, and immunogenicity of a human monoclonal antibody targeting the G glycoprotein of henipaviruses in healthy adults: a first-in-human, randomised, controlled, phase 1 study. *Lancet Infect Dis* **2020**, *20*, 445-454.
89. Zamora, J.L.R.; Ortega, V.; Johnston, G.P.; Li, J.; Andre, N.M.; Monreal, I.A.; Contreras, E.M.; Whittaker, G.R.; Aguilar, H.C. Third Helical Domain of the Nipah Virus Fusion Glycoprotein Modulates both Early and Late Steps in the Membrane Fusion Cascade. *J Virol* **2020**, *94.*
90. Douglas, J.; Drummond, A.J.; Kingston, R.L. Evolutionary history of cotranscriptional editing in the paramyxoviral phosphoprotein gene. *Virus Evol* **2021,** *7*(1):veab028.
91. Aguilar, H.C.; Iorio, R.M. Henipavirus membrane fusion and viral entry. *Curr Top Microbiol Immunol* **2012,** *359*, 79-94.
92. Erlenhöfer, C.; Duprex, W.P.; Rima, B.K.; Ter Meulen, V.; Schneider-Schaulies, J. Analysis of receptor (CD46, CD150) usage by measles virus. *J Gen Virol* **2002,** *83,* 1431-1436.

CHAPTER 2

Feline morbillivirus, a new paramyxovirus possibly associated with feline kidney disease

Content from this chapter was partially published in:

Choi, E.J.; Ortega, V.; Aguilar, H.C. Feline Morbillivirus, a New Paramyxovirus Possibly Associated with Feline Kidney Disease. *Viruses* **2020**, *12*.

2.1 Abstract

Feline morbillivirus (FeMV) was first isolated in stray cats in Hong Kong in 2012. Since its discovery, the virus has been reported in domestic cats worldwide, including in Hong Kong, Japan, Italy, US, Brazil, Turkey, UK, Germany, and Malaysia. FeMV is classified in the *Morbillivirus* genus within the *Paramyxoviridae* family. FeMV research has focused primarily on determining the host range, symptoms, and characteristics of persistent infections in vitro. Importantly, there is a potential association between FeMV infection and feline kidney diseases, such as tubulointerstitial nephritis (TIN) and chronic kidney diseases (CKD), which are known to significantly affect feline health and survival. However, the tropism and viral entry mechanism(s) of FeMV remain unknown. In this review, we summarize the FeMV studies up to date, including the discoveries of various FeMV strains, basic virology, pathogenicity, and disease signs.

2.2 Introduction

2.2.1 FeMV Belongs to Family *Paramyxoviridae*.

The family *Paramyxoviridae* includes many pathogenic and infectious viruses such as measles virus (MeV), mumps virus (MuV), newcastle disease virus (NDV), rinderpest virus (RPV), and the two deadly zoonotic Hendra virus (HeV) and Nipah virus (NiV) (1, 3, 4, 8, 9). Therefore, the outbreak of these viruses can cause critical human and veterinary health burdens, as well economic damage to several livestock industries (10–13). Paramyxovirus RBPs bind to cellular receptors, such as neuraminidase-proteinaceous receptors (for HN), ephrinB2 and ephrinB3 (for G), and SLAM (also known as CD150, for H) (23–26). After receptor binding, the two surface

glycoproteins, F and RBP, undergo conformational changes and trigger F to induce the viral-cell membrane fusion cascade that results in viral entry. This process facilitates the fusion of viral and host cell membranes and viral entry into host cells (19-22, 27, 28).

The *Morbillivirus* genus within the *Paramyxoviridae* family contains highly infectious animal viruses, including peste des petits ruminants virus (PPRV), canine distemper virus (CDV), and cetacean morbillivirus (CeMV), which can cause severe and sometimes fatal systemic disorders (14–16). In 2012, a previously unknown virus now named feline morbillivirus (FeMV, formerly abbreviated FmoPV), was discovered in Hong Kong to infect cats and subsequently classified in the Morbillivirus genus (1, 17, 18).

2.2.2 Discovery of Various FeMV Strains

FeMV is an emerging morbillivirus that has been isolated and studied by numerous research groups worldwide. Cats infected with FeMV have been detected in Hong Kong, Japan, Italy, United States, Brazil, Turkey, United Kingdom, Germany, Malaysia (Figure 2.1). FeMV RNA was first detected in 56 out of 457 stray cats (12.3%, 53 urine samples, four rectal swabs, and one blood sample) by reverse transcription polymerase chain reaction (RT-PCR) utilizing consensus primers designed using the partial sequence of the morbillivirus L gene, a highly conserved sequence within the genome (1, 10). The three complete genome sequences (761U, 776U, and M252A) had less than 80% nucleotide identities to known paramyxoviruses (1). The three genomes followed the characteristic paramyxovirus genome layout as 3’-N-P/V/W/C-M-F-HN/H/G-L-5’, the rule of six, and the herringbone nucleoprotein

morphology (1, 29, 30). Based on these observations and the phylogenetic analysis, the three strains were added to the *Morbillivirus* genus (1).

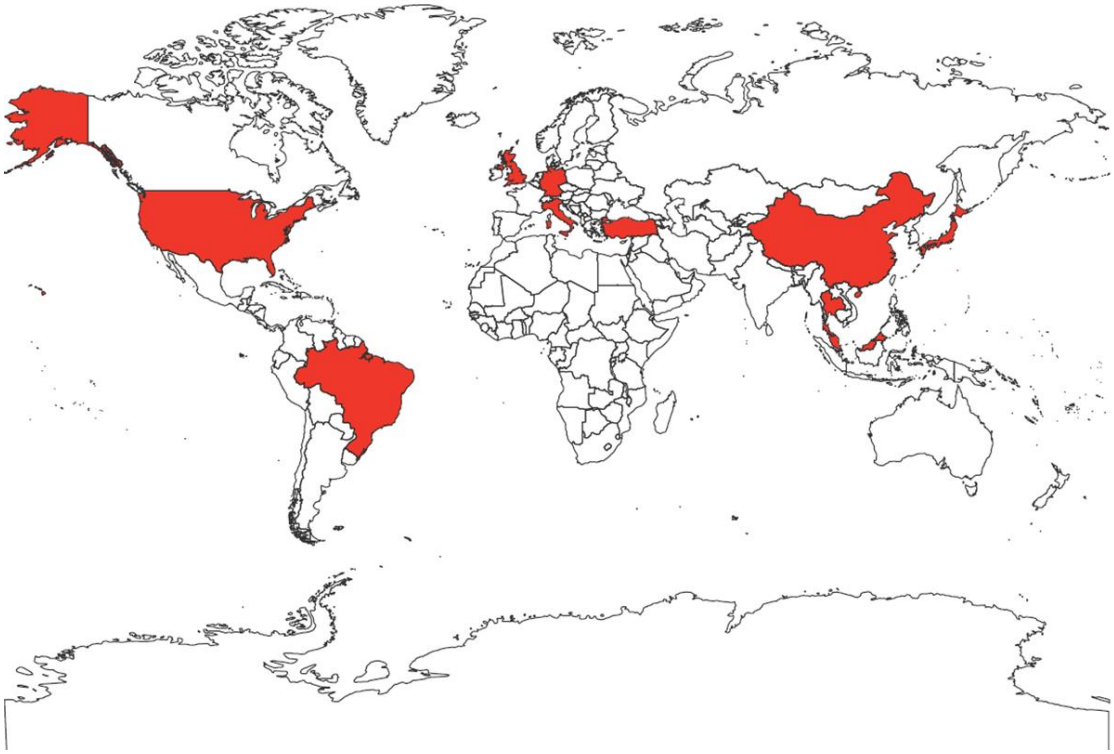

Figure 2.1: World map showing the countries with reported FeMV infections in felines in red.

Since then, new FeMV strains have been continuously isolated from cat urine samples and identified by RT-PCR based on the partial L gene sequences. In 2014, viral RNA was detected in five out of 82 urine samples (6.1%) and one among ten blood samples (10%) in Japan. The six unknown viruses were determined to be FeMV strains (SE4, CL5, SE7, SE14, MS25, and MS26), as they shared 92–94% identity with the three viruses identified in Hong Kong (31). Furthermore, three strains (SS1, SS2, and SS3) were isolated from 13 cat urine samples and had a 90–99% nucleotide

similarity to the isolates from Hong Kong. SS3 showed an around 99% similarity to strain M252A (32). Based on the high similarity between FeMV strains identified in Japan and Hong Kong, the researchers suggested a possible transmission of FeMV by unidentified vectors. For instance, infected cats may have been transported between the two countries (32).

Partial L gene sequences of FeMV strains were amplified using RT-PCR from samples such as cat urine, kidney, and blood (2, 31). The large protein sequences from the different FeMV strains were aligned in Figure 2.2. Whole genome sequences of some viruses were determined by various techniques, such as overlapping RT-PCR amplicons, next-generation sequencing (NGS), and sequence-independent single primer amplification (SISPA) (2, 5). The partial and whole genome sequences known to date are shown in Table 1. MiJP003 is one of the FeMV strains whose complete genome sequence has been determined (2). Interestingly, the genomic organization and the similarity analysis results showed that the intragenomic region, F and H, is different from other strains (2). This suggests a possible recombination event among the known FeMV strains (2, 33).

The rate of FeMV-positive urine samples has varied between studies. One possible explanation is the different clinical and environmental backgrounds of the samples and donors. Stray cats are more easily infected, as they have a higher risk of exposure to infectious agents and conditions, thus the positive rate of the virus in stray cats is higher than that in household cats (10, 31, 34, 35). Interestingly, unneutered male cats showed a higher risk of FeMV infection than female cats. This may be due to higher activity and aggressive tendencies of male cats, such as territorial fighting

and marking behaviors (33, 35).

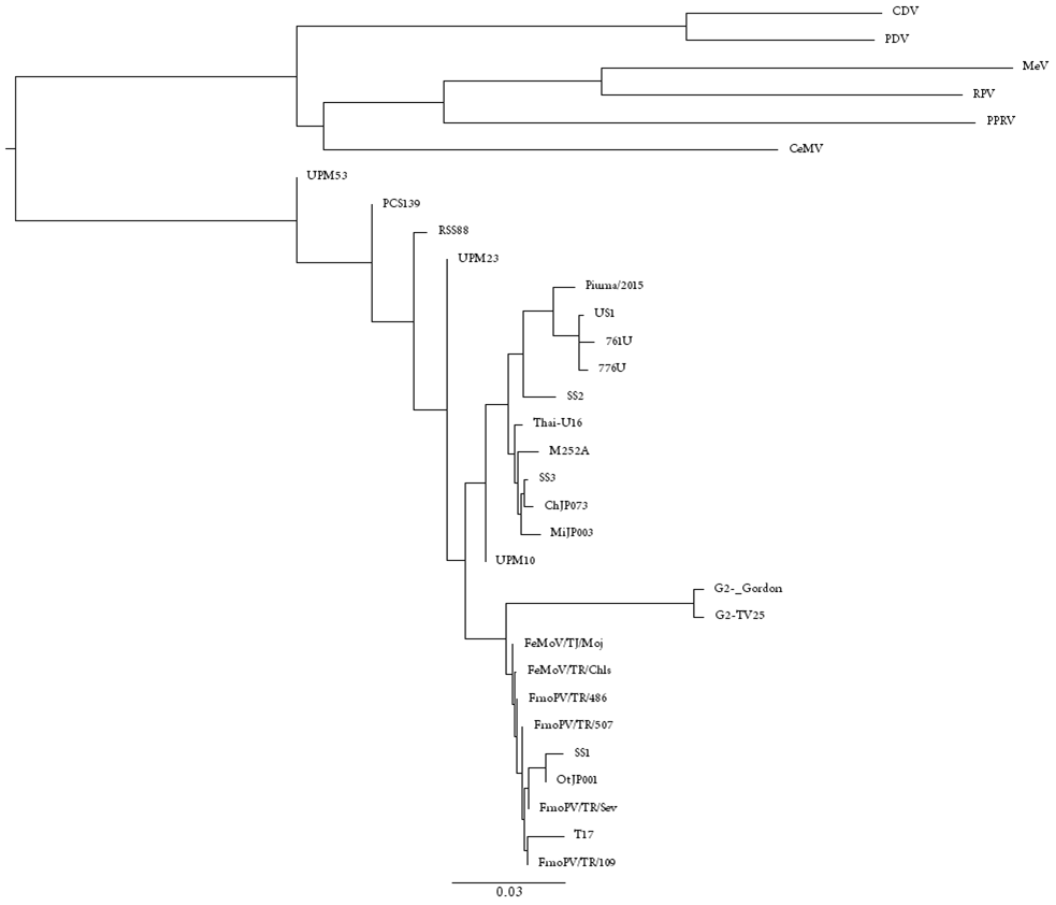

Figure 2.2: Diagram of the Morbillivirus family.
The phylogenetic tree was built after obtaining the RNA polymerase/large protein sequences of the viruses from the NCBI Protein Database. The protein sequences were aligned by using the COBALT multiple alignment tool and the fast-minimum evolution method and visualized using FigTree. The virus names and GenBank accession numbers are as follows: Feline morbillivirus (FeMV) strains TV17 (AVH81382.1), Thai-U16 (AVD98481.1), Piuma/2015 (AMM62640.1), US1 (AMH87247.1), 761U (YP_009512964.1), 776U (AFH55526.1), M252A (AFH55534.1), SS3 (BAR91703.1), SS2 (BAR91698.1), SS1 (BAO58314.1), ChJP073 (BAP74678.1), MiJP003 (BAP74672.1), OtJP001 (BAP74666.1), A1 (AVT56121.1), H10 (AVT56123.1), H1 (AVT56124.1), S1 (AVT56126.1), H3 (AVT56127.1), S2 (VT56128.1), FmoPV/TR/Sev (AMZ80122.1), FmoPV/TR/507 (AMZ80121.1), FmoPV/TR/486 (AMZ80120.1), FmoPV/TR/109 (AMZ80119.1), FeMoV/TR/Moj (ALM58465.1), FeMoV/TR/Chls(ALJ78003.1), PCS139 (AQV13350.1), RSS88 (AQV13353.1), UPM53 (AQV13352.1), UPM10 (AQV13351.1), UPM23 (AQV13349.1), GT2-Gordon (QBC65287.1), GT2-TV25

(QBC65293.1); cetacean morbillivirus (CeMV)—2990 (AYR16899.1), phocine distemper virus (PDV)—Wadden (YP_009177604.1), rinderpest virus (RPV)—LA96 (AEX65767.1), peste des petits ruminants virus (PPRV)—Turkey2000 (CAH61259.1), canine distemper virus (CDV)—PS (AFG24211.1), measles virus (MeV)—Edmonton (AAA75501.1).

2.3 FeMV Detection Techniques

To isolate new FeMV strains, several techniques have been developed to increase detection efficiency. For instance, a real-time RT-PCR system showed an over ten times higher sensitivity relative to the conventional RT-PCR method. Using real- time RT-PCR, 25 FeMV positive urine samples were detected out of 166 samples (15.1%). This was about twice the positive rate than the previous study, which showed only six positives out of 82 (7.3%) (31, 36). Furthermore, the reverse transcription loop-mediated isothermal amplification (RT-LAMP) assay has a 100 times higher sensitivity and is time-efficient as compared to conventional RT-PCR (37). An enzyme-linked immunosorbent assay (ELISA) was also developed and applied for serological detection of FeMV (38). The purified FeMV P protein was used in the assay as an antigen, because [1] it is important in viral replication, [2] is highly expressed in infected cells, [3] has less conserved gene sequence, and [4] antigenicity does not require glycosylation (38). The P protein-based ELISA assays have been developed for other paramyxoviruses and show higher accuracy and specificity as compared to conventional methods of detection (39, 40). Using ELISA, P protein antibodies were detected in 22 of 100 cats (22%), supporting previous study results (1, 32, 33).

Virus	Strain	Country	Reference	Sequence	GenBank accession no.
FeMV	761U	Hong Kong	Woo et al., 2012	Complete	JQ411014
	776U				JQ411015
	M252A				JQ411016
	SE4	Japan	Furuya et al., 2014	Partial (L gene)	AB828138
	CL5				AB828139
	SE7				AB828140
	SE14				AB828141
	MS25				AB828142
	MS26				AB828143
	SS1	Japan	Sakaguchi et al., 2014	Complete	AB910309
	SS2				AB910310
	SS3				AB910311
	OtJP001	Japan	Park et al., 2014	Complete	AB924120
	MiJP003				AB924121
	ChJP073				AB924122
	Piuma/2015	Italy	Lorusso et al., 2015	Partial (L gene)	KT306750
			Marcacci et al., 2016	Complete	KT825132
	US1	US	Sharp et al., 2016	Complete	KR014147
	BR1	Brazil	Darold et al., 2017	Partial (L gene)	KX452077
	FmoPV/TR/109	Turkey	Yilmaz et al., 2017	Partial (L gene)	KU053510
	FmoPV/TR/486				KU053511
	FmoPV/TR/507				KU053512
	FmoPV/TR/Sev				KU053513
	A1	UK	McCallum et al., 2018	Partial (L gene)	MG640027
	S9				MG640028
	H10				MG640029
	H1				MG640030
	S6				MG640031
	S1				MG640032
	H3				MG640033
	S2				MG640034
	TV17	Germany	Sieg et al., 2018	Complete	MG563820
	1073U	Italy	Stranieri et al., 2019	Partial (L gene)	N/A
	434K				
	1568K				
	Tremedino/2018	Italy	Donato et al., 2019	Complete	MK088516
	Pepito/2018				MK088517
	UPM23	Malaysia	Isa et al., 2019	Partial (L gene)	KU646847
	PCS139				KU646848
	UPM10				KU646849
	UPM53				KU646850
	RSS88				KU646851
	UPM23			Partial (N gene)	KU646852
	PCS139				KU646853
	UPM10				KU646854
	UPM53				KU646855
	RSS88				KU646856
FeMV-GT2	Gordon	Germany	Sieg et al., 2019	Complete	MK182089
	TV25				MK182090

Table 2.1: Reported FeMV complete/partial sequences.
*N/A indicates not available.

2.4 Signs of FeMV-Infected Cells and Cats

In vitro, FeMV has been shown to cause cytopathic effects that include cell rounding, detachment, lysis, and syncytia formation in infected Crandall–Reese Feline

Kidney (CRFK) cells (1, 32). Clinically, FeMV-positive cats have shown urinary tract signs (renal disorders and residue in urine), gastrointestinal signs (anorexia, diarrhea, and vomiting), as well as weight loss, fever, and depression. Additionally, infected cats had decreased red blood cell, hemoglobin, albumin, and urobilinogen counts, as well as higher alanine transaminase, alkaline phosphatase, and bilirubin levels as compared to uninfected cats (10). However, the authors did not state whether the six FeMV-positive cats were all hospitalized or healthy. Furthermore, this study indicated that some FeMV-positive cats were also positive for other viruses, such as Feline Coronavirus, feline immunodeficiency virus, and feline leukemia virus. Therefore, the symptoms observed cannot be concluded as caused solely by FeMV.

German strain GT2 (FeMV-GT2), identified in 2019, was isolated from a cat with polyuria-polydipsia syndrome. FeMV-GT2 is phylogenetically distinct and belongs to a different subgroup than other known FeMV strains. FeMV-GT2 can infect cells, such as renal and pulmonary epithelial cells and primary cells from the cerebrum and cerebellum. FeMV-GT2 also infected immune cells, such as CD4+ T cells (40–70%), CD20+ B cells, and monocytes (20–40%) (46). However, some of the authors' observations in this study did not match the previous studies. First, the authors did not observe any cytopathic effects, including syncytia formation, in feline kidney cell lines. Second, the authors suggested that the prevalence of the strain was only 0.83% in urine, which is much less as compared to other studies. This may be due to (1) possible RNA degradation during sample storage before RNA extraction and (2) the high genetic diversity between strains (2, 33, 46, 47).

2.5 Virology, Tropism, and FeMV Entry into Host Cells

The in vitro host range of FeMV infectivity has been studied in 32 different cell lines originating from 13 animal species, including human, cat, dog, mouse, rat, African green monkey, rabbit, ferret, mink, quail, cattle, horse, and swine (47). The cells were incubated with the FeMV SS1 strains and cultured for two weeks, and the viral infection was detected by RT-PCR that amplified the L gene. Kidney cell lines derived from both cats and African green monkeys, as well as other feline cell lines, including epithelial, fibroblastic, lymphoid, and glial cells, were susceptible to the viral infection. This suggests the receptor(s) for FeMV, which remain(s) unknown, is(are) ubiquitously expressed, at least in cats. Human cell lines were not susceptible to FeMV, suggesting there is a low risk of cross-species transmission between humans and felids (47). Similarly, transmission between cats remains undetermined. So far, cohabitation has not caused most cats to become FeMV-positive (10). However, due to the high genetic diversity of the virus and the relatively high mutation rate of the paramyxoviruses, including potential gene recombination, FeMV may have the capacity to adapt to new host species such as humans through physical contact with cats (2, 33, 47).

Little is known about the specific viral entry mechanism for FeMV. However, host cell receptors such as SLAM (CD150) and nectin-4 are potential candidates, since other morbilliviruses, such as CDV, MeV, RPV, and PPRV use them as their primary receptors for their respective hosts (2, 48, 49). For example, MeV suppresses the immune system by binding to the human SLAM on dendritic cells (50, 51). CDV interacts with monkey, dog, and feline SLAM, but less efficiently with the cells

expressing human SLAM (52–54). Since receptors are one of the crucial factors to determine the tissue tropism and host range of a virus, it is important to identify the receptor of FeMV (2, 53) Interestingly, the cleavage site of the FeMV F protein is different from the typical cleavage site of other known morbillivirus F proteins. Although immunoblot analysis showed FeMV F cleaved into the typical F_1 and F_2 subunits, the FeMV F protein has a single basic proteolytic cleavage site, while other morbillivirus F proteins have multibasic cleavage sites (1, 32, 55). This observation suggests that different proteases may cleave the FeMV F protein, which may affect viral entry and host cell tropism.

2.6 Possibility of Persistent FeMV Infection

Several studies have shown evidence of persistent infection with FeMV (13, 32, 33, 43, 46). For example, FeMV strain US1 was obtained from a male domestic cat in 2013, and the identical strain was detected in the same cat 15 months later based on amplification and sequencing of the H gene (43). Furthermore, almost half of the infected cats (14 out of 29) were positive not only for RNA but also for antibodies against the N protein (33). Further, two cats infected by FeMV strain GT2 shed the virus in their urine for up to several years (46). These results suggest that persistent FeMV infection is possible. Interestingly, while cat urine (50.8%) and kidney (80.0%) samples were found FeMV-positive as determined via nested RT-PCR targeting the L gene, blood samples were all FeMV-negative (35). This suggests that the cats were not viremic when the samples were collected. These observations suggest that FeMV either has a long incubation period or a short viremic duration (35). Another possibility is that during the early stages of infection, FeMV in circulation may infect

lymphocytes and remain below the threshold of PCR detection (56, 57). Overall, the pathogenesis of FeMV remains not well understood. Further studies will be required with larger sample size and various incubation periods to understand persistent FeMV infections.

2.7 Controversies of FeMV Studies

A controversy surrounding FeMV research is whether the virus is involved in tubulointerstitial nephritis (TIN). This is one of the primary causes of renal failure, which can lead to and may trigger chronic kidney disease (CKD). This is one of the most common metabolic diseases of cats, particularly for older cats, frequently causing feline death (42, 58, 59). There has been a suggested association between FeMV and TIN after the discovery that seven out of 12 FeMV-infected cats had TIN (1). Additionally, four of the fixed kidney tissues from ten cats with nephritis (40%) were FeMV-positive (31, 60). Furthermore, a significant association between FeMV infection and TIN was found based on immunohistochemistry (IHC) (60). The pathology observed in 38 kidney tissue samples was consistent with chronic kidney disease, including interstitial cell infiltration, glomerulosclerosis, tubular atrophy, and fibrosis. The authors also compared FeMV-positive and negative samples, scored and statistically evaluated the correlation between FeMV infection and TIN, and found particular statistical significance in tubular atrophy, luminal expansion, urinary casts for renal tubules, inflammatory cell infiltration, and fibrosis in the interstitial areas. The differences were significant for the thickness of capillaries and glomerulosclerosis in renal tubules (60). On the other hand, other conducted studies were unable to find a clear statistical relationship between cat nephritis and FeMV infection (10, 12, 32, 34,

35, 44). FeMV, however, might be involved in CKD or lower urinary tract diseases (LUTD), based on the reported IHC detected in 19 cat kidney tissues of FeMV-infected cats (33). However, the authors proposed that FeMV may not necessarily cause feline urinary tract diseases, but simply act as a helper or bystander (33). Several possible explanations of this controversy have been proposed. First, some feline chronic diseases, including TIN and CKD, can still develop when no FeMV RNA is detected in urine. Second, the research that showed no clear association between FeMV and TIN or CKD might have chosen indirect markers for detection. Finally, the primers used for FeMV detection may be relatively poorly optimized (60). Another controversy in the field is the potential cross-reactivity between FeMV and CDV. Sakaguchi et al. showed immunoreactivity of the anti-FeMV N antibody to CDV N, and of anti-CDV dog serum to FeMV (32). However, other studies did not find any cross-reactivity between these two viruses using an immunofluorescence (IF) test for anti-FeMV serum binding to CDV N, an ELISA assay to test cross-reactivity between CDV P and FeMV P, and an RT-LAMP assay using the RNA extracted from CDV-infected Vero cells (33, 37, 38).

2.8 Conclusions

Cats are among the most common household pets. Feline kidney diseases such as TIN and CKD are among the leading causes of death in domesticated cats, particularly in geriatric cats. Although the link between FeMV and kidney diseases has not been clearly defined, an association is possible, even if it is not causal. It is possible that some cats establish persistent FeMV infection, shedding FeMV RNA in their urine for extended periods. Moreover, considering the high genetic diversity of

FeMV, there is a possibility for cross-species infections. Therefore, FeMV research may have significance beyond feline health. Since FeMV is a relatively newly identified virus, currently, there are not enough case studies or clinical data available. Therefore, further studies with larger sample numbers or full genome sequences of the identified strains would be beneficial to understand the effects of FeMV in worldwide feline health.

2.9 References

1. Woo, P.C.; Lau, S.K.; Wong, B.H.; Fan, R.Y.; Wong, A.Y.; Zhang, A.J.; Wu, Y.; Choi, G.K.; Li, K.S.; Hui, J., et al. Feline morbillivirus, a previously undescribed paramyxovirus associated with tubulointerstitial nephritis in domestic cats. *Proc Natl Acad Sci U S A* **2012**, *109*, 5435-5440.
2. Park, E.S.; Suzuki, M.; Kimura, M.; Maruyama, K.; Mizutani, H.; Saito, R.; Kubota, N.; Furuya, T.; Mizutani, T.; Imaoka, K., et al. Identification of a natural recombination in the F and H genes of feline morbillivirus. *Virology* **2014**, *468-470*, 524-531.
3. Aguilar, H.C.; Henderson, B.A.; Zamora, J.L.; Johnston, G.P. Paramyxovirus Glycoproteins and the Membrane Fusion Process. *Curr Clin Microbiol Rep* **2016**, *3*, 142-154.
4. Clayton, B.A. Nipah virus: transmission of a zoonotic paramyxovirus. *Curr Opin Virol* **2017**, *22*, 97-104.
5. Marcacci, M.; De Luca, E.; Zaccaria, G.; Di Tommaso, M.; Mangone, I.; Aste, G.; Savini, G.; Boari, A.; Lorusso, A. Genome characterization of feline morbillivirus from Italy. *J Virol Methods* **2016**, *234*, 160-163.
6. Thibault, P.A.; Watkinson, R.E.; Moreira-Soto, A.; Drexler, J.F.; Lee, B. Zoonotic Potential of Emerging Paramyxoviruses: Knowns and Unknowns. *Adv Virus Res* **2017**, *98*, 1-55.
7. Hyndman, T.H.; Shilton, C.M.; Marschang, R.E. Paramyxoviruses in reptiles: a review. *Vet Microbiol* **2013**, *165*, 200-213.
8. Cox, R.M.; Plemper, R.K. Structure and organization of paramyxovirus particles. *Curr Opin Virol* **2017**, *24*, 105-114.
9. Bradel-Tretheway, B.G.; Zamora, J.L.R.; Stone, J.A.; Liu, Q.; Li, J.; Aguilar, H.C. Nipah and Hendra Virus Glycoproteins Induce Comparable Homologous but Distinct Heterologous Fusion Phenotypes. *J Virol* **2019**, *93*.
10. Yilmaz, H.; Tekelioglu, B.K.; Gurel, A.; Bamac, O.E.; Ozturk, G.Y.; Cizmecigil, U.Y.; Altan, E.; Aydin, O.; Yilmaz, A.; Berriatua, E., et al. Frequency, clinicopathological features and phylogenetic analysis of feline morbillivirus in cats in Istanbul, Turkey. *J Feline Med Surg* **2017**, *19*, 1206-1214.
11. de Vries, R.D.; Duprex, W.P.; de Swart, R.L. Morbillivirus infections: an introduction. *Viruses* **2015**, *7*, 699-706.
12. Darold, G.M.; Alfieri, A.A.; Muraro, L.S.; Amude, A.M.; Zanatta, R.; Yamauchi, K.C.; Alfieri, A.F.; Lunardi, M. First report of feline morbillivirus in South America. *Arch Virol* **2017**, *162*, 469-475.
13. De Luca, E.; Crisi, P.E.; Di Domenico, M.; Malatesta, D.; Vincifori, G.; Di Tommaso, M.; Di Guardo, G.; Di Francesco, G.; Petrini, A.; Savini, G., et al. A real-time RT-PCR assay for molecular identification and quantitation of feline morbillivirus RNA from biological specimens. *J Virol Methods* **2018**, *258*, 24-28.

14. Kumar, N.; Maherchandani, S.; Kashyap, S.K.; Singh, S.V.; Sharma, S.; Chaubey, K.K.; Ly, H. Peste des petits ruminants virus infection of small ruminants: a comprehensive review. *Viruses* **2014**, *6*, 2287-2327.
15. Rendon-Marin, S.; da Fontoura Budaszewski, R.; Canal, C.W.; Ruiz-Saenz, J. Tropism and molecular pathogenesis of canine distemper virus. *Virol J* **2019**, *16*, 30.
16. Van Bressem, M.F.; Duignan, P.J.; Banyard, A.; Barbieri, M.; Colegrove, K.M.; De Guise, S.; Di Guardo, G.; Dobson, A.; Domingo, M.; Fauquier, D., et al. Cetacean morbillivirus: current knowledge and future directions. *Viruses* **2014**, *6*, 5145-5181.
17. Amarasinghe, G.K.; Ayllon, M.A.; Bao, Y.; Basler, C.F.; Bavari, S.; Blasdell, K.R.; Briese, T.; Brown, P.A.; Bukreyev, A.; Balkema-Buschmann, A., et al. Taxonomy of the order Mononegavirales: update 2019. *Arch Virol* **2019**, *164*, 1967-1980. 19. Morrison, T.G. Structure and function of a paramyxovirus fusion protein. *Biochim Biophys Acta* **2003**, *1614*, 73-84.
18. Rima, B.; Balkema-Buschmann, A.; Dundon, W.G.; Duprex, P.; Easton, A.; Fouchier, R.; Kurath, G.; Lamb, R.; Lee, B.; Rota, P., et al. ICTV Virus Taxonomy Profile: Paramyxoviridae. *J Gen Virol* **2019**, *100*, 1593-1594.
19. Morrison, T.G. Structure and function of a paramyxovirus fusion protein. Biochim. Biophys. Acta 2003, 1614, 73–84.
20. El Najjar, F.; Schmitt, A.P.; Dutch, R.E. Paramyxovirus glycoprotein incorporation, assembly and budding: a three way dance for infectious particle production. *Viruses* **2014**, *6*, 3019-3054.
21. Schmitt, A.P.; Leser, G.P.; Waning, D.L.; Lamb, R.A. Requirements for budding of paramyxovirus simian virus 5 virus-like particles. *J Virol* **2002**, *76*, 3952-3964.
22. Alayyoubi, M.; Leser, G.P.; Kors, C.A.; Lamb, R.A. Structure of the paramyxovirus parainfluenza virus 5 nucleoprotein-RNA complex. *Proc Natl Acad Sci U S A* **2015**, *112*, E1792-1799.
23. Tatsuo, H.; Yanagi, Y. The morbillivirus receptor SLAM (CD150). *Microbiol Immunol* **2002**, *46*, 135-142.
24. Nakano, H.; Kameo, Y.; Andoh, K.; Ohno, Y.; Mochizuki, M.; Maeda, K. Establishment of canine and feline cells expressing canine signaling lymphocyte activation molecule for canine distemper virus study. *Vet Microbiol* **2009**, *133*, 179-183.
25. Negrete, O.A.; Levroney, E.L.; Aguilar, H.C.; Bertolotti-Ciarlet, A.; Nazarian, R.; Tajyar, S.; Lee, B. EphrinB2 is the entry receptor for Nipah virus, an emergent deadly paramyxovirus. *Nature* **2005**, *436*, 401-405.
26. Chang, A.; Dutch, R.E. Paramyxovirus fusion and entry: multiple paths to a common end. *Viruses* **2012**, *4*, 613-636.
27. Iorio, R.M.; Melanson, V.R.; Mahon, P.J. Glycoprotein interactions in paramyxovirus fusion. *Future Virol* **2009**, *4*, 335-351.

28. Aguilar, H.C.; Iorio, R.M. Henipavirus membrane fusion and viral entry. *Curr Top Microbiol Immunol* **2012**, *359*, 79-94.
29. Kolakofsky, D.; Roux, L.; Garcin, D.; Ruigrok, R.W.H. Paramyxovirus mRNA editing, the "rule of six" and error catastrophe: a hypothesis. *J Gen Virol* **2005**, *86*, 1869-1877.
30. Cox, R.; Plemper, R.K. The paramyxovirus polymerase complex as a target for next-generation anti-paramyxovirus therapeutics. *Front Microbiol* **2015**, *6*, 459.
31. Furuya, T.; Sassa, Y.; Omatsu, T.; Nagai, M.; Fukushima, R.; Shibutani, M.; Yamaguchi, T.; Uematsu, Y.; Shirota, K.; Mizutani, T. Existence of feline morbillivirus infection in Japanese cat populations. *Arch Virol* **2014**, *159*, 371-373.
32. Sakaguchi, S.; Nakagawa, S.; Yoshikawa, R.; Kuwahara, C.; Hagiwara, H.; Asai, K.I.; Kawakami, K.; Yamamoto, Y.; Ogawa, M.; Miyazawa, T. Genetic diversity of feline morbilliviruses isolated in Japan. *J Gen Virol* **2014**, *95*, 1464-1468.
33. Park, E.S.; Suzuki, M.; Kimura, M.; Mizutani, H.; Saito, R.; Kubota, N.; Hasuike, Y.; Okajima, J.; Kasai, H.; Sato, Y., et al. Epidemiological and pathological study of feline morbillivirus infection in domestic cats in Japan. *BMC Vet Res* **2016**, *12*, 228.
34. Stranieri, A.; Lauzi, S.; Dallari, A.; Gelain, M.E.; Bonsembiante, F.; Ferro, S.; Paltrinieri, S. Feline morbillivirus in Northern Italy: prevalence in urine and kidneys with and without renal disease. *Vet Microbiol* **2019**, *233*, 133-139.
35. Mohd Isa, N.H.; Selvarajah, G.T.; Khor, K.H.; Tan, S.W.; Manoraj, H.; Omar, N.H.; Omar, A.R.; Mustaffa-Kamal, F. Molecular detection and characterisation of feline morbillivirus in domestic cats in Malaysia. *Vet Microbiol* **2019**, *236*, 108382.
36. Furuya, T.; Wachi, A.; Sassa, Y.; Omatsu, T.; Nagai, M.; Fukushima, R.; Shibutani, M.; Yamaguchi, T.; Uematsu, Y.; Shirota, K., et al. Quantitative PCR detection of feline morbillivirus in cat urine samples. *J Vet Med Sci* **2016**, *77*, 1701-1703.
37. Koide, R.; Sakaguchi, S.; Miyazawa, T. Basic biological characterization of feline morbillivirus. *J Vet Med Sci* **2015**, *77*, 565-569.
38. Arikawa, K.; Wachi, A.; Imura, Y.; Sutummaporn, K.; Kai, C.; Park, E.S.; Morikawa, S.; Uematsu, Y.; Yamaguchi, T.; Furuya, T. Development of an ELISA for serological detection of feline morbillivirus infection. *Arch Virol* **2017**, *162*, 2421-2425.
39. Das, M.; Kumar, S. Recombinant phosphoprotein based single serum dilution ELISA for rapid serological detection of Newcastle disease virus. *J Virol Methods* **2015**, *225*, 64-69.
40. Dillon, P.J.; Parks, G.D. Role for the phosphoprotein P subunit of the paramyxovirus polymerase in limiting induction of host cell antiviral responses. *J Virol* **2007**, *81*, 11116-11127.

41. Donato, G.; De Luca, E.; Crisi, P.E.; Pizzurro, F.; Masucci, M.; Marcacci, M.; Cito, F.; Di Sabatino, D.; Boari, A.; D'Alterio, N., et al. Isolation and genome sequences of two Feline Morbillivirus genotype 1 strains from Italy. *Vet Ital* **2019**, *55*, 179-182.
42. Lorusso, A.; Di Tommaso, M.; Di Felice, E.; Zaccaria, G.; Luciani, A.; Marcacci, M.; Aste, G.; Boari, A.; Savini, G. First report of feline morbillivirus in Europe. *Vet Ital* **2015**, *51*, 235-237.
43. Sharp, C.R.; Nambulli, S.; Acciardo, A.S.; Rennick, L.J.; Drexler, J.F.; Rima, B.K.; Williams, T.; Duprex, W.P. Chronic Infection of Domestic Cats with Feline Morbillivirus, United States. *Emerg Infect Dis* **2016**, *22*, 760-762.
44. McCallum, K.E.; Stubbs, S.; Hope, N.; Mickleburgh, I.; Dight, D.; Tiley, L.; Williams, T.L. Detection and seroprevalence of morbillivirus and other paramyxoviruses in geriatric cats with and without evidence of azotemic chronic kidney disease. *J Vet Intern Med* **2018**, *32*, 1100-1108.
45. Sieg, M.; Vahlenkamp, A.; Baums, C.G.; Vahlenkamp, T.W. First Complete Genome Sequence of a Feline Morbillivirus Isolate from Germany. *Genome Announc* **2018**, *6*.
46. Sieg, M.; Busch, J.; Eschke, M.; Bottcher, D.; Heenemann, K.; Vahlenkamp, A.; Reinert, A.; Seeger, J.; Heilmann, R.; Scheffler, K., et al. A New Genotype of Feline Morbillivirus Infects Primary Cells of the Lung, Kidney, Brain and Peripheral Blood. *Viruses* **2019**, *11*.
47. Sakaguchi, S.; Koide, R.; Miyazawa, T. In vitro host range of feline morbillivirus. *J Vet Med Sci* **2015**, *77*, 1485-1487.
48. Khosravi, M.; Bringolf, F.; Rothlisberger, S.; Bieringer, M.; Schneider-Schaulies, J.; Zurbriggen, A.; Origgi, F.; Plattet, P. Canine Distemper Virus Fusion Activation: Critical Role of Residue E123 of CD150/SLAM. *J Virol* **2016**, *90*, 1622-1637.
49. Lin, L.T.; Richardson, C.D. The Host Cell Receptors for Measles Virus and Their Interaction with the Viral Hemagglutinin (H) Protein. *Viruses* **2016**, *8*.
50. Hahm, B.; Arbour, N.; Oldstone, M.B. Measles virus interacts with human SLAM receptor on dendritic cells to cause immunosuppression. *Virology* **2004**, *323*, 292-302.
51. Tatsuo, H.; Ono, N.; Tanaka, K.; Yanagi, Y. SLAM (CDw150) is a cellular receptor for measles virus. *Nature* **2000**, *406*, 893-897.
52. Feng, N.; Liu, Y.; Wang, J.; Xu, W.; Li, T.; Wang, T.; Wang, L.; Yu, Y.; Wang, H.; Zhao, Y., et al. Canine distemper virus isolated from a monkey efficiently replicates on Vero cells expressing non-human primate SLAM receptors but not human SLAM receptor. *BMC Vet Res* **2016**, *12*, 160.
53. Seki, F.; Ono, N.; Yamaguchi, R.; Yanagi, Y. Efficient isolation of wild strains of canine distemper virus in Vero cells expressing canine SLAM (CD150) and their adaptability to marmoset B95a cells. *J Virol* **2003**, *77*, 9943-9950.

54. Hara, Y.; Suzuki, J.; Noguchi, K.; Terada, Y.; Shimoda, H.; Mizuno, T.; Maeda, K. Function of feline signaling lymphocyte activation molecule as a receptor of canine distemper virus. *J Vet Med Sci* **2013**, *75*, 1085-1089.
55. Visser, I.K.; van der Heijden, R.W.; van de Bildt, M.W.; Kenter, M.J.; Orvell, C.; Osterhaus, A.D. Fusion protein gene nucleotide sequence similarities, shared antigenic sites and phylogenetic analysis suggest that phocid distemper virus type 2 and canine distemper virus belong to the same virus entity. *J Gen Virol* **1993**, *74 (Pt 9)*, 1989-1994.
56. Denman, A.M. Lymphocyte function and virus infections. *J Clin Pathol Suppl (R Coll Pathol)* **1979**, *13*, 39-47.
57. von Messling, V.; Milosevic, D.; Cattaneo, R. Tropism illuminated: lymphocyte-based pathways blazed by lethal morbillivirus through the host immune system. *Proc Natl Acad Sci U S A* **2004**, *101*, 14216-14221.
58. Joyce, E.; Glasner, P.; Ranganathan, S.; Swiatecka-Urban, A. Tubulointerstitial nephritis: diagnosis, treatment, and monitoring. *Pediatr Nephrol* **2017**, *32*, 577-587.
59. Brown, C.A.; Elliott, J.; Schmiedt, C.W.; Brown, S.A. Chronic Kidney Disease in Aged Cats: Clinical Features, Morphology, and Proposed Pathogeneses. *Vet Pathol* **2016**, *53*, 309-326.
60. Sutummaporn, K.; Suzuki, K.; Machida, N.; Mizutani, T.; Park, E.S.; Morikawa, S.; Furuya, T. Association of feline morbillivirus infection with defined pathological changes in cat kidney tissues. *Vet Microbiol* **2019**, *228*, 12-19.

CHAPTER 3

Three cysteines in the Mojiang virus receptor binding protein stalk domain modulate tetrameric stability and membrane fusogenicity.

3.1 Abstract

Mojiang virus (MojV) is a recently identified rat-borne virus classified in the Henipavirus genus within the Paramyxoviridae family, a genus that typically comprises bat-borne viruses. The receptor binding protein (RBP) G binds to a host cell receptor and triggers the fusion glycoprotein (F) to undergo a conformational cascade that results in viral entry into cells and cell-cell fusion, a typical pathognomonic feature of paramyxoviral infections. MojV G appears to be relatively distinct from other henipaviral G proteins, sharing only ~20% amino acid identity. To investigate their roles, we mutated the three cysteine residues within the MojV G stalk domain (C141, C143, and C188) into serines. We discovered these cysteine residues are important for maintaining a stronger than typical henipaviral tetrameric structure, modulating membrane fusogenicity, and F protein avidity. Notably, some of the MojV G serine mutants were capable of functionally and structurally interacting with the deadly henipaviral Nipah virus (NiV) F. Also, removing the MojV G cysteine residues increased, rather than decreased, fusogenicity, the typical phenotype observed for other henipaviral G glycoproteins. The functional interactions of MojV and NiV glycoproteins confirm the placement of MojV in the Henipaviridae genus and highlight novel and highly diverse aspects of oligomerization and membrane fusion mechanisms amongst the henipaviruses.

3.2 Importance

The *Henipavirus* genus includes highly virulent pathogens, such as Nipah (NiV) and Hendra (HeV) viruses, which can have a major global impact in veterinary and medical health. The recent discovery of ~20 new henipaviruses highlights their

importance. Henipaviral entry is coordinated by the interactions between the receptor binding (G) and fusion (F) glycoproteins. Mojiang virus (MojV) was discovered in 2012 after being circumstantially associated with three human deaths caused by a respiratory illness. We found that MojV G displays a stronger tetrameric structure than NiV G, and that a MojV G cysteine cluster in the stalk domain has significant effects on maintaining oligomeric structure, protein expression, interactions with F, and modulation of membrane fusion. Interestingly, despite sequence differences, mutant MojV G proteins were able to functionally interact with NiV F, confirming placement of MojV as a henipavirus, and highlighting an interesting conservation and unique aspects of henipaviral membrane fusion.

3.3 Introduction

Paramyxoviral entry into a host cell is mediated through a pH-independent process whereby the viral lipid envelope fuses with the host cell membrane. Two viral surface glycoproteins promote viral attachment and membrane fusion, the tetrameric receptor binding protein (RBP) and the trimeric fusion protein (F) (4, 5). Henipaviral F proteins are class I viral fusion proteins characterized by having N-terminal trimeric α-helical coiled-coils (6). F is synthesized as an inactivated precursor (F_0), transported to the cell surface, and subsequently endocytosed (7) and thus activated through proteolytic cleavage, generating the heterodimer F_1 and F_2 (8, 9). The paramyxoviral RBPs are termed either hemagglutinin-neuraminidase (HN), hemagglutinin (H), or glycoprotein (G) (5). HNs (e.g. for mumps virus, avian paramyxovirus-1, and parainfluenza viruses 1 to 5 (PIV 1-5)) bind to sialic acid-containing receptors. The H and G proteins (e.g. for morbilliviruses and henipaviruses, respectively) recognize

proteinaceous cell surface receptors (2, 10-12). G is a homotetramer made up of dimer-of-dimers (13), and a type II transmembrane protein composed of cytoplasmic tail, transmembrane, stalk, and globular head domains from N- to C-terminus. Binding of paramyxoviral RBPs to their host cell receptor induces conformational changes in the RBP that leads to F triggering (14-18), which harpoons F into the host cell membrane, leading to membrane fusion. Once viral infection occurs, the host cell expresses the RBP and F glycoproteins on its membrane, which will trigger fusion with neighboring naïve receptor-expressing cells to form syncytia (cell-cell fusion) (19).

Although the overall genome structure is similar to other henipaviruses, MojV G has several unique characteristics compared to other henipaviral G proteins. First, the amino acid identity between MojV G and other henipaviral G proteins is only ~20%, lower than among other henipaviral G proteins (Table 1). Second, MojV G has four putative N-glycosylation sites located in the stalk and head domain's C-terminal extension (CTE), while other henipaviral G proteins have more N-glycosylation sites in their globular heads (20). Lastly, while other henipaviral G proteins use conserved ephrin receptors such as A2, A5, B1, B2, and/or B3, the MojV G host cell receptor(s) remain unknown in spite of previous extensive investigations (2, 21-24).

We and others have shown that the paramyxoviral attachment protein stalk domain is important for triggering the F protein (9, 10, 25-27). For example, mutations in the MeV H stalk domain significantly reduced fusion and altered F-G avidity (28), and the henipaviral G stalk domain is important for G expression, oligomerization, F-G interactions, and membrane fusogenicity (13, 26, 29). Henipaviruses have three

cysteine residues in the stalk domain, important for the formation of disulfide-linked dimers and tetramers. We found that the cysteine-disrupted NiV G mutants do not induce NiV F-triggering and represent fusion-dead phenotypes (13). The MojV G stalk domain has a cluster of three cysteine residues (C141, C143, and C188) with unknown functions. To study the roles of these cysteines, we mutated each cysteine individually to serines, and investigated the cell-cell fusion and viral entry mechanisms of MojV G when co-expressed with MojV F and NiV F. We determined that the cysteines are involved in many important roles, including G oligomeric structure, protein expression/stability, interactions with F, viral entry, and cell-cell fusion modulation, which differed from the functions of the cysteins for the NiV G stalk (13). The heterologous combination of the MojV G cysteine mutants with NiV F showed complementarity between the two henipaviral glycoproteins, suggesting that MojV G shares functionally conserved, but also distinct cell-cell fusion mechnism compared with other henipaviral G proteins.

3.4 Materials and Methods

3.4.1 Cell line, expression plasmids, and mutagenesis

HEK293T cells (ATCC, Manassas, VA) were cultured in Dulbecco's modified Eagle's medium (DMEM) supplemented with 10% fetal bovine serum (FBS), 1% HEPES, and 1% Pen/Strep at 37 °C and 5% CO2. MojV G (GenBank YP_009094095.1) and MojV F (GenBank YP_009094094.1) nucleotide sequences were codon optimized and synthesized by Biomatik. The genes were subcloned into the pcDNA3.1+ and PCAGGS backbone vectors. MojV G was tagged at its C terminus with a hemagglutinin (HA) tag (YPYDVPDYA). For MojV F F1 band

detection, a C-terminal AU1 tag was inserted (DTYRYI). The MojV F extracellular 1X FLAG tag (DYKDDDDK) was inserted at the C-terminal F2 region after residue S102 by Gibson assembly with primer pairs of MojV F- F (5'-GAATAATGTGAAGAGCGATTACAAGGATGACGACGATAAGGGCAATAAT AAG-3') and MojV F-R (5'-CTTATTATTGCCCTTATCGTCGTCATCCTTGTAA TCGCTCTTCACATTATTC-3'), and pCDNA-F (5'-CATCACGAGATTTCGATT CCAC-3' and pCDNA-R (5'-GTGGAATCGAAATCTCGTGATG-3'). We used codon-optimized NiV F and G genes with C-terminal hemagglutinin (HA) and C-terminal region of F2 FLAG tags, respectively, as previously described (33, 47). MojV G stalk cysteine residue mutations were introduced to the MojV G stalk by site-directed mutagenesis using the QuickChange II XL site-directed mutagenesis kit (Agilent Technologies, Foster City, CA), and mutations and whole gene sequences were verified through DNA sequencing.

3.4.2 SDS-PAGE and immunoblotting under reducing and nonreducing conditions

HEK293T cells were transfected at 90% confluency in 6 well plates with 3µg/well of wild-type MojV or NiV F and either wild-type MojV G or mutant plasmids at a 3:1 F/G ratio. At 18-24 hours post-transfection (hpt), cells were harvested and lysed using 1X RIPA buffer (Merck Millipore) supplemented with a cOmplete protease inhibitor tablet (Roche Applied Science, Indianapolis, IN). Cell lysate samples undergoing non-reducing SDS-PAGE conditions were loaded onto gels without further treatment. For immunoblotting, the G and F proteins were detected using rabbit anti-HA (1:2,000) and mouse anti-FLAG (1:1,000) antibodies,

respectively. Fluorescently labeled anti-rabbit Alexa Fluor 647 and goat anti-mouse Alexa Fluor 488 antibodies (Life Technologies, NY) were used as a secondary antibodies (1:2,000). The proteins were detected and quantitated using a ChemiDoc MP Imager system with Image Lab software (Bio-Rad, CA).

3.4.3 Cell-cell fusion assay

HEK293T cells were transfected with 3 µg total DNA of MojV or NiV F and MojV G wild-type/mutant plasmid at a 3:1 (F:G) ratio in 6-well plates. At 18-20 hpt, syncytial nuclei (4 or more nuclei per cell) were counted from 20 microscopic fields. Four fields were combined as one 200X field count due to the low levels of cell-cell fusion for MojV (31, 38)

3.4.4 Cell surface expression using flow cytometry

Cells were transfected as described above and harvested in FACS buffer (1% FBS in PBS). The rabbit anti-HA antibody in FACS buffer (1:1,000) was incubated with the cells for 1 hr. Cells were washed twice with FACS buffer and incubated with fluorescently labeled anti-rabbit Alexa Fluor 488 and FLAG-APC (1:2,000) for 30 minutes. Quantification of cell surface expression (CSE) was performed by flow cytometry using a Guava easyCyte8 HT (EMD Millipore, MA).

3.4.5 Co-immunoprecipitation

MojV F and/or G expression plasmids were transfected as described above at ~90% confluence. At 24 hpt, supernatant and cells were harvested using 1 mL 1X PBS per well. Cells were vortexed every 5 min and kept on ice for a total of 20 min. Cell lysates were then centrifuged at 12,500 x g for 20 min at 4°C with the supernatant kept

for downstream analysis. One half of cell lysate was used for direct SDS-PAGE analysis and the other for co-immunoprecipitation using a µMACS protein G isolation kit (Miltenyi Biotec, Auburn, CA). 30 µL µMACS protein G microbeads were mixed with 4 uL of mouse anti-FLAG antibody and kept at 4°C overnight. 34 uL of the bead/Ab mixture was added to 100 uL of cell lysate and incubated at 4°C for 2.5 hr. The mixture was added to µMACS columns and allowed to flow through completely. The columns were washed 4 times with 300 µL lysis buffer (0.025 M Tris-HCl, 0.15 M NaCl, 1.0 mM EDTA, 1% NP-40, 5% glycerol) followed by one 100 µL low salt lysis buffer wash (1% NP-40, 50 mM Tris HCl pH 8.0).

3.4.6 Statistical analysis

The statistical significances were analyzed in consultation with the Cornell Statistical Consulting Unit, and using GraphPad Prism 8 (GraphPad Software, Inc., CA). *P* values were calculated by unpaired Student *t* test and corrected by using the respective Bonferroni correction factors. The data represent averages ± standard error of the mean (SEM) from at least three independent experiments.

3.5 Results

3.5.1 Extracellular tag insertions on the MojV glycoproteins do not alter total protein expression or F maturation.

Henipaviral F glycoproteins consist of N-terminal ectodomain, transmembrane, and C-terminal cytoplasmic tail domains (6, 8, 30) (Figure 3.1.A). Previous studies have established that intracellular F_1 C-terminal tags, such as AU1, do not alter the function of the F glycoproteins (25, 31, 32). However, due to the lack of polyclonal

antisera or monoclonal antibodies to detect MojV F expression, determining how to quantitatively compare the MojV F to other functional henipaviral F glycoproteins is essential. Previous studies on related henipaviruses and morbilliviruses, where a FLAG tag sequence was inserted within the F_2 subunit near the protease cleavage site of F, determined this insertion site allows the protein's bioactivity (16, 33-35). To determine whether a tag will alter the MojV F bioactivity, we designed MojV F with either a FLAG tag located within the F_2 subunit or an intracellular AU1 tag at the C-terminus.

The well characterized henipaviral NiV F and G glycoproteins were used to compare with MojV F and G for total protein expression. HEK293T cells were harvested 18 hours hpt and Western blot analysis was conducted using the cell lysates. Both MojV F and NiV F FLAG or AU1 tagged proteins underwent protease cleavage and expressed either the F_0+F_2 or F_0+F_1, respectively, as shown in Figure 3.1.B. Interestingly, compared to the cleavage of FLAG-tagged NiV F (46% and 43%, MojV F alone and cotransfected with MojV G, respectively), lower levels of MojV F were cleaved to F_2 (12% and 11%, F alone or with G, respectively) (Fig. 3.1.B). When MojV F had a C-terminal AU1 tag, a decreased percentage of cleavage to F_1 was observed (20% and 22%, F alone and with G, respectively) as compared to NiV F (31% and 37%, F alone and with G, respectively) (Fig. 3.1.B). We then compared the fusogenicity levels of the transfected cells expressing MojV G (with HA) and MojV F (with Flag, AU1, or no tag). Syncytia levels of both of the cases were similar, suggesting the tags do not alter the function of MojV F and G glycoproteins (data not shown). Furthermore, when non-reduced MojV G yielded primarily tetramers

regardless of the presence of F, consistent to the previous findings (2). However, NiV G was mostly a dimer (Fig. 3.1.C). Altogether, these results suggest that both the MojV F and G are expressed well in host cells. Further, MojV F showed less F_1/F_2 cleavage than NiV F, and MojV G showed a higher tetramer forming propensity than NiV G.

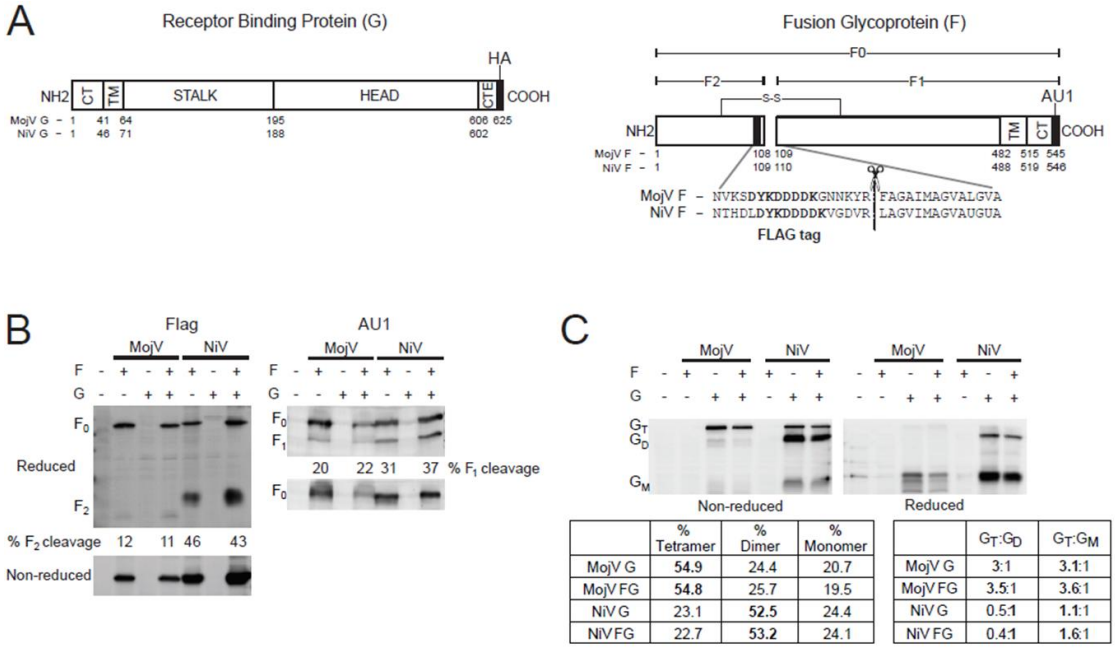

	% Tetramer	% Dimer	% Monomer
MojV G	54.9	24.4	20.7
MojV FG	54.8	25.7	19.5
NiV G	23.1	52.5	24.4
NiV FG	22.7	53.2	24.1

	$G_T:G_D$	$G_T:G_M$
MojV G	3:1	3.1:1
MojV FG	3.5:1	3.6:1
NiV G	0.5:1	1.1:1
NiV FG	0.4:1	1.6:1

Figure 3.1: Tag insertions, total protein expression levels, and oligomerization of the attachment and fusion glycoproteins.
(A) Schematic diagrams of the MojV and NiV G and F glycoproteins. For the RBPs, the HA tags were inserted at the C-terminal ends. For the Fs, the tag was inserted either in the C-terminus of the F2 region (1X FLAG tag) or at the C-terminal cytoplasmic tail (AU1 tag). The comparative sequences near the protease cleavage site are shown for MojV and NiV F proteins. Transmembrane (TM) and cytoplasmic tail (CT) domains are labelled. CTE; C-terminal extension region, present in MojV G, but not in NiV G. **(B)** Total protein expression of F in HEK293T cells in the presence of MojV F/G or NiV F/G in either reducing (top) or non-reducing (bottom) conditions. Percentage of F1 or F2 cleavage was determined by densitometry using semi-quantitative fluorescent Western blot analysis (N=4). **(C)** Total protein expression of G in HEK293T cells in the presence of MojV F or NiV F in non-reducing (upper left) and reducing (upper right) conditions. Percentage (left table) and ratio (right table) of tetramer, dimer, or monomer formation were based on densitometry. N=3. Each of the percentages were not significantly different between G when transfected alone or cotransfected with MojV or NiV F. Tetramer to dimer ($G_T:G_D$) and tetramer to

monomer (G_T:G_M) quantification for each of the glycoproteins post individual or homologous glycoprotein transfection is shown. The percentage and ratio were determined from an average of the three independent immunoblots.

3.5.2 MojV F and G induce lower cell surface expression and fusion levels than NiV F and G.

As cell-cell fusion is highly dependent on cell surface expression (CSE) of F and G glycoproteins, we then quantitatively compared cell-cell fusion (syncytia) and CSE levels for MojV and NiV F and G. To determine the CSE levels, cells were transfected with F and G expression plasmids at a 3:1 ratio. This ratio was chosen since it yielded the highest levels of fusion for both MojV and NiV (Fig. 3.2.A). After ratios between 1:300 and 300:1 were tested, cells were harvested 18 to 20 hpt. CSE levels were analyzed by flow cytometry and normalized to the levels of MojV F and G when coexpressed. When the F and G plasmids were individually transfected, there was no significant difference in the expression levels between MojV and NiV (Fig. 3.2.B). However, when F and G plasmids were cotransfected, the CSE levels for both of NiV F and G significantly increased as compared to MojV F and G. To measure fusogenicity, cells were transfected and observed at similar conditions and times as described above. Cells with 4 or more nuclei were designated as syncytia as previously described (36-38). As shown in Fig. 3.2.C, cells transfected with MojV F and G had less syncytia than those transfected with NiV F and G. To quantitatively compare the fusogenicity of MojV and NiV, we determined their fusion indices. The fusion and CSE values were normalized to those of NiV F and G, set to 1. When F and G plasmids were transfected at a total of 3 ug/well of a 6-well plate, the fusion indices

of MojV calculated using the CSE of F or G were 0.01 and 0.02, respectively as compared to NiV (Fig. 3.2.C). This means MojV had less the 5% of the fusogenic level of NiV. To further corroborate this result, we repeated the experiments with ten times lower total DNA for NiV F and G (0.3 ug), while keeping the level of MojV plasmids at 3 ug/well. MojV F and G still had less the 5% of the fusogenic level of NiV, although MojV F and G CSE levels were approximately 3X higher than those of NiV F and G (Fig. 3.2.D). Altogether, our data suggested that MojV F and G are significantly hypofusogenic compared to those of NiV.

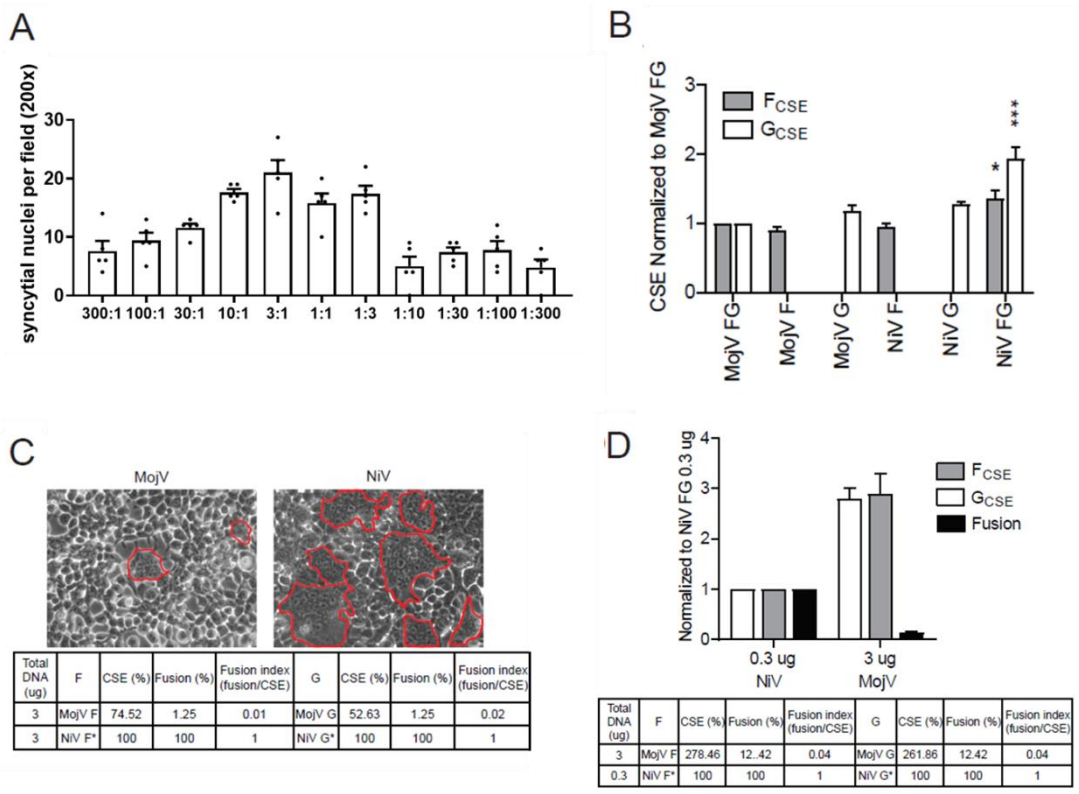

Total DNA (ug)	F	CSE (%)	Fusion (%)	Fusion index (fusion/CSE)	G	CSE (%)	Fusion (%)	Fusion index (fusion/CSE)
3	MojV F	74.52	1.25	0.01	MojV G	52.63	1.25	0.02
3	NiV F*	100	100	1	NiV G*	100	100	1

Total DNA (ug)	F	CSE (%)	Fusion (%)	Fusion index (fusion/CSE)	G	CSE (%)	Fusion (%)	Fusion index (fusion/CSE)
3	MojV F	278.46	12..42	0.04	MojV G	261.86	12.42	0.04
0.3	NiV F*	100	100	1	NiV G*	100	100	1

Figure 3.2: MojV glycoproteins are less fusogenic than NiV.
(A) Syncytia counting of multinuclei HEK293T cells after transfecting MojV F and G plasmids at ratios between 300:1 and 1:300 (F:G). The plasmids were transfected at a total of 3 ug per well of 6-well plates. **(B)** CSE of the wild-type MojV F and G glycoproteins was quantified through flow cytometry using anti-HA and anti-FLAG tag antibodies. Data were corrected for background with empty vector backbone alone and normalized with co-expressed MojV F and G. The data represented averages ±

SEM from six biological repeats. *, $p<0.05$; ***, $p<0.001$. **(C)** HEK293T were transfected with MojV or NiV F and G. Red lines highlight syncytia from microscopic field at 200X. Fusion indicies were determined for each condition (fusion/CSE). **(D)** CSE and fusion indicies of co-expressed MojV F and G (3 ug) was normalized with those of co-expressed NiV F and G (0.3 ug).

3.5.3 The three cysteines in the MojV G stalk domain are involved in the oligomerization, expression, and host cell fusogenicity.

Multiple studies reported the importance of the paramyxoviral G stalk domains for viral entry, integrity, and expression of G glycoproteins, F/G interaction, F-triggering, and host cell fusogenicity during the membrane fusion process (25, 27, 28, 33, 39-41). The cysteine residues within the G stalk domain have been determined to be important for disulfide-linked dimer formation for the paramyxoviruses (13, 26, 42, 43). Based on previous studies, we hypothesized that the three cysteines in the MojV G stalk domain, C141, C143, and C188, influence oligomerization and membrane fusion (Fig. 3.3.A). To cause minimal secondary effects to the protein structure, we mutated the three cysteins to serines individually (C141S, C143S, and C188S) or in combination as double (C141S/C143S, C141S/C188S, and C143S/C188S) or triple (C141S/C143S/C188S) mutants, to determine their synergistic roles. Each mutant was transfected into HEK293T cells with its homologous wild-type MojV F. We observed syncytia from all the mutants as well as the wild-type MojV G after co-expressing with MojV F (data not shown). Western blot and CSE analyses of MojV F showed no significant differences between samples, suggesting that MojV F is not affected by the MojV G stalk cysteins (Fig. 3.3.B and 3.3.C). However, MojV G mutants showed different oligomerization patterns from wild-type MojV G (Fig. 3.3.B). While wild-

type MojV G displayed a high tetramer forming propensity in a non-reducing gel, both the C141S and C143S mutants were mostly dimers, and the C141S/C143S mutant showed mostly monomers. These results suggest that C141 and C143 are critical for mediating covalent dimerization, and each individually affect the tetramerization of MojV G. While the mutants with C188S (C188S, C141S/C188S, C143S/C188S, and C141S/C143S/C188S) had tetramer forming propensity, their CSE and total protein expression levels were significantly reduced compared to wild-type G and other mutants (Fig. 3.3.B and 3.3.C). This suggests that C188 is involved in the expression of MojV G, but not in its oligomerization propensity, potentially maintaining protein stability to refrain from protein recycling. A potential explanation for this phenotype is that the C188 residue is directly upstream to a putative N-glycosylation site, and the mutation from cysteine to serine in the residue preceding the NXS/T motif could be an important determinant of glycosylation efficiency (44). Most importantly, mutant C141S showed cell-cell fusion levels above wild-type MojV G levels besides having wild-type CSE levels (fusion index = 1.48), and the C188S mutants had fusion indexes between 2.54 – 3.67, despite their low CSE levels. Overall, our results indicate that the MojV G stalk cysteines play important roles in protein expression, oligomerization, and membrane fusion.

3.5.4 Wild-type or mutant MojV and NiV glycoproteins functionally complement.

Due to the low amino acid identity between MojV G and other henipaviral G proteins, we sought to determine whether the surface glycoproteins of MojV and NiV may complement functionally. Homologous and heterologous combinations of MojV

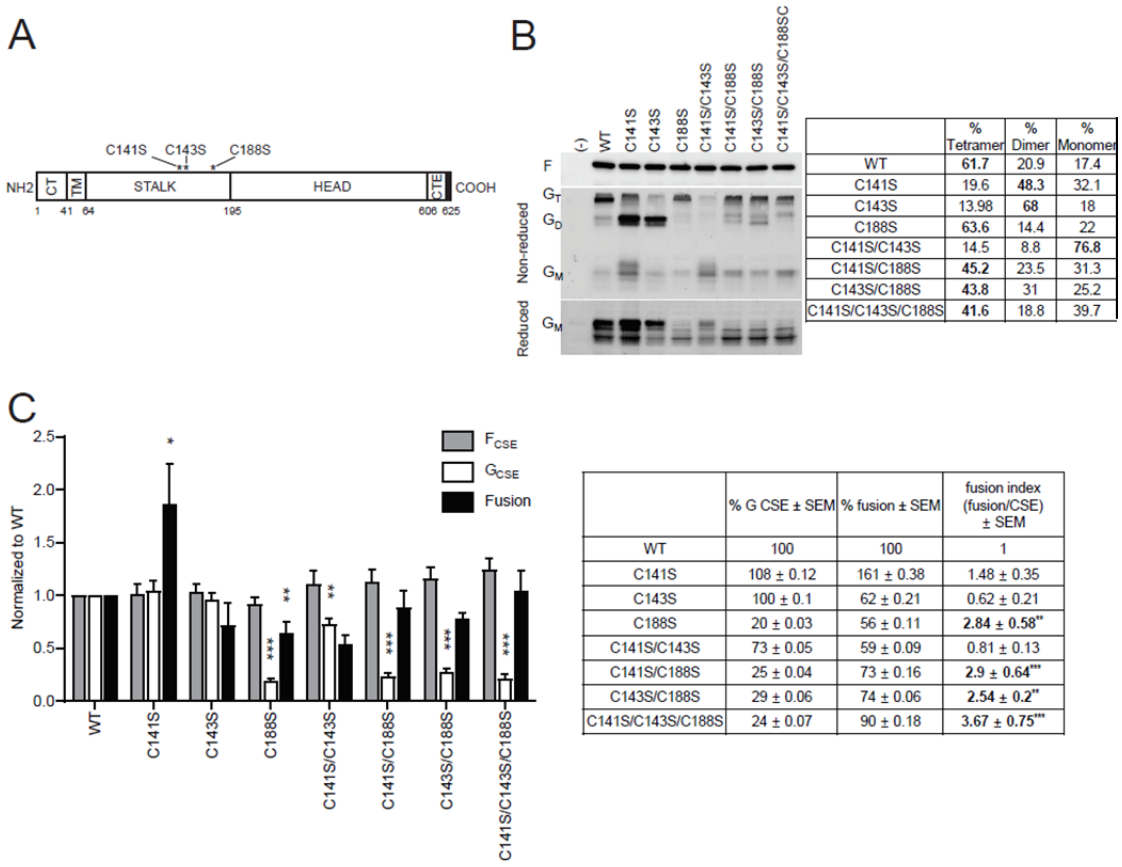

	% Tetramer	% Dimer	% Monomer
WT	**61.7**	20.9	17.4
C141S	19.6	**48.3**	32.1
C143S	13.98	**68**	18
C188S	**63.6**	14.4	22
C141S/C143S	14.5	8.8	**76.8**
C141S/C188S	**45.2**	23.5	31.3
C143S/C188S	**43.8**	31	25.2
C141S/C143S/C188S	**41.6**	18.8	39.7

	% G CSE ± SEM	% fusion ± SEM	fusion index (fusion/CSE) ± SEM
WT	100	100	1
C141S	108 ± 0.12	161 ± 0.38	1.48 ± 0.35
C143S	100 ± 0.1	62 ± 0.21	0.62 ± 0.21
C188S	20 ± 0.03	56 ± 0.11	**2.84 ± 0.58****
C141S/C143S	73 ± 0.05	59 ± 0.09	0.81 ± 0.13
C141S/C188S	25 ± 0.04	73 ± 0.16	**2.9 ± 0.64*****
C143S/C188S	29 ± 0.06	74 ± 0.06	**2.54 ± 0.2****
C141S/C143S/C188S	24 ± 0.07	90 ± 0.18	**3.67 ± 0.75*****

Figure 3.3: MojV G stalk domain cysteine mutants express well and alter fusogenicity. **(A)** Schematic of MojV G glycoprotein. Asterisks indicate the locations of the C141S, C143S, and C188S mutations within the stalk domain. **(B)** Western blot analysis of MojV G cysteine mutants. HEK293T cell lysates were harvested at 18-20 hpt and separated using 10% SDS-PAGE gel under non-reducing (top) or reducing (bottom) conditions. Anti-HA antibodies detected the MojV G glycoproteins. G_T=tetramer, G_D=dimer, G_M=monomer. Table indicates quantified tetramer, dimer, and monomer structures as percentages of the total G signals (G_T+G_D+G_M). **(C)** Cell surface expression (CSE) of MojV F and G (wild-type or serine mutants) determined by flow cytometry and normalized to either wild-type MojV F or G (F_{CSE} and G_{CSE}, respectively). Nuclei inside syncytia formed by MojV F and G (wild-type or C to S mutants) were counted and normalized to the fusion levels of the cells transfected with wild-type MojV F and G (Fusion). Fusion indexes (fusion/CSE) were normalized to those of wild-type MojV G. The data represents averages ± SEM from four a minimum of four biological replicates. *, $p<0.05$; **, $p<0.01$; ***, $p<0.001$.

and NiV G and F were coexpressed in HEK293T cells. Notably, both heterologous combinations of proteins were fusogenic, and the heterologous combinations with

mutant MojV G proteins were fusogenic with similar patterns when co-transfecting with NiV F as when co-transfecting with MojV F, indicating functional complementary for all heterologous combinations (data not shown). As expected, Western blot analysis showed similar results for oligomerization of wild-type and mutant MojV G (Fig. 3.4.A). These results further support the notion that MojV is a member of the genus *Henipavirus* genus, since its glycoproteins are able to functionally complement those of NiV.

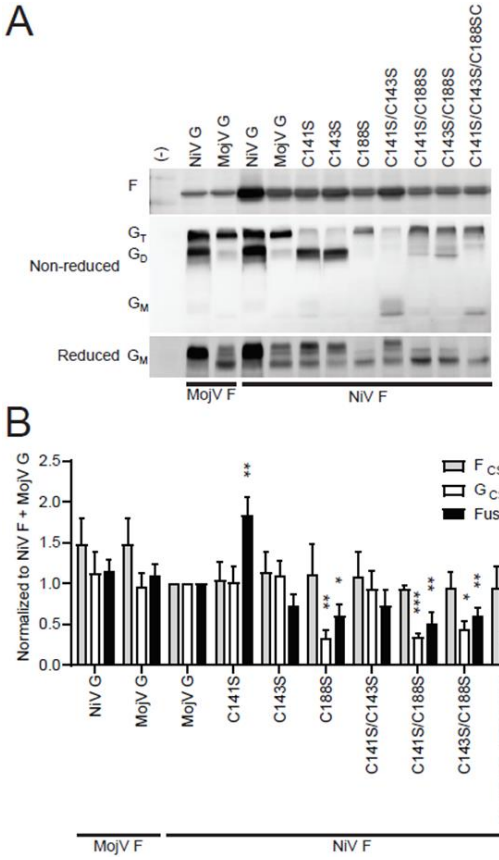

		% Tetramer	% Dimer	% Monomer
MojV F	NiV G	44.8	**48.4**	6.8
	MojV G	**60.5**	38.1	1.4
NiV F	NiV G	40.8	**53.4**	5.8
	MojV G	**67.1**	26.9	6.0
	C141S	16.3	**73.4**	10.3
	C143S	12.9	**81.6**	5.5
	C188S	**71.4**	9.4	19.2
	C141S/C143S	15.1	8.1	**76.8**
	C141S/C188S	**48.7**	21.3	30.0
	C143S/C188S	**45.0**	30.1	24.9
	C141S/C143S/C188S	**54.6**	4.5	40.9

		% G CSE ± SEM	% Fusion ± SEM	fusion index (fusion/CSE) ± SEM
MojV F	MojV G	102.5 ± 0.03	100.4 ± 0.14	1.0 ± 0.13
	NiV G	107.4 ± 0.06	113.8 ± 0.14	1.1 ± 0.13
NiV F	MojV G	100.0	100.0	1.0
	C141S	95.3 ± 0.05	173.6 ± 0.23	**1.8 ± 0.24****
	C143S	95.9 ± 0.08	73.6 ± 0.14	0.8 ± 0.14
	C188S	20.2 ± 0.03	57.5 ± 0.13	**2.8 ± 0.65***
	C141S/C143S	79.3 ± 0.08	67.8 ± 0.19	0.9 ± 0.24
	C141S/C188S	25.4 ± 0.02	47.1 ± 0.14	**1.9 ± 0.55***
	C143S/C188S	31.7 ± 0.03	59.8 ± 0.09	**1.9 ± 0.27***
	C141S/C143S/C188S	29.4 ± 0.04	50.6 ± 0.19	1.7 ± 0.63

Figure 3.4: Heterologous henipavirus glycoproteins are capable of complemeting MojV in the promotion of fusion.
(A) NiV F and MojV G (wild-type or serine mutants) were cotransfected into HEK293T cells and harvested at 18-20 hpt in preparation for Western blot analysis under non-reducing (middle) or reducing (bottom) conditions, and ran in a 10% SDS-PAGE gel. The table contains quantified tetramer, dimer, and monomer structures values, shown as percentages. **(B)** Cell surface expression (CSE) of HEK293T cells

cotransfected with NiV F and MojV G (wild-type or serine mutants) (F_{CSE} and G_{CSE}, respectively) and Fusion values for NiV F and MojV G samples. All values were normalized to NiV F (F_{CSE}), MojV G (G_{CSE}), or NiV F and MojV G (Fusion) and fusion index was determined for each cotransfection as in Fig. 3. The data represents averages ± SEM from at least three biological repeats. *, $p<0.05$; **, $p<0.01$; ***, $p<0.001$.

3.5.5 MojV G stalk cysteine mutants interact with F and alter F/G avidities.

To determine whether the MojV G stalk mutants affect the ability of G and F to interact, we performed co-immunoprecipitation (co-IP) assays using cell lysates of HEK293T cells cotransfected with MojV G and either of MojV F or NiV F. Affinity purification was against the F FLAG tag, therefore, only the HA-tagged G that is directly associated with F was co-IP'd. The F and G proteins were detected from cell lysates or the immunoprecipitated (IP) fractions through immunoblotting using anti-FLAG and HA antibodies, respectively (Fig. 3.5.A). We normalized the densitometric values for each of the serine mutants to the values for wild-type MojV F and G, set to 1. The avidities (strengths) of all F and G interactions were measured as $G_{IP}/(G_{lys} \times F_{IP})$, to account for the amount of G IP'd, but also for the amounts of F effectively IP'd, and the amounts of G in the cell lysates (31-33, 38). We observed that the hyperfusogenic C188S mutants have 5 to 12 times increased F/G avidities with their homologous F proteins (Fig. 3.5.B). Notably, Fig. 3.5.D and 3.5.E showed similar trends for the heterologous glycoprotein interactions, and with NiV F, the avidity levels of the C188S mutants increased up to 30-50 times, even higher than the levels between MojV F and G. C188 is located near the C-terminal end of the MojV G stalk domain, thus we posit that C188 may modulate F/G interactions so that the two glycoproteins do not interact too tightly, thus C188S may increase F/G interactions.

This suggests that this region in the C-terminal end of the stalk domain is important for modulating both G/F interactions and fusogenicity. Henipaviruses, including NiV and HeV, have been proposed to follow a “dissociation” or “clamp model” (45). Briefly, in these models the F and G glycoproteins bind to each other prior to receptor binding, upon which F-triggering and F/G dissociation occurs. The reported inverse correlations between F/G binding avidities and fusogenicity provide evidence for the dissociation model for the henipaviruses (33, 38). However, surprisingly we observed a positive correlation between fusogenicity and the avidities of F/G interactions for both homologous and heterologous MojV G mutants and MojV or NiV F combinations (Fig. 3.5.C and 3.5.F). These results suggest that MojV F and G do not follow a dissociation model, and that this aspect of F/G interactions in the fusion cascade is different between MojV and NiV.

3.6 Discussion

The MojV sequence was first obtained from mine rats in 2012 (1). Previous studies reported cell-cell fusion events for MojV in a variety of cells, including human and rodent cell lines, with syncytial levels being visually lower compared to other established henipaviruses. However, no studies had quantified such syntycia levels accounting for CSE levels of the glycoproteins, and comparing them to the better characterized NiV or HeV. In addition, MojV G and F are suggested to undergo the fusion cascade kinetically slower (46). Here, we delved into the function of the MojV G stalk domain cysteine residues and their influence on oligomerization and on the fusion cascade when interacting with their homologous MojV F or the related

heterologous NiV F glycoproteins.

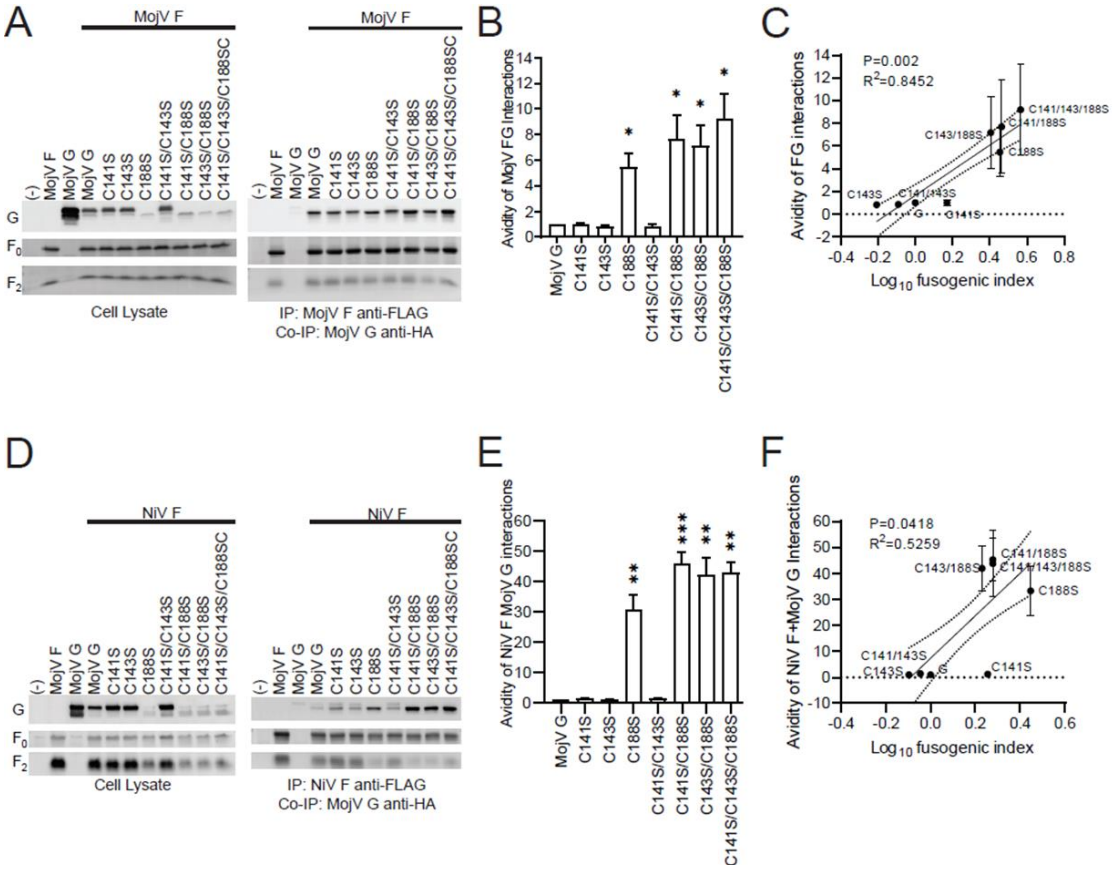

Figure 3.5: MojV G cysteine mutants alter avidities of F and G interactions.
(A) Representative immunoblot image of MojV F and G interactions, determined by immunoprecipitation of MojV F using protein G microbeads against the FLAG tag, and co-immunoprecipitation of MojV G. HEK293T cells cotransfected with MojV F and G and cell lysates were harvested at 24 hpt. **(B)** F/G interaction avidity values were determined by densitometry, normalized to the value of wild-type MojV F/G, and measured using the Biorad ImageLab software. **(C)** Representatitve image of Pierson correlation between fusogenicity and MojV G and F interaction avidities determined via co-immunoprecipitation. **(D)** Representative immunoblot image of MojV G and NiV F interactions using the same method as A, but NiV F was used instead of MojV F. **(E)** F/G interaction avidity values were determined and measured by the same method as B. The values were normalized to the NiV F/MojV G avidity level. **(F)** Correlation graph between fusogenicity and MojV G and NiV F interaction avidities determined via co-immunoprecipitation.

To aid quantitative analysis, we inserted a FLAG tag into the F2 domain of MojV F and an HA tag at the C-terminus of MojV G, since we had successfully shown these tags did not affect NiV glycoproteins functionally (33). Both MojV G and F were determined to be structurally and functionally stable and expressed well. MojV G maintained its strong tetrameric structure while NiV showed its majority of dimers as previously established (Figs. 3.1.B and 3.1.C) (2, 13). This suggests that MojV G monomers may be in a lower movement environment in the tetrameric structure. This is important since the cysteine residues within the henipaviral stalk domains are known to play roles in bringing together the monomers to form dimers of dimers, and these G tetrameric interactions are known to affect interactions with the F glycoproteins, and the fusion cascade (13, 31, 36).

We also discovered the levels of cleavage for MojV F were lower as compared to NiV F, suggesting the amount of mature, kinetically active F may contribute to the decrease in fusion events for MojV. CSE levels for MojV F and G were somewhat decreased as compared to those of NiV F and G when the glycoproteins were co-expressed, but not when expressed individually. Lower cell surface expression levels have been associated with decreased cell-cell fusion events (6, 25). Interestingly, when both NiV G and F were co-expressed, the levels of each glycoprotein increased as compared to when individually expressed. However, there was no significant difference in the levels of MojV G and F between individual and co-expression (Fig. 3.2.A). A possible explanation for this observation may be that NiV and MojV glycoprotein transport mechanisms may differ. Ghana virus (GhV) G was suggested to undergo a delayed release from the endoplasmic reticulum as compared to NiV G

(31). Similarly studies may reveal similar trends for MojV.

MojV G has 3 cysteine residues on its stalk domain (C141, C143, and C188) (Fig. 3.3.A) (13, 43, 46). We discovered that a serine substitution that removes the C188 leads to a significant drop in MojV G protein expression (Figs. 3.3.B and 3.3.D). The C188 residue is near the C-terminal end of the stalk domain, and a residue upstream a putative N-glycosylation site, beginning at residue N189. Mutating this site from a cysteine to serine may have altered the glycosylation efficiency, proper folding of MojV G, and potentially its transport to the cell surface. Studies focusing on the putative MojV N-glycosylation sites have not been reported and are needed to observe whether this N-glycosylation site is used and affects protein expression and transport. As for the C141S mutation, it led to a significant increase in cell-cell fusion levels without affecting the glycoproteins' CSE levels (Fig. 3.3.D). This suggests the C141 plays a role in inhibiting cell-cell fusion in wild-type MojV G. Interestingly, this phenomenon is unique to MojV and has not been observed for other henipaviral G proteins (13, 31). In addition, both the C141 and C143 residues were involved in G tetrameric strength, as when mutated to serine residues, showed lower tetrameric and higher dimeric propensity. This dimeric propensity is relatively more similar to that observed from NiV G (2, 13). Therefore, we suggest that the wild-type MojV G stalk domain cysteine residues may contribute to excessive stalk domain tetrameric rigidity, sub-optimal for fusion promotion, whereas the relatively looser NiV-G tetrameric structure, with higher dimeric propensity, may be more prone to fusion promotion.

We next delved into determining the strength of the interactions between the MojV G and F glycoproteins, and determined that while these interactions for C141S

and C143S were unaffected, those for the C188S mutants had a significantly increase, suggesting a previously unexposed potential contact point between G and F (Fig. 3.5.A and 3.5.B). Interesting, as similar trend was observed with NiV F, but with even higher levels of F/G interaction avidities (Fig. 3.5.D and 3.5.E). These results suggest that the MojV G stalk domain influences the level of its interaction with. Further, we observed a positive correlation between the avidity of MojV G/F interactions and fusogenicity, which suggests a unique and distinct method of interaction for MojV glycoproteins and how they modulate the membrane fusion process, which needs to be further investigated.

When the MojV G serine mutants were co-expressed with the heterologous NiV F, we observed similar results as when co-expressed with the homologous MojV F, suggesting an ability for cross-talk between the two glycoproteins across the two viruses. Since MojV G and F have low sequence conservation, our data suggest structural conservation, with further studies needed to confirm this. However, our results more comfortably place MojV in the henipavirus genus, which has been debated. Further studies are also needed to understand the pathogenicity of MojV, to identify the MojV G receptor(s), to determine the G and F structures, and the role of the CTE region in the MojV G globular head.

3.7 References

1. Wu Z, Yang L, Yang F, Ren X, Jiang J, Dong J, Sun L, Zhu Y, Zhou H, Jin Q. 2014. Novel Henipa-like virus, Mojiang Paramyxovirus, in rats, China, 2012. Emerg Infect Dis 20:1064-6.
2. Rissanen I, Ahmed AA, Azarm K, Beaty S, Hong P, Nambulli S, Duprex WP, Lee B, Bowden TA. 2017. Idiosyncratic Mòjiāng virus attachment glycoprotein directs a host-cell entry pathway distinct from genetically related henipaviruses. Nat Commun 8:16060.
3. Drexler JF, Corman VM, Müller MA, Maganga GD, Vallo P, Binger T, Gloza-Rausch F, Cottontail VM, Rasche A, Yordanov S, Seebens A, Knörnschild M, Oppong S, Adu Sarkodie Y, Pongombo C, Lukashev AN, Schmidt-Chanasit J, Stöcker A, Carneiro AJ, Erbar S, Maisner A, Fronhoffs F, Buettner R, Kalko EK, Kruppa T, Franke CR, Kallies R, Yandoko ER, Herrler G, Reusken C, Hassanin A, Krüger DH, Matthee S, Ulrich RG, Leroy EM, Drosten C. 2012. Bats host major mammalian paramyxoviruses. Nat Commun 3:796.
4. Azarm KD, Lee B. 2020. Differential Features of Fusion Activation within the Paramyxoviridae. Viruses 12:161.
5. Aggarwal M, Plemper RK. 2020. Structural Insight into Paramyxovirus and Pneumovirus Entry Inhibition. Viruses 12:342.
6. White JM, Delos SE, Brecher M, Schornberg K. 2008. Structures and mechanisms of viral membrane fusion proteins: multiple variations on a common theme. Critical reviews in biochemistry and molecular biology 43:189-219.
7. Dutch RE. 2010. Entry and fusion of emerging paramyxoviruses. PLoS Pathog 6:e1000881.
8. Diederich S, Moll M, Klenk H-D, Maisner A. 2005. The Nipah Virus Fusion Protein Is Cleaved within the Endosomal Compartment. Journal of Biological Chemistry 280:29899-29903.
9. Iorio RM, Melanson VR, Mahon PJ. 2009. Glycoprotein interactions in paramyxovirus fusion. Future Virol 4:335-351.
10. Bose S, Song AS, Jardetzky TS, Lamb RA. 2014. Fusion activation through attachment protein stalk domains indicates a conserved core mechanism of paramyxovirus entry into cells. J Virol 88:3925-41.
11. Aguilar HC, Ataman ZA, Aspericueta V, Fang AQ, Stroud M, Negrete OA, Kammerer RA, Lee B. 2009. A novel receptor-induced activation site in the Nipah virus attachment glycoprotein (G) involved in triggering the fusion glycoprotein (F). J Biol Chem 284:1628-35.
12. Takimoto T, Taylor GL, Connaris HC, Crennell SJ, Portner A. 2002. Role of the Hemagglutinin-Neuraminidase Protein in the Mechanism of Paramyxovirus-Cell Membrane Fusion. Journal of Virology 76:13028-13033.
13. Maar D, Harmon B, Chu D, Schulz B, Aguilar HC, Lee B, Negrete OA. 2012. Cysteines in the Stalk of the Nipah Virus G Glycoprotein Are

Located in a Distinct Subdomain Critical for Fusion Activation. Journal of Virology 86:6632-6642.
14. Deng R, Wang Z, Mahon PJ, Marinello M, Mirza A, Iorio RM. 1999. Mutations in the Newcastle disease virus hemagglutinin-neuraminidase protein that interfere with its ability to interact with the homologous F protein in the promotion of fusion. Virology 253:43-54.
15. Bose S, Zokarkar A, Welch BD, Leser GP, Jardetzky TS, Lamb RA. 2012. Fusion activation by a headless parainfluenza virus 5 hemagglutinin-neuraminidase stalk suggests a modular mechanism for triggering. Proc Natl Acad Sci U S A 109:E2625-34.
16. Ader N, Brindley MA, Avila M, Origgi FC, Langedijk JP, Örvell C, Vandevelde M, Zurbriggen A, Plemper RK, Plattet P. 2012. Structural rearrangements of the central region of the morbillivirus attachment protein stalk domain trigger F protein refolding for membrane fusion. J Biol Chem 287:16324-34.
17. Navaratnarajah CK, Negi S, Braun W, Cattaneo R. 2012. Membrane fusion triggering: three modules with different structure and function in the upper half of the measles virus attachment protein stalk. J Biol Chem 287:38543-51.
18. Navaratnarajah CK, Oezguen N, Rupp L, Kay L, Leonard VH, Braun W, Cattaneo R. 2011. The heads of the measles virus attachment protein move to transmit the fusion-triggering signal. Nat Struct Mol Biol 18:128-34.
19. Aguilar HC, Henderson BA, Zamora JL, Johnston GP. 2016. Paramyxovirus Glycoproteins and the Membrane Fusion Process. Curr Clin Microbiol Rep 3:142-154.
20. Ortega V, Stone JA, Contreras EM, Iorio RM, Aguilar HC. 2019. Addicted to sugar: roles of glycans in the order Mononegavirales. Glycobiology 29:2-21.
21. Zeltina A, Bowden TA, Lee B. 2016. Emerging Paramyxoviruses: Receptor Tropism and Zoonotic Potential. PLOS Pathogens 12:e1005390.
22. Negrete OA, Levroney EL, Aguilar HC, Bertolotti-Ciarlet A, Nazarian R, Tajyar S, Lee B. 2005. EphrinB2 is the entry receptor for Nipah virus, an emergent deadly paramyxovirus. Nature 436:401-5.
23. Laing ED, Navaratnarajah CK, Cheliout Da Silva S, Petzing SR, Xu Y, Sterling SL, Marsh GA, Wang L-F, Amaya M, Nikolov DB, Cattaneo R, Broder CC, Xu K. 2019. Structural and functional analyses reveal promiscuous and species specific use of ephrin receptors by Cedar virus. Proceedings of the National Academy of Sciences 116:20707-20715.
24. Pryce R, Azarm K, Rissanen I, Harlos K, Bowden TA, Lee B. 2019. A key region of molecular specificity orchestrates unique ephrin-B1 utilization by Cedar virus. Life science alliance 3:e201900578.
25. Liu Q, Stone JA, Bradel-Tretheway B, Dabundo J, Benavides Montano JA, Santos-Montanez J, Biering SB, Nicola AV, Iorio RM, Lu X, Aguilar HC. 2013. Unraveling a three-step spatiotemporal mechanism of

triggering of receptor-induced Nipah virus fusion and cell entry. PLoS pathogens 9:e1003770-e1003770.
26. Brindley MA, Takeda M, Plattet P, Plemper RK. 2012. Triggering the measles virus membrane fusion machinery. Proc Natl Acad Sci U S A 109:E3018-27.
27. Melanson VR, Iorio RM. 2004. Amino Acid Substitutions in the F-Specific Domain in the Stalk of the Newcastle Disease Virus HN Protein Modulate Fusion and Interfere with Its Interaction with the F Protein. Journal of Virology 78:13053-13061.
28. Corey EA, Iorio RM. 2007. Mutations in the stalk of the measles virus hemagglutinin protein decrease fusion but do not interfere with virus-specific interaction with the homologous fusion protein. J Virol 81:9900-10.
29. Liu Q, Bradel-Tretheway B, Monreal AI, Saludes JP, Lu X, Nicola AV, Aguilar HC. 2015. Nipah virus attachment glycoprotein stalk C-terminal region links receptor binding to fusion triggering. J Virol 89:1838-50.
30. Diederich S, Sauerhering L, Weis M, Altmeppen H, Schaschke N, Reinheckel T, Erbar S, Maisner A. 2012. Activation of the Nipah virus fusion protein in MDCK cells is mediated by cathepsin B within the endosome-recycling compartment. J Virol 86:3736-45.
31. Bradel-Tretheway BG, Liu Q, Stone JA, McInally S, Aguilar HC. 2015. Novel Functions of Hendra Virus G N-Glycans and Comparisons to Nipah Virus. Journal of Virology 89:7235-7247.
32. Aguilar HC, Matreyek KA, Choi DY, Filone CM, Young S, Lee B. 2007. Polybasic KKR motif in the cytoplasmic tail of Nipah virus fusion protein modulates membrane fusion by inside-out signaling. J Virol 81:4520-32.
33. Bradel-Tretheway BG, Zamora JLR, Stone JA, Liu Q, Li J, Aguilar HC. 2019. Nipah and Hendra Virus Glycoproteins Induce Comparable Homologous but Distinct Heterologous Fusion Phenotypes. J Virol 93.
34. Avila M, Alves L, Khosravi M, Ader-Ebert N, Origgi F, Schneider-Schaulies J, Zurbriggen A, Plemper RK, Plattet P. 2014. Molecular Determinants Defining the Triggering Range of Prefusion F Complexes of Canine Distemper Virus. Journal of Virology 88:2951-2966.
35. Avila M, Khosravi M, Alves L, Ader-Ebert N, Bringolf F, Zurbriggen A, Plemper RK, Plattet P. 2015. Canine Distemper Virus Envelope Protein Interactions Modulated by Hydrophobic Residues in the Fusion Protein Globular Head. Journal of Virology 89:1445-1451.
36. Biering SB, Huang A, Vu AT, Robinson LR, Bradel-Tretheway B, Choi E, Lee B, Aguilar HC. 2012. N-Glycans on the Nipah virus attachment glycoprotein modulate fusion and viral entry as they protect against antibody neutralization. Journal of virology 86:11991-12002.
37. Aguilar HC, Matreyek KA, Choi DY, Filone CM, Young S, Lee B. 2007. Polybasic KKR Motif in the Cytoplasmic Tail of Nipah Virus Fusion Protein Modulates Membrane Fusion by Inside-Out Signaling. Journal of Virology 81:4520-4532.

38. Aguilar HC, Matreyek KA, Filone CM, Hashimi ST, Levroney EL, Negrete OA, Bertolotti-Ciarlet A, Choi DY, McHardy I, Fulcher JA, Su SV, Wolf MC, Kohatsu L, Baum LG, Lee B. 2006. N-Glycans on Nipah Virus Fusion Protein Protect against Neutralization but Reduce Membrane Fusion and Viral Entry. Journal of Virology 80:4878-4889.
39. Lee JK, Prussia A, Paal T, White LK, Snyder JP, Plemper RK. 2008. Functional Interaction between Paramyxovirus Fusion and Attachment Proteins. Journal of Biological Chemistry 283:16561-16572.
40. Melanson VR, Iorio RM. 2006. Addition of N-Glycans in the Stalk of the Newcastle Disease Virus HN Protein Blocks Its Interaction with the F Protein and Prevents Fusion. Journal of Virology 80:623-633.
41. Talekar A, Moscona A, Porotto M. 2013. Measles virus fusion machinery activated by sialic acid binding globular domain. J Virol 87:13619-27.
42. Yuan P, Swanson KA, Leser GP, Paterson RG, Lamb RA, Jardetzky TS. 2011. Structure of the Newcastle disease virus hemagglutinin-neuraminidase (HN) ectodomain reveals a four-helix bundle stalk. Proceedings of the National Academy of Sciences 108:14920-14925.
43. Behner L, Zimmermann L, Ringel M, Weis M, Maisner A. 2018. Formation of high-order oligomers is required for functional bioactivity of an African bat henipavirus surface glycoprotein. Veterinary Microbiology 218:90-97.
44. Bañó-Polo M, Baldin F, Tamborero S, Marti-Renom MA, Mingarro I. 2011. N-glycosylation efficiency is determined by the distance to the C-terminus and the amino acid preceding an Asn-Ser-Thr sequon. Protein Sci 20:179-86.
45. Aguilar HC, Henderson BA, Zamora JL, Johnston GP. 2016. Paramyxovirus Glycoproteins and the Membrane Fusion Process. Current clinical microbiology reports 3:142-154.
46. Cheliout Da Silva S, Yan L, Dang HV, Xu K, Epstein JH, Veesler D, Broder CC. 2021. Functional Analysis of the Fusion and Attachment Glycoproteins of Mojiang Henipavirus. Viruses 13:517.
47. Levroney EL, Aguilar HC, Fulcher JA, Kohatsu L, Pace KE, Pang M, Gurney KB, Baum LG, Lee B. 2005. Novel innate immune functions for galectin-1: galectin-1 inhibits cell fusion by Nipah virus envelope glycoproteins and augments dendritic cell secretion of proinflammatory cytokines. J Immunol 175:413-20.
48. Madeira F, Park YM, Lee J, Buso N, Gur T, Madhusoodanan N, Basutkar P, Tivey ARN, Potter SC, Finn RD, Lopez R. 2019. The EMBL-EBI search and sequence analysis tools APIs in 2019. Nucleic acids research 47:W636-W641.

CHAPTER 4

N-glycans on the Mojiang virus fusion (F) modulate membrane fusogenicity and viral entry

4.1 Abstract

Mojiang virus (MojV) is a novel rat-borne virus identified in China in 2012, classified in the *Henipavirus* genus within the *Paramyxoviridae* family. The receptor-binding protein (G) triggers the fusion glycoprotein (F) to undergo a conformational cascade that results in cell-cell fusion and viral entry into cells. N-glycosylation occurs at Asp residues in NXS/T sites and is used by many pathogens to evade host immune responses. Prior studies showed that several of the N-glycans of henipaviral G and F modulate host cell-cell fusion and viral entry. We sought to determine if N-glycans of the MojV F and G glycoproteins play similar roles to those of other henipaviral glycoproteins. Here we found that MojV is significantly less N-glycosylated than other henipaviruses since two out of four and at least one out of four potential N-glycosylation sites were glycosylated on MojV F and G, respectively. We found that MojV F N-glycan deficient mutants affected proteolytic F cleavage, cell-cell fusion, and viral entry levels. In contrast to other henipaviruses, the N-glycan in the MojV G did not affect cell-cell fusion and viral entry, and only one MojV F N-glycan modulated host cell fusogenicity. Alignment of N-glycan positions between henipaviral G proteins indicated that the N-glycosylation site on MojV G is not conserved with others. Our results highlight the diverse roles of N-glycans in the mechanism of membrane fusion and viral entry amongst henipaviruses.

4.2 Importance

N-glycosylation is an important protein modification process in host cells, that is utilized by pathogens to invade host cells and to evading host immune responses. Different from bat-originated henipaviruses, MojV is a rodent-originated novel

henipavirus. We found that both of the two surface glycoproteins of MojV, F and G, are far less N-glycosylated than those of other henipaviruses. By constructing N-glycan deficient mutants, we determined that MojV F and G have only two and at least one actually utilized N-glycosylation sites, respectively. Our data suggested that the N-glycans on MojV F are involved in many roles such as proteolytic F cleavage, F/G interaction, and viral entry. On the other hand, the N-glycan on MojV G did not significantly modulate cell-cell fusion and viral entry mechanisms, suggesting that its N-glycosylation only plays minor roles. Furthermore, the N-glycosylation site of MojV G was not aligned with those of other henipaviral G proteins. Our study suggests that N-glycans affect at a wide range of cell-cell fusion and viral entry and they are not always conserved among henipaviruses.

4.3 Introduction

Paramyxovirus membrane fusion is induced by intricate interaction between the two surface glycoproteins, the fusion (F) and the receptor-binding protein (RBP, designated as G for the genus *Henipavirus*). The tetrameric G protein binds to its host cell receptor and triggers a conformational change of the F protein. In the process of structural reorganization of F protein from metastable pre-fusion to post-fusion state, the membranes of virus and a host cell are pulled in and eventually fused (viral-cell fusion). The viral genetic materials enter into the host cell via created fusion pore. Additionally, an infected host cell expresses the F and G glycoproteins on the cell surface which can trigger membrane fusion with nearby naïve cells (cell-cell fusion) (3, 4). This induces formation of multinuclei cells called syncytia, as the fusion cascade continues.

Glycosylation is an important protein modification process in a host cell, involving many cellular functions such as intracellular trafficking, cell-cell signaling, protein folding, and receptor binding (5). This process is critical to host cells, but it is also utilized by pathogens for invading host cells and evading detection from the host immune system. N-glycosylation, one of the main protein glycan modifications, occurs when N-acetylglucosamine (GlcNAc) binds to Asp (N) residues in the conserved NXS/T motifs (5). It has been shown that many paramyxoviruses such as Nipah (NiV), Hendra (HeV), Sendai (SeV) and canine distemper virus (CDV) take advantage of N-glycans for proteolytic processing, protein folding and trafficking (8-13). Furthermore, N-glycans on the paramyxoviral F and RBP glycoproteins are also known to be important for cell-cell fusion and viral entry (5, 7, 9-12, 15, 32). For example, previous studies showed that some of the N-glycan-deficient NiV G head mutants showed increased fusogenic capabilities, but the mutants represented fusion-dead phenotype when the N-glycans were eliminated from NiV G stalk domain (7-9). Also, NiV and HeV F glycoproteins altered fusion level when some of the N-glycans were lost (7, 9). Additionally, the previous study in our lab firstly reported that O-glycosylation, another glycosylation process occurring at S/T residues, also modulates fusogenicity, F/G avidities, and viral entry capabilities of NiV and HeV G glycoproteins (14).

To understand the roles of N-glycans on the MojV F and G glycoproteins, we bioinformatically predicted N-glycosylated sites on the two surface glycoproteins and constructed each of the N-glycan deficient mutants by switching N to Q from NXS/T motif. We discovered that two sites are N-glycosylated on MojV F, and they are

involved in many roles such as proteolytic F cleavage, cell fusogenicity, F/G interaction, and viral entry level. We also found that there is at least one actual N-glycosylation site on MojV G but it has no significant impact. The structural comparison of the N-glycosylation sites between henipaviral G proteins indicated that the sole N-glycan on MojV G is not conserved with any of the sites on other henipaviral G proteins. This study highlights that the degree of N-glycan usage is various amongst henipaviruses in cell-cell fusion and viral entry.

4.4 Material and Methods

4.4.1 Expression plasmids and mutagenesis

The codon-optimized MojV G (GenBank YP_009094095.1) and MojV F (GenBank YP_009094094.1) nucleotide sequences were synthesized by Biomatik and subcloned into the PCAGGS and pcDNA3.1+ backbone vectors, respectively. MojV G was tagged at its C terminus with a hemagglutinin (HA) tag (YPYDVPDYA). MojV F was tagged at its C-terminal F2 region with a 1X FLAG tag (DYKDDDDK). N-glycosylation sites of MojV F and G were predicted based on the NetNGlyc 1.0 server (30). N to Q mutations were introduced by site-directed mutagenesis using the QuickChange II XL site-directed mutagenesis kit (Agilent Technologies, Foster City, CA) at amino acid positions 61 (G1), 64 (G2), 189 (G3), and 619 (G4) in the MojV G glycoprotein, and at the positions 69 (F1), 283 (F2), 463 (F3), and 484 (F4) in the MojV F glycoprotein. The mutations and constructs were verified through DNA sequencing.

4.4.2 Cell culture

Human Embryonic Kidney (HEK) 293T and BSR-T7 cell lines were cultured with Dulbecco's modified Eagle's medium (DMEM) supplemented with 10% fetal bovine serum (FBS), 1% HEPES, and 1% Pen/Strep at 37 °C and 5% CO_2.

4.4.3 Reducing and non-reducing SDS-PAGE and immunoblotting

HEK293T and BSR-T7 cells were transfected in 6-well plates with 3 ug total DNA of either wild type or N-glycan deficient mutant MojV F and G plasmids at 3:1 (F:G) ratio. At 20-22 hpt, cells were collected and lysed using 100 ul 1X RIPA buffer (Merck Millipore). Cell lysates or MojV pseudotyped virions undergoing non-reducing SDS-PAGE conditions were loaded onto 10% gels without further treatment. The reducing samples were treated with ß-mercaptoethanol and denatured for 8 mins at 95°C, and were loaded onto 12% gels. The MojV F and G proteins were detected using mouse anti-FLAG (1:1,000) and rabbit anti-HA (1:1,000) antibodies, respectively. Fluorescently labeled anti-rabbit Alexa Fluor 488 and goat anti-mouse Alexa Fluor 647 antibodies (Life Technologies, NY) were used as secondary antibodies (1:2,000). The proteins were detected and quantified using a ChemiDoc MP Imager system with Image Lab software (Bio-Rad, CA).

4.4.4 PNGaseF, Endo H, and Tunicamycin treatment

HEK293T cell lysates collected as described above were further treated with either PNGaseF or Endo H to remove N-glycans. PNGaseF (New England Biolabs [NEB], Inc., Ipswich, MA) was incubated with cell lysates as described in the previous paper (7). Endo H (NEB) was treated to cell lysates according to the manufacturer's protocol and incubated overnight at 37°C. Additionally, to inhibit N-glycosylation

process, 1 ug/ml tunicamycin (Research Products Internationals [RPI], Corp., Mount Prospect, IL) was treated when cells were transfected with MojV F and G plasmids. All cell lysates were reduced and immunoblotted as mentioned above.

4.4.5 Cell surface expression using flow cytometry

HEK293T and BSR-T7 cells were transfected as described above and collected in FACS buffer (1% FBS in PBS) in 20-22 hpt. Cells were also transfected with an empty pcDNA3.1+ as a negative control. The rabbit anti-HA antibody in FACS buffer (1:1,000) was incubated with the cells for 1 hour on ice. Cells were washed twice with FACS buffer and incubated with fluorescently labeled anti-rabbit Alexa Fluor 488 and FLAG-APC (1:2,000) for 30 minutes on ice. Cells were washed twice as before. Cell surface expression analysis was performed by flow cytometry (Guava easyCyte8 HT; EMD Millipore, MA).

4.4.6 Cell-cell fusion assay

BSR-T7 cells were transfected and collected as described above. At 20-22 hpt, syncytial nuclei (4 or more nuclei per cell) were counted from 20 random microscopic fields (50X). Four fields were combined as one microscopic field (200X).

4.4.7 Co-immunoprecipitations

MojV F and G plasmids were transfected into HEK293T cells in a 6 well plate. Cell lysates were collected and lysed as described above. A half amount (50 uL) of each lysate was kept for immunoblotting and the other (50 uL) was used for co-immunoprecipitation via µMACS protein G isolation kit (Miltenyi Biotec, Auburn, CA). 4 uL of rabbit anti-FLAG antibody was added to 30 µL µMACS protein G

microbeads and incubated overnight at 4 ℃. The bead/Ab mixture was added to 50 uL of cell lysate and incubated at 4 ℃ for 2.5 h and completely flew through μMACS columns. The columns were washed 4 times with 300 μL lysis buffer (0.025 M Tris-HCl, 0.15 M NaCl, 1.0 mM EDTA, 1% NP-40, 5% Glycerol) and then washed once with 100 μL low salt lysis buffer wash (1% NP-40, 50 mM Tris HCl pH 8.0).

4.4.8 Pseudotyped MojV/VSV∆G rLuc virion synthesis, RT-qPCR, and viral entry assay.

MojV pseudotyped virions were made from the VSV-ΔG-Luc virus, as described previously (7, 15, 16). The MojV F and G wild-type/mutants plasmids were transfected to the cells at 1:3 (F:G) ratio. The cells were infected with VSVΔG rLuc at 48 hpt (1:300), and the pseudotyped virions were collected at 48 hours post-infection (hpi). Viral RNA was extracted using QIAamp Viral RNA mini kit (Qiagen, CA). VSV RNA genomes were reverse transcribed and quantified by RT-qPCR using UltraPlex 1-Step (Quantabio) with Taqman VSV Ind-1 specific probe (15, 17, 18). The VSV genome copy numbers were quantified as previously detailed (18, 19). For viral entry assay, HEK293T cells were seeded in a 96 well plate and infected with the appropriate VSV pseudotyped virions when ~50% confluent using serial virus dilutions. DMEM with 10% FBS was added at 2 hpi. At 22-24 hpi, cells were lysed and Renilla luciferase activity was measured as relative light units (RLU) using the Renilla Luciferase Assay System (Promega) and the Tecan Spark microplate reader (Tecan Group Ltd., Männedorf, Switzerland).

4.5 Results

4.5.1 Two and at least one out of the four potential N-glycosylated sites are utilized on MojV F and G, respectively.

N-glycosylation occurs at asparagine residue followed by a random amino acid residue except for proline, and either of serine or threonine sites (NXS/T) (5). MojV G has four potential N-glycosylated sites, located at Asn residues 61, 64, 189, and 619 (Fig. 4.1.A). MojV F also was predicted to have four putative N-glycosylated sites, at residues 69, 283, 463 and 484 (Fig. 4.1.B). To determine which sites that are N-glycosylated, we mutated each of the Asn to Gln and constructed N-glycan deficient mutants (G1-G4, G1G2, and G3G4 for MojV G and F1-F4 for MojV F) (Fig. 4.1.A and 4.1.B). Each of the N-glycan deficient MojV F and G mutants were co-transfected to HEK293T cells with either wild-type MojV F or G at 3:1 ratio (F:G) in total DNA of 3 ug. After 20-22 hours of post-transfection (hpt), cells were lysed and lysates were collected for measuring total protein expression using Western blot analysis. The non-reduced wild-type MojV G and its mutants mostly formed tetramers, suggesting that N-glycan(s) do not affect the oligomerization of the G protein. When reduced, only G3 represented different glycosylation pattern compared to wild-type MojV G (Fig. 4.1.C). This suggests that the G3 site, which is located at the C terminus of the MojV G stalk domain, is N-glycosylated. Interestingly, the two double mutants, G1G2 and G3G4, as well as G4 could not be detected by Western analysis (Fig. 4.1.C). This suggests that the asparagines of these sites are crucial for their protein stability or membrane trafficking. Although it is unclear if G4 is N-glycosylated due to no protein expression, the result indicated that at least one of the four putative sites is actually N-glycosylated. The Western blot results of MojV F showed that F1 and F3 migrated

further than the wild-type F protein for both of non-reduced and reduced conditions (Fig. 4.1.D). This indicates that F1 and F3 sites, located on the C terminus of the F2 and F1 region, respectively, are N-glycosylated. Additionally, all the F1 to F4 mutants showed low protein expression compared to the wild-type F protein (Fig. 4.1.D). This means that the four asparagines are involved in MojV F expression. Overall, the Western blot results of MojV F protein show that two out of the four potential N-glycosylated sites are utilized.

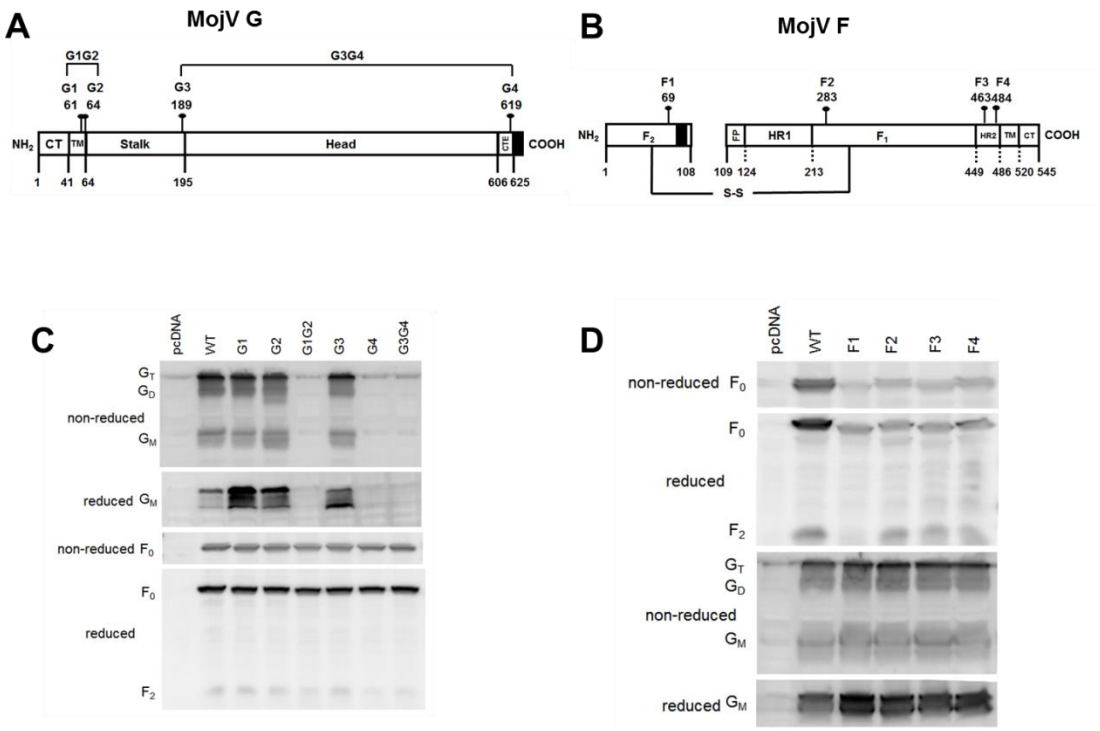

Figure 4.1: Analysis of predicted N-glycan sites on MojV G and F proteins.
(A, B) Diagrams of MojV G (A) and F (B) glycoproteins. N-glycosylation sites were predicted using NetNGlyc 1.0 Server. The black lollypop-like structures represent potential N-glycosylation sites on MojV G (G1 to G4) and MojV F (F1 to F4). **(A)** Locations of functional domains of MojV G were predicted by sequence alignment of henipaviral RBPs using Clustal Omega. CT, cytoplasmic tail; TM, transmembrane; CTE, C-terminal extension. **(B)** Locations of each domain of MojV F which are indicated as dashed lines were based on Cheliout Da Silva *et al* (12). F_1 and F_2 regions are connected by a disulfide bond. FP; fusion peptide; HR; heptad repeat. **(C)** HEK293T was co-transfected with wild-type (WT) MojV F and either wild-type

MojV G or N-glycan mutant candidates and lysed 20 to 22 hpt. Lysates were separated under non-reduced and reduced conditions and immunoblotted using rabbit anti-HA antibody and mouse anti-FLAG antibody against G and F, respectively. The top two membranes indicate Western blot results of MojV G, and the bottom two represent MojV F results. **(D)** HEK293T was co-transfected with wild-type MojV G and either wild-type MojV F or N-glycan mutant candidates. Western blot analysis was conducted similar to **(C)**. The top two membranes indicate Western blot results of MojV F, and the two bottom ones represent MojV G result.

4.5.2 The site of G3 on MojV G and those of F1, and F3 on MojV F are N-glycosylated.

To make certain that G3, F1, and F3 are N-glycan-deficient mutants, we first treated the cell lysates with Endo H (endoglycosidase H), which cleaves the bond between two N-acetylglucosamines (GlcNAc) from both high-mannose and hybrid N-glycans, but not from complex type N-glycans (5, 31). We found that Endo H-treated wild-type MojV G showed similar gel shift to Endo H-untreated G3 (Fig. 4.2.A). We also incubated cells with tunicamycin, which is an antibiotic that disrupts protein maturation by blocking N-glycosylation (33). The band migration patterns of wild-type MojV G and G3 were similar when their N-glycosylation was inhibited by tunicamycin (Fig. 4.2.A). This confirms that the different band phenotypes were induced by N-glycan deficiency of G3. Furthermore, PNGaseF (Peptide-N-glucosidase F) cleaves all N-glycans except for GlcNAc containing α 1-3 fucose (23). The different band phenotypes between wild-type G and G3 also indicated that G3 is an actual N-glycan deficient mutant (Fig. 4.2.B).

The previous Western blot result suggested the two N-glycosylated sites, F1 and F3. This means that N-glycan of F1 site was eliminated from mutant F1 but its F3 site is still N-glycosylated. Similarly, F3 is lack of its own N-glycan but F1 site still

possesses N-glycan. When treated with Endo H, almost a half of N-glycans on F1 were not cleaved (Fig. 4.2.C). This indicates that not all N-glycans were eliminated from F3 site, suggesting that F3 may be a complex type. Additionally, when treated with PNGaseF, F1 showed almost no gel shift, meaning that most of N-glycans on F1 were not eliminated (Fig. 4.2.D). As expected from Endo H treatment result, the complex type N-glycans on F3 site may be fucosylated on their α 1-3 sites (5). This may explain why there was no cleavage since PNGaseF cannot cleave α 1-3 fucose. Overall, these results suggest that G3, F1 and F3 sites are indeed N-glycosylated.

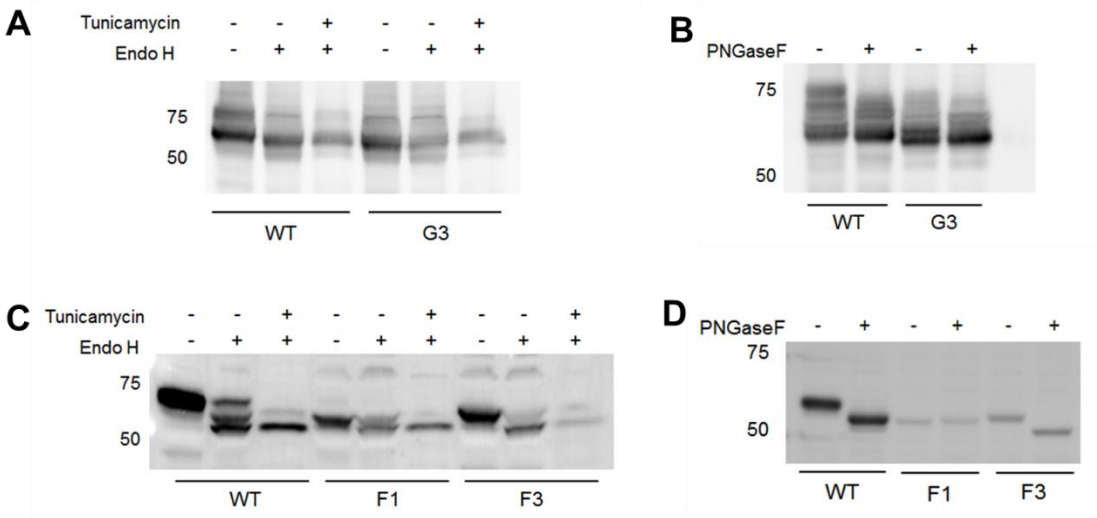

Figure 4.2: Confirming actual N-glycan-deficient MojV F and G mutants.
(A, C) Western blot analysis of MojV G **(A)** or F **(C)** with or without Endo H and tunicamycin treatment. Tunicamycin was treated to HEK293T when transfected. Endo H was incubated with HEK293T cell lysates at 37°C overnight. -, incubated without treatment; +, incubated with treatment. Numbers on the left indicate protein size (kDa). **(B, D)** Western blot results of MojV G **(B)** or F **(D)** with or without PNGaseF treatment. PNGaseF was treated to cell lysates similar to Endo H.

4.5.3 The N-glycans on MojV F are involved in many functions in cell-cell fusion.

Next, we sought to determine if the N-glycosylation of the MojV F and G

glycoproteins affect cell-cell fusion and viral entry mechanisms. The wild-type MojV F or N-glycan deficient mutants, F1 and F3, were co-transfected with wild-type MojV G to HEK293T (simply labeled as F1 and F3). The wild-type MojV G or the mutant G3 were co-expressed with wild-type MojV F (simply labeled as G3). The syncytial cells were observed from all the cases, showing that all of the mutants are functionally competent (data not shown). However, unfortunately, it was not easy to obtain robust data of the number of syncytial nuclei using HEK293T due to the slow fusion kinetics and low fusion levels of MojV F and G (21). Instead, we decided to use hamster kidney cell-derived BSR-T7 considering that MojV is rodent-originated. We observed clearer and higher level of syncytia from BSR-T7 when transfected both the cell lines under the same condition. Also, there was no difference in the protein bands' phenotypes from Western blot results using both cell lines (compare Fig. 4.1.C and 4.1.D with Fig. 4.3.A).

Interestingly, Western blot results consistently showed that intensity of F2 band of the mutant F1 was lower than those of others (Fig. 4.3.A). This suggests that N-glycans on the F1 site affect proteolytic F cleavage. We then counted number of nuclei from syncytial cells and tested if N-glycosylation modulates fusogenic capability of MojV F and G. We observed that the fusion level of F3 was significantly increased (Fig. 4.3.B). The cell surface expression (CSE) levels of both the F1 and F3 were also significantly reduced than that of wild-type MojV F (Fig. 4.3.C). We quantified fusion level of each mutant by calculating fusion index. Briefly, both the CSE and fusion levels were converted to percentage and normalized to the levels of wild-type MojV F and G, which were both set to 1. The fusion index of F3 was

approximately five times higher than that of wild-type MojV F, indicating that it confers hyperfusogenic capability (Fig. 4.3.C). Altogether, the results suggest that the N-glycosylation on F1 site (located in F_2 region) is involved in proteolytic F cleavage and that on F3 site (located in F_1 region) modulates fusogenicity. On the other hand, the phenotypes between wild-type MojV G and G3 were similar, suggesting that N-glycan(s) on MojV G does not significantly affect cell-cell fusion.

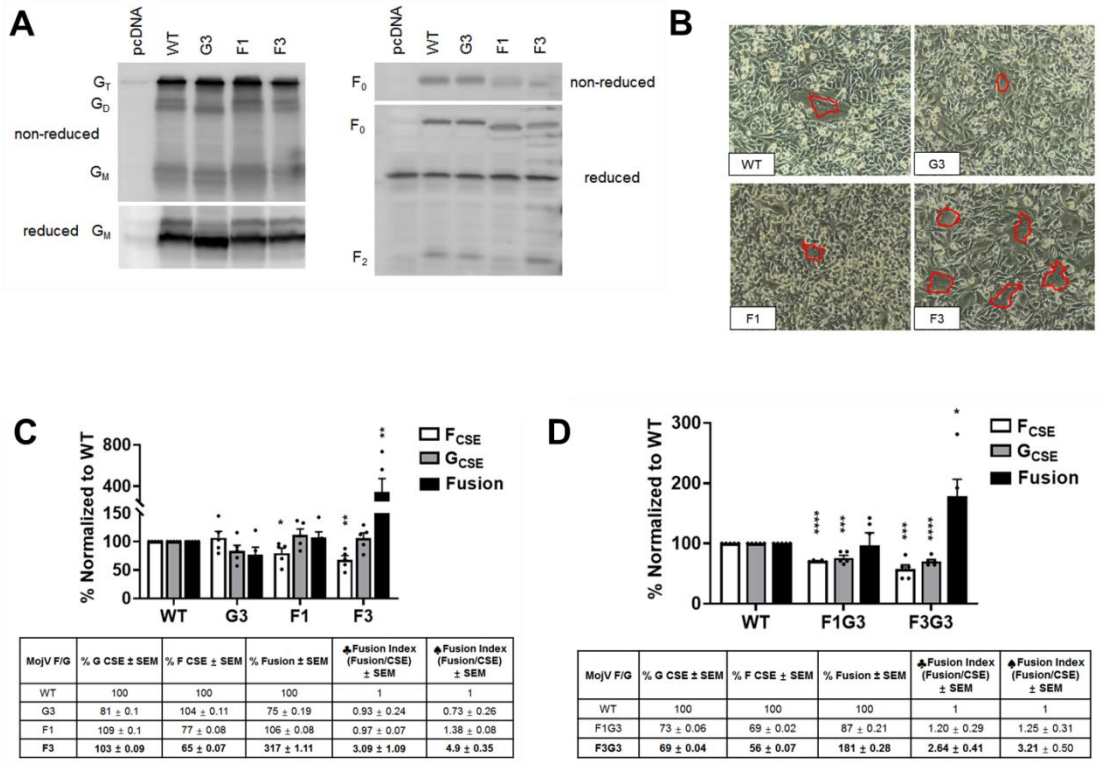

MojV F/G	% G CSE ± SEM	% F CSE ± SEM	% Fusion ± SEM	♣Fusion Index (Fusion/CSE) ± SEM	♠Fusion Index (Fusion/CSE) ± SEM
WT	100	100	100	1	1
G3	81 ± 0.1	104 ± 0.11	75 ± 0.19	0.93 ± 0.24	0.73 ± 0.26
F1	109 ± 0.1	77 ± 0.08	106 ± 0.08	0.97 ± 0.07	1.38 ± 0.08
F3	103 ± 0.09	65 ± 0.07	317 ± 1.11	3.09 ± 1.09	4.9 ± 0.35

MojV F/G	% G CSE ± SEM	% F CSE ± SEM	% Fusion ± SEM	♣Fusion Index (Fusion/CSE) ± SEM	♠Fusion Index (Fusion/CSE) ± SEM
WT	100	100	100	1	1
F1G3	73 ± 0.06	69 ± 0.02	87 ± 0.21	1.20 ± 0.29	1.25 ± 0.31
F3G3	69 ± 0.04	56 ± 0.07	181 ± 0.28	2.64 ± 0.41	3.21 ± 0.50

Figure 4.3: The N-glycans on MojV F alter CSE and fusogenicity levels.
(A) MojV F and G proteins were detected from BSR-T7 cell lysates by Western blot analysis. **(B)** Syncytial nuclei were observed at 200X. Red lines highlight each syncytial field. **(C)** Cell surface expression (CSE) and fusion levels of MojV F and G proteins. The CSE levels of MojV F and G were quantified by flow cytometry using anti-mouse FLAG-APC antibodies and rabbit anti-HA, respectively. The CSE levels were normalized to wild-type MojV F (F_{CSE}) and G (G_{CSE}). Syncytial nuclei were counted at 20-22 hpi and normalized to fusion level of wild-type MojV F and G (indicated as Fusion). ♣ and ♠ indicate fusion levels divided by G CSE or F CSE, respectively. The data represented averages ± standard errors of the means (SEM) from five independent biological repeats. *, $p<0.05$; **, $p<0.01$. **(D)** Normalized

values of CSE and fusion levels of combined N-glycan mutants. ***, $p<0.001$; ****, $p<0.0001$.

To investigate if there is any synergistic effect between the N-glycans on MojV F and G, we co-expressed F1 and G3 (labeled as F1G3), or F3 and G3 (labeled as F3G3) as combined mutants. The Western blot results were similar between the combined and single mutants, meaning that there is no significant difference in total protein expression levels for both cases (data not shown). F3 was still hyperfusogenic when co-expressed with G3, but its fusion index was reduced by almost 50% comparing to that of F3 as a single mutant (Fig. 4.3.D). This suggests that the F and G glycoproteins become less able to induce cell-cell fusion when N-glycans are eliminated from both of them.

4.5.4 N-glycans modulate avidity between MojV F and G.

Next, we investigated if the N-glycans on MojV F and G proteins affect F/G interactions by co-immunoprecipitation (co-IP) assays using HEK293T cell lysates after co-expressing MojV F and G. Since affinity purification was conducted against the FLAG tag-attached MojV F, only the HA-tagged MojV G that binds to F was co-immunoprecipitated. The F and G proteins were detected from cell lysates (Fig. 4.4.A, left) and the immunoprecipitated (IP) fractions through immunoblotting (Fig. 4.4.A, right) using anti-FLAG and anti-HA antibodies, respectively. To quantify each of the MojV F and G avidity levels, we measured densitometry of each band and normalized it to the values for the wild-type F and G proteins, which are set to 1. The avidity levels were calculated following the fomula $G_{IP}/(G_{lys} \text{ X } F_{IP})$ based on the previous papers (15, 17). We found that the avidity levels of both F1 and F3 were increased by twice than those of wild-type F and G, and those of F1G3 and F3G3 were even higher

than others (Fig. 4.4.B). This suggests that F/G interaction gets stronger when N-glycans are eliminated. On the other hand, the F/G avidity levels between wild-type MojV F and either wild-type G or G3 showed no significant difference (Fig. 4.4.B).

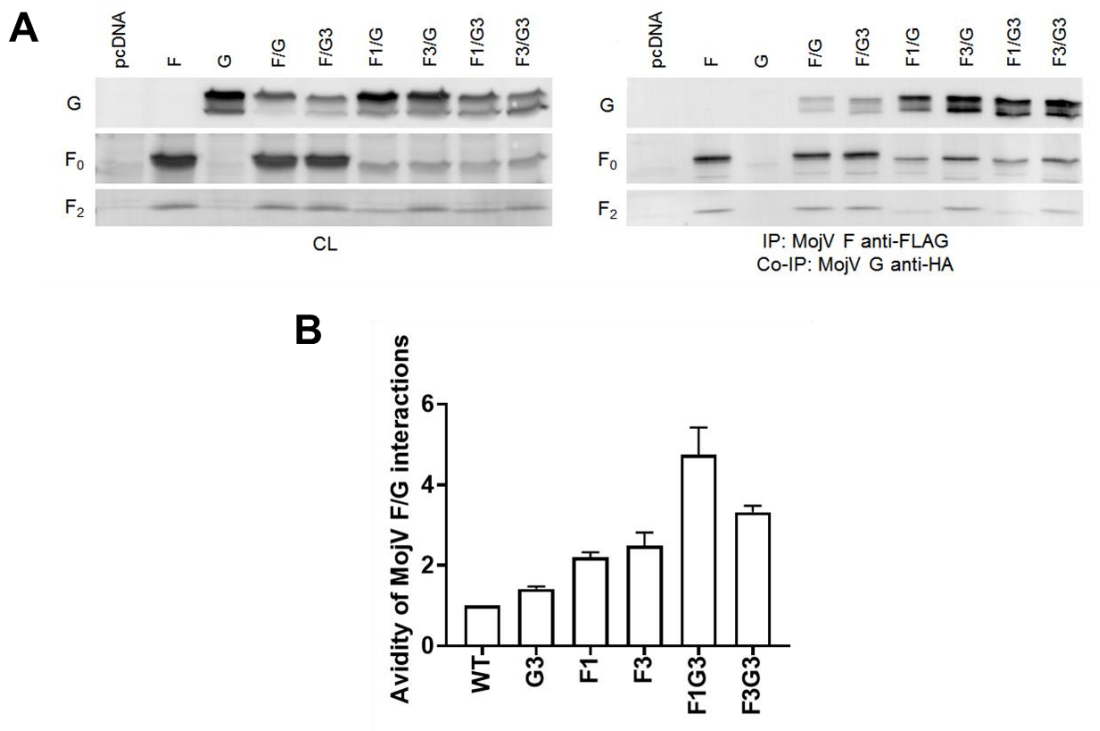

Figure 4.4: N-glycans on MojV F affect F/G interaction.
(A) Representing immunoblot images of MojV F and G interactions. The wild-type MojV F and G or mutants were detected from HEK293T cell lysates (CL, left). MojV F was immunoprecipitated (IP) and MojV G was co-immunoprecipitated (co-IP) using anti-FLAG and anti-HA antibodies, respectively (right). **(B)** Avidity values were analyzed by densitometry using the Biorad ImageLab software. Each values were normalized to the value of co-expressed wild-type F and G (WT), which is set to 1. The data indicate the average ± SEM from five biological repeats.

However, in spite of little influence of N-glycosylation on MojV G in F/G avidity, the combined mutants showed significantly increased F/G affinity levels compared to others (Fig. 4.4.B). This suggests that there may be synergistic impact between N-

glycans on the F and G glycoproteins. Additionally, it was previously reported that henipaviral F and G proteins such as NiV and HeV F and G follow dissociation model (3). In this model, the two proteins bind and interact to each other prior to receptor binding. Previous studies demonstrated that there is a negative correlation between fusogenic index and F/G avidity from this model (8, 17). However, we could not find any correlations from MojV F and G proteins, suggesting that they may not follow dissociation model (data not shown). Overall, the results suggest that N-glycans on MojV F synergistically interact with that of MojV G and modulate F/G interaction levels in a proper range so they do not interact too tightly.

4.5.5 N-glycans of MojV F affect viral entry.

Viral entry (viral-cell membrane fusion) and cell-cell membrane fusion mechanisms have been suggested to have a correlation (25). To investigate whether N-glycans on the MojV F and G proteins are involved in both membrane fusion mechanisms, we used our previously established VSV pseudotyped viral entry assay (7, 15, 18). Either wild-type MojV F or G with the mutants were pseudotyped onto the membrane of vesicular stomatitis virus (VSV) which contains the *Renilla* luciferase reporter gene instead of its own glycoprotein (VSV-ΔG-rLuc). As a negative control, VSV that is pseudotyped only with wild-type MojV G (labeled as MojV G in figure 4.5.B) was constructed to exclude any nonspecific entry (15, 17). To accurately compare viral entry levels, we conducted quantitative reverse transcription PCR and measured viral genome copy numbers. The values were then normalized to have an equal amount of virions for viral entry measurement.

The Western blot results of the pseudotyped indicate that the F and G

glycoproteins were well incorporated onto the VSV membranes (Fig. 4.5.A). As expected, viral entry level of wild-type MojV F and G (labeled as MojV FG in figure 4.5.B) were higher than that of MojV G, confirming that the pseudotyped VSV induced viral entry via virus-cell membrane fusion mechanism. The viral entry level of G3 was similar to that of wild-type MojV FG, suggesting that N-glycosylation of MojV G does not significantly modulate viral entry (Fig. 4.5.B). However, F1 and F3 showed more than ten times increased entry level compared to MojV FG (Fig. 4.5.B). We additionally tried to harvest VSV pseudoparticles of F1G3 and F3G3 to investigate if there is any synergistic effect between N-glycans on F and G proteins. However, the cells were consistently detached after VSV infection, suggesting that eliminating N-glycans from both the glycoproteins may induce toxicity (data not shown). Overall, the results suggest that the N-glycans on MojV F greatly modulate viral entry into host cells.

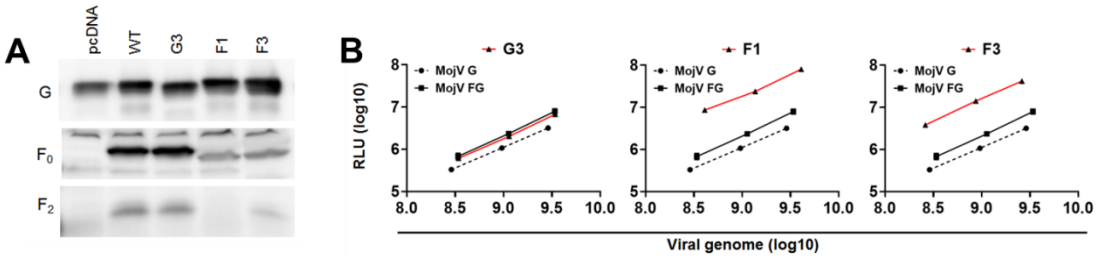

Figure 4.5: N-glycans on MojV F affect viral entry.
(A) Western blot analysis of MojV F and G that are incorporated onto VSV pseudotyped virions in reduced condition. **(B)** Relative entry levels of VSV-rluc virions pseudotyped with designated wild-type MojV F and G or mutants. HEK293T was transfected and lysed 22-24 hours post-infection (hpi). Relative Light Units (RLU) were quantified and plotted against the number of viral genomes/ul. Each dots represents the mean value of three biological repeats.

4.6 Discussion

N-glycosylation is a commonly occurring protein modification process in host cells and it is also utilized by pathogens for viral entry and avoiding host immune reactions. We found that MojV G has at least one N-glycosylated site, G3, on the stalk domain (Fig. 4.1.C). There is an additional Asp residue that is located in the CTE region of the head domain. Our result showed that it is critical for the G expression. So far, the function of CTE is unknown. As one of the possibilities, the CTE region may need to be cleaved in an endosomal compartment before MojV G is expressed onto host cell membrane. Disrupting the Asp may inhibit proper protein cleavage and affect surface expression of MojV G. Another double mutant G1G2 also showed no expression although both single mutants, G1 and G2, were expressed well (Fig. 4.1.C). This suggests that the two Asp residues on both sites are critical and at least one of them is required for G protein expression. Due to an absence of the crystal structure of MojV G stalk, the location of each domain was merely predicted by amino acid alignment with other henipaviruses. Therefore, the G1 and G2 may be located on either of N terminus of the stalk or C terminus of the transmembrane domains. Revealing the crystal structure of the entire MojV G protein will be necessary to clarify this.

MojV F has two actual N-glycosylation sites, one is on F2 and the other is on F1 region (Fig. 4.1.B). F3, which is located on the C terminus of F1 region, showed surprisingly increased fusion level. Its location was predicted to be in the heptad repeat (HR) 2 on the F protein (21). During the membrane fusion process, the alpha-

helical domain of HR2 interacts with HR1 and forms F protein as a post-fusion conformation of the 6-helix bundle (3, 26). The hyperfusogenicity of F3 corresponds to the previous study of the F protein of Newcastle Disease virus (NDV), which yielded hyperfusogenic phenotype when N-glycans were eliminated from its HR1 and HR2 (27). Therefore, this suggests that the N-glycan(s) on the HR2 region of MojV F modulates fusion level, and this fusion-controlling mechanism by N-glycosylation may be conserved among paramyxoviruses.

The henipaviral G proteins have 7 to 12 bioinformatically predicted N-glycosylation sites that are mostly located on their head regions while there are only four sites throughout entire MojV G (Fig. 4.6.A). We found that the N-glycosylation site on G stalk, N189, is not conserved with any other predicted sites on the henipaviral G proteins. The predicted N-glycan positions of MojV F were relatively more conserved to other henipaviral F proteins except for Ghana virus (GhV) F, suggesting that the roles of N-glycans are relatively more conserved among henipaviral F proteins compared to the G proteins (Fig. 4.6.B).

Several studies still remain to be determined to understand more roles of N-glycosylation on MojV F and G glycoproteins. For example, the N-glycan(s) on MojV G may play significant roles as a “glycan shield” to protect the virus against neutralizing antibodies or modulates binding affinity to receptors (7, 8, 15, 28). Furthermore, since MojV F and G are far less N-glycosylated than others, other post-translational modifications such as O-glycosylation may also affect the cell-cell fusion and viral entry (14).

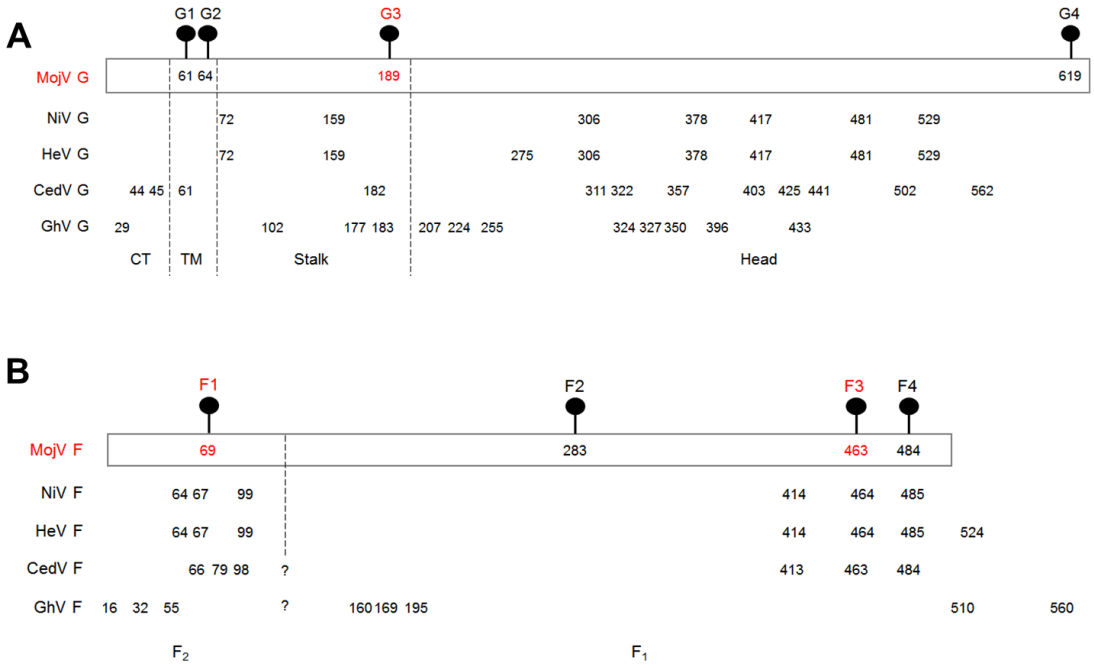

Figure 4.6: Comparison of N-glycan positions between henipaviral G (A) and F (B) glycoproteins.
Numbers indicate predicted N-glycosylation sites based on NetNGlyc 1.0 Server. The numbers in red represent the actual N-glycosylated sites in MojV G and F. **(A)** Each domain of G proteins were separated by dashed lines. **(B)** A dashed line indicates F protein cleavage. Locations of both CedV and GhV F cleavage sites are unknown and shown as question marks. The GenBank accession numbers of each of the amino acid sequences are as follows: MojV G (YP_009094095.1), NiV G (NP_112027.1), HeV G (NP_047112.2), CedV G (YP_009094086.1), GhV G (AFH96011.1), MojV F (YP_009094094.1), NiV F (NP_112026.1), HeV F (NP_047111.2), CedV F (YP_009094085.1), GhV F (YP_009091837.1).

4.7 References

1. Hyndman, T.H.; Shilton, C.M.; Marschang, R.E. Paramyxoviruses in reptiles: a review. Vet Microbiol 2013, 165, 200-213.
2. Thibault, P.A.; Watkinson, R.E.; Moreira-Soto, A.; Drexler, J.F.; Lee, B. Zoonotic Potential of Emerging Paramyxoviruses: Knowns and Unknowns. Adv Virus Res 2017, 98, 1-55.
3. Aguilar, H.C.; Henderson, B.A.; Zamora, J.L.; Johnston, G.P. Paramyxovirus Glycoproteins and the Membrane Fusion Process. Curr Clin Microbiol Rep 2016, 3, 142-154.
4. Azarm, K.D.; Lee, B. Differential Features of Fusion Activation within the Paramyxoviridae. Viruses 2020, 12.
5. Ortega, V.; Stone, J.A.; Contreras, E.M.; Iorio, R.M.; Aguilar, H.C. Addicted to sugar: roles of glycans in the order Mononegavirales. Glycobiology 2019, 29, 2-21.
6. Vigerust, D.J.; Shepherd, V.L. Virus glycosylation: role in virulence and immune interactions. Trends Microbiol 2007, 15, 211-218.
7. Biering, S.B.; Huang, A.; Vu, A.T.; Robinson, L.R.; Bradel-Tretheway, B.; Choi, E.; Lee, B.; Aguilar, H.C. N-Glycans on the Nipah virus attachment glycoprotein modulate fusion and viral entry as they protect against antibody neutralization. J Virol 2012, 86, 11991-12002.
8. Aguilar, H.C.; Matreyek, K.A.; Filone, C.M.; Hashimi, S.T.; Levroney, E.L.; Negrete, O.A.; Bertolotti-Ciarlet, A.; Choi, D.Y.; McHardy, I.; Fulcher, J.A., et al. N-glycans on Nipah virus fusion protein protect against neutralization but reduce membrane fusion and viral entry. J Virol 2006, 80, 4878-4889.
9. Carter, J.R.; Pager, C.T.; Fowler, S.D.; Dutch, R.E. Role of N-linked glycosylation of the Hendra virus fusion protein. J Virol 2005, 79, 7922-7925.
10. Bagai, S.; Lamb, R.A. Individual roles of N-linked oligosaccharide chains in intracellular transport of the paramyxovirus SV5 fusion protein. Virology 1995, 209, 250-256.
11. El Najjar, F.; Schmitt, A.P.; Dutch, R.E. Paramyxovirus glycoprotein incorporation, assembly and budding: a three way dance for infectious particle production. Viruses 2014, 6, 3019-3054.
12. Sawatsky, B.; von Messling, V. Canine distemper viruses expressing a hemagglutinin without N-glycans lose virulence but retain immunosuppression. J Virol 2010, 84, 2753-2761.
13. Segawa, H.; Inakawa, A.; Yamashita, T.; Taira, H. Functional analysis of individual oligosaccharide chains of Sendai virus hemagglutinin-neuraminidase protein. Biosci Biotechnol Biochem 2003, 67, 592-598.
14. Stone, J.A.; Nicola, A.V.; Baum, L.G.; Aguilar, H.C. Multiple Novel Functions of Henipavirus O-glycans: The First O-glycan Functions Identified in the Paramyxovirus Family. PLoS Pathog 2016, 12, e1005445.

15. Bradel-Tretheway, B.G.; Liu, Q.; Stone, J.A.; McInally, S.; Aguilar, H.C. Novel Functions of Hendra Virus G N-Glycans and Comparisons to Nipah Virus. J Virol 2015, 89, 7235-7247.
16. Liu, Q.; Bradel-Tretheway, B.; Monreal, A.I.; Saludes, J.P.; Lu, X.; Nicola, A.V.; Aguilar, H.C. Nipah virus attachment glycoprotein stalk C-terminal region links receptor binding to fusion triggering. J Virol 2015, 89, 1838-1850.
17. Bradel-Tretheway, B.G.; Zamora, J.L.R.; Stone, J.A.; Liu, Q.; Li, J.; Aguilar, H.C. Nipah and Hendra Virus Glycoproteins Induce Comparable Homologous but Distinct Heterologous Fusion Phenotypes. J Virol 2019, 93.
18. Zamora, J.L.R.; Ortega, V.; Johnston, G.P.; Li, J.; Andre, N.M.; Monreal, I.A.; Contreras, E.M.; Whittaker, G.R.; Aguilar, H.C. Third Helical Domain of the Nipah Virus Fusion Glycoprotein Modulates both Early and Late Steps in the Membrane Fusion Cascade. J Virol 2020, 94.
19. Zamora, J.L.R.; Ortega, V.; Johnston, G.P.; Li, J.; Aguilar, H.C. Novel Roles of the N1 Loop and N4 Alpha-Helical Region of the Nipah Virus Fusion Glycoprotein in Modulating Early and Late Steps of the Membrane Fusion Cascade. J Virol 2021, 95.
20. Rissanen, I.; Ahmed, A.A.; Azarm, K.; Beaty, S.; Hong, P.; Nambulli, S.; Duprex, W.P.; Lee, B.; Bowden, T.A. Idiosyncratic Mojiang virus attachment glycoprotein directs a host-cell entry pathway distinct from genetically related henipaviruses. Nat Commun 2017, 8, 16060.
21. Cheliout Da Silva, S.; Yan, L.; Dang, H.V.; Xu, K.; Epstein, J.H.; Veesler, D.; Broder, C.C. Functional Analysis of the Fusion and Attachment Glycoproteins of Mojiang Henipavirus. Viruses 2021, 13.
22. Maley, F.; Trimble, R.B.; Tarentino, A.L.; Plummer, T.H., Jr. Characterization of glycoproteins and their associated oligosaccharides through the use of endoglycosidases. Anal Biochem 1989, 180, 195-204.
23. Tarentino, A.L.; Trimble, R.B.; Plummer, T.H., Jr. Enzymatic approaches for studying the structure, synthesis, and processing of glycoproteins. Methods Cell Biol 1989, 32, 111-139.
24. Wu, Z.; Yang, L.; Yang, F.; Ren, X.; Jiang, J.; Dong, J.; Sun, L.; Zhu, Y.; Zhou, H.; Jin, Q. Novel Henipa-like virus, Mojiang Paramyxovirus, in rats, China, 2012. Emerg Infect Dis 2014, 20, 1064-1066.
25. White, J.M.; Delos, S.E.; Brecher, M.; Schornberg, K. Structures and mechanisms of viral membrane fusion proteins: multiple variations on a common theme. Crit Rev Biochem Mol Biol 2008, 43, 189-219.
26. Bossart, K.N.; Zhu, Z.; Middleton, D.; Klippel, J.; Crameri, G.; Bingham, J.; McEachern, J.A.; Green, D.; Hancock, T.J.; Chan, Y.P., et al. A neutralizing human monoclonal antibody protects against lethal disease in a new ferret model of acute nipah virus infection. PLoS Pathog 2009, 5, e1000642.
27. Samal, S.; Khattar, S.K.; Kumar, S.; Collins, P.L.; Samal, S.K. Coordinate deletion of N-glycans from the heptad repeats of the fusion F

protein of Newcastle disease virus yields a hyperfusogenic virus with increased replication, virulence, and immunogenicity. J Virol 2012, 86, 2501-2511.
28. Vuorio, J.; Skerlova, J.; Fabry, M.; Veverka, V.; Vattulainen, I.; Rezacova, P.; Martinez-Seara, H. N-Glycosylation can selectively block or foster different receptor-ligand binding modes. Sci Rep 2021, 11, 5239.
29. Parsons, L.M.; Bouwman, K.M.; Azurmendi, H.; de Vries, R.P.; Cipollo, J.F.; Verheije, M.H. Glycosylation of the viral attachment protein of avian coronavirus is essential for host cell and receptor binding. J Biol Chem 2019, 294, 7797-7809.
30. Gupta, R.; Brunak, S. Prediction of glycosylation across the human proteome and the correlation to protein function. Pac Symp Biocomput 2002, 310-322.
31. Kim, M.S.; Leahy, D. Enzymatic deglycosylation of glycoproteins. Methods Enzymol 2013, 533, 259-63.
32. von Messling, V.; Cattaneo, R. N-linked glycans with similar location in the fusion protein head modulate paramyxovirus fusion. J Virol 2003, 77, 10202-12.
33. Wu, J.; Chen, S.; Liu, H.; Zhang, Z.; Ni, Z.; Chen, J.; Yang, Z.; Nie, Y.; Fan, D. Tunicamycin specifically aggravates ER stress and overcomes chemoresistance in multidrug-resistant gastric cancer cells by inhibiting N-glycosylation. J Exp Clin Cancer Res 2018. 37, 272.

CHAPTER 5

Overall conclusions and future directions

5.1 The current knowledge and future paths of Feline Morbillivirus (FeMV) research

Since FeMV was firstly detected from stray cats in Hong Kong in 2012, there have been many reports and case studies on the virus throughout the world. Chapter two summarized the current knowledge on FeMV, including the discoveries of each novel FeMV strain, cell tropism of both *in vivo* and *in vitro*, experimental techniques of FeMV RNA detection, and so on. Although study on FeMV is actively ongoing, there are still controversies between reports (e.g. possibility of persistent infection and association with other kidney diseases) and unidentified characteristics (e.g. cell entry mechanisms and host cell receptor). Therefore, to clarify these controversies and reveal undetermined characteristics, more case studies and clinical data with precise detection methods are strongly required. The recently proposed TaqMan-based real-time RT-PCR assay targeting the N gene can is promising because it shows higher sensitivity and detection rate than the conventional detection methods, and it also detects an early phase of FeMV infection (1).

Although it was reported that the risk of human-to-cat transmission is low since human cell lines are not susceptible to FeMV, it has a lot of potential of causing future pandemic outbreaks due to multiple reasons (2). First, the experiment of determining its host range was conducted *in vitro* only. Furthermore, the infectivity of the virus was tested with limited human cell lines including human embryonic kidney (HEK293T), rhabdomyosarcoma (TE671), fibrosarcoma (HT1080), epithelioid carcinoma (HeLa), and leukemia (MT-4 and Molt-4) (2). This cannot represent *in vivo* environment in the human body. Also, SLAM (CD150) and Nectin-4, which are the potential candidate receptors of FeMV, are widely expressed at immune and epithelial cells, respectively (3). This suggests that the possibility of FeMV transmission from cat to human cannot be completely excluded until *in vivo* infectivity tests are

conducted. Second, there is a probability of recombination between FeMV strains. A previous paper suggested that one of the FeMV strains from Japan, MiJP003, showed a possible recombination event between two strains isolated from Hong Kong and Japan (4). Third, although it is controversial, cross-reactivity was reported between FeMV and CDV (2). Therefore, it may have a capacity to adapt to new host species considering its high genetic diversity and possible gene recombination and cross-reactivity. (5). Not surprisingly, the viral RNA of the virus was recently detected from a white-eared opossum (*Didelphis albiventris*) in southern Brazil, in 2021 (6). This was the first FeMV detection from a non-feline host, showing its ability to infect other mammal species (6). Therefore, humans can also be a highly desirable host target considering the high frequency of direct contact with cats.

Due to the lack of a cell culture system, the pathogenicity of FeMV is still unclear (3). However, several studies showed the possibility of using Crandall–Reese Feline Kidney (CRFK) cells as a model of viral infection (6-9). Since FeMV-infected CRFK cells showed syncytia formation, studying its cell-cell fusion and viral entry mechanisms using this cell line would be helpful to understand its pathogenesis. Additionally, the proteolytic cleavage site of FeMV F may not be conserved with the typical cleavage sites of other morbilliviral F proteins. Overall, understanding its pathogenicity would expand our knowledge of the genus *Morbillivirus* (7, 8, 10).

5.2 The current knowledge and future paths of Mojiang virus (MojV) research

MojV is the first rat-originated henipavirus. Since it is only known by sequence data and does not share receptor(s) with any other henipaviruses, its characteristics including pathogenicity, symptoms, and species tropism have not been established yet. What hampers MojV cell fusion studies is the low levels and slow fusion kinetics of MojV F and G surface glycoproteins (11). Chapter 3 defines the

functions of the three cysteine residues on the MojV G stalk domain. We found that these residues are involved in many roles in the cell-cell fusion mechanism of MojV, such as maintaining tetrameric structure, G protein expression, cell fusogenicity, and F/G interaction. Interestingly, the F and G proteins of MojV and another deadly henipaviral NiV were functionally interacting with each other despite the low amino acid similarity between the two G proteins. This confirms the phylogenic placement of MojV as a member of the genus *Henipavirus* which has been controversial in the field. In Chapter 4, we discovered the roles of N-glycosylation on the MojV F and G glycoproteins in cell-cell fusion and viral entry mechanisms. Our data indicate that the two N-glycans on MojV F modulate proteolytic F cleavage, cell fusogenicity, F/G interaction, and viral entry. MojV G has at least one N-glycosylated site on its stalk domain. However, it did not play any significant role in membrane fusion mechanisms and was not conserved with N-glycosylation sites on other henipaviral G proteins.

MojV can be easily underestimated comparing to other deadly pathogenic henipaviruses such as NiV and HeV. However, its unique origin implies that bats are not the only host reservoirs of henipaviruses (13). Hence, studying MojV both *in vitro* and *in vivo* will expand our understanding of henipaviruses. As further *in vitro* study, revealing the crystal structure of MojV G will be very helpful to deeply understand its cell-cell fusion and viral entry mechanisms. Recently, the atomic structure of the MojV G head domain has been determined and through comparisons with other henipaviral G head domains it was predicted that the MojV G head does not have a binding site of Ephrin B2 by comparing the crystal structure of MojV and NiV G ß-propeller domains (12). Obtaining the crystal structure of the MojV G stalk domain will provide critical insight into its functional role especially as a tertiary structure. For example, one of the three cysteine residues in MojV G stalk, C188, is closely located to an N-glycosylated site (N189). There is a possibility that the N-glycan may

functionally obstruct C188.

5.3 Overall conclusion

Studying cell-cell fusion and viral entry mechanisms is critical to understand the early stages of viral infection. Our study on MojV revealed similarities of the mechanisms amongst henipaviruses (e.g. similar phenotypes between homologous and heterologous combinations of MojV G with either of MojV F or NiV F, respectively) and differences (e.g. low levels of N-glycosylation on MojV G, increased fusogenicity after disrupting cysteine residues of MojV G stalk). Also, the summary of current knowledge on FeMV highlighted its high potential for human transmission and emphasized the significance of future studies on its cell-cell membrane fusion and viral entry mechanisms. Overall, by shedding light on the two understudied paramyxoviruses, FeMV and MojV, we will be able to be more prepared against possible future pandemics induced by paramyxoviruses.

5.2 References

1. Makhtar, S.T.; Tan, S.W.; Nasruddin, N.A.; Abdul Aziz, N.A.; Omar, A.R.; Mustaffa-Kamal, F. Development of TaqMan-based real-time RT-PCR assay based on N gene for the quantitative detection of feline morbillivirus. *BMC Vet Res* **2021**, *17*, 128.
2. Sakaguchi, S.; Koide, R.; Miyazawa, T. In vitro host range of feline morbillivirus. *J Vet Med Sci* **2015**, *77*, 1485-1487.
3. De Luca, E.; Sautto, G.A.; Crisi, P.E.; Lorusso, A. Feline Morbillivirus Infection in Domestic Cats: What Have We Learned So Far? *Viruses* **2021**, *13*.
4. Park, E.S.; Suzuki, M.; Kimura, M.; Maruyama, K.; Mizutani, H.; Saito, R.; Kubota, N.; Furuya, T.; Mizutani, T.; Imaoka, K., et al. Identification of a natural recombination in the F and H genes of feline morbillivirus. *Virology* **2014**, *468-470*, 524-531.
5. Choi, E.J.; Ortega, V.; Aguilar, H.C. Feline Morbillivirus, a New Paramyxovirus Possibly Associated with Feline Kidney Disease. *Viruses* **2020**, *12*.
6. Lavorente, F.L.P.; de Matos, A.; Lorenzetti, E.; Oliveira, M.V.; Pinto-Ferreira, F.; Michelazzo, M.M.Z.; Viana, N.E.; Lunardi, M.; Headley, S.A.; Alfieri, A.A., et al. First detection of Feline morbillivirus infection in white-eared opossums (Didelphis albiventris, Lund, 1840), a non-feline host. *Transbound Emerg Dis* **2021**, 10.1111/tbed.14109.
7. Woo, P.C.; Lau, S.K.; Wong, B.H.; Fan, R.Y.; Wong, A.Y.; Zhang, A.J.; Wu, Y.; Choi, G.K.; Li, K.S.; Hui, J., et al. Feline morbillivirus, a previously undescribed paramyxovirus associated with tubulointerstitial nephritis in domestic cats. *Proc Natl Acad Sci U S A* **2012**, *109*, 5435-5440.
8. Furuya, T.; Sassa, Y.; Omatsu, T.; Nagai, M.; Fukushima, R.; Shibutani, M.; Yamaguchi, T.; Uematsu, Y.; Shirota, K.; Mizutani, T. Existence of feline morbillivirus infection in Japanese cat populations. *Arch Virol* **2014**, *159*, 371-373.
9. Donato, G.; De Luca, E.; Crisi, P.E.; Pizzurro, F.; Masucci, M.; Marcacci, M.; Cito, F.; Di Sabatino, D.; Boari, A.; D'Alterio, N., et al. Isolation and genome sequences of two Feline Morbillivirus genotype 1 strains from Italy. *Vet Ital* **2019**, *55*, 179-182.
10. Visser, I.K.; van der Heijden, R.W.; van de Bildt, M.W.; Kenter, M.J.; Orvell, C.; Osterhaus, A.D. Fusion protein gene nucleotide sequence similarities, shared antigenic sites and phylogenetic analysis suggest that phocid distemper virus type 2 and canine distemper virus belong to the same virus entity. *J Gen Virol* **1993**, *74 (Pt 9)*, 1989-1994.
11. Cheliout Da Silva, S.; Yan, L.; Dang, H.V.; Xu, K.; Epstein, J.H.; Veesler, D.; Broder, C.C. Functional Analysis of the Fusion and Attachment Glycoproteins of Mojiang Henipavirus. *Viruses* **2021**, *13*.

12. Rissanen, I.; Ahmed, A.A.; Azarm, K.; Beaty, S.; Hong, P.; Nambulli, S.; Duprex, W.P.; Lee, B.; Bowden, T.A. Idiosyncratic Mojiang virus attachment glycoprotein directs a host-cell entry pathway distinct from genetically related henipaviruses. *Nat Commun* **2017**, *8*, 16060.
13. Wu, Z.; Yang, L.; Yang, F.; Ren, X.; Jiang, J.; Dong, J.; Sun, L.; Zhu, Y.; Zhou, H.; Jin, Q. Novel Henipa-like virus, Mojiang Paramyxovirus, in rats, China, 2012. *Emerg Infect Dis* **2014**, *20*, 1064-1066.